https://www.mdc-berlin.de/de/veroeffentlichungstypen/clinical-journal-club

Als gemeinsame Einrichtung von MDC und Charité fördert das Experimental and Clinical Research Center die Zusammenarbeit zwischen Grundlagenwissenschaftlern und klinischen Forschern. Hier werden neue Ansätze für Diagnose, Prävention und Therapie von Herz-Kreislauf- und Stoffwechselerkrankungen, Krebs sowie neurologischen Erkrankungen entwickelt und zeitnah am Patienten eingesetzt. Sie sind eingeladen, um uns beizutreten. Bewerben Sie sich!

A 76-year-old man presented to the dermatology clinic with a 2-day history of blood-filled blisters on the tongue. He reported no prior trauma or other bleeding symptoms. Physical examination was notable for hemorrhagic bullae on the tongue and gingiva, and purpura on the arms and legs. Which of the following lab abnormalities is most likely present?

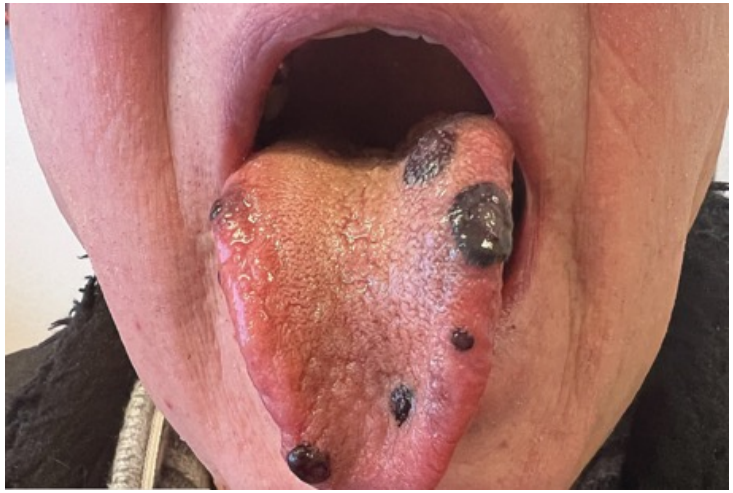

Anemia

Elevated PT and PTT

Leukopenia

Thrombocytopenia

Vitamin C deficiency

Peripheral blood smear showed thrombocytopenia with megakaryocytes and bone marrow biopsy showed elevated number of megakaryocytes, and a diagnosis of immune thrombocytopenia was made. Primary immune thrombocytopenia is a diagnosis of exclusion that is made after other causes of thrombocytopenia and secondary immune thrombocytopenia are ruled out. The patient was treated with an 8-week tapering course of prednisolone. At 12-week follow-up, his mucocutaneous lesions had abated and platelet count had normalized.

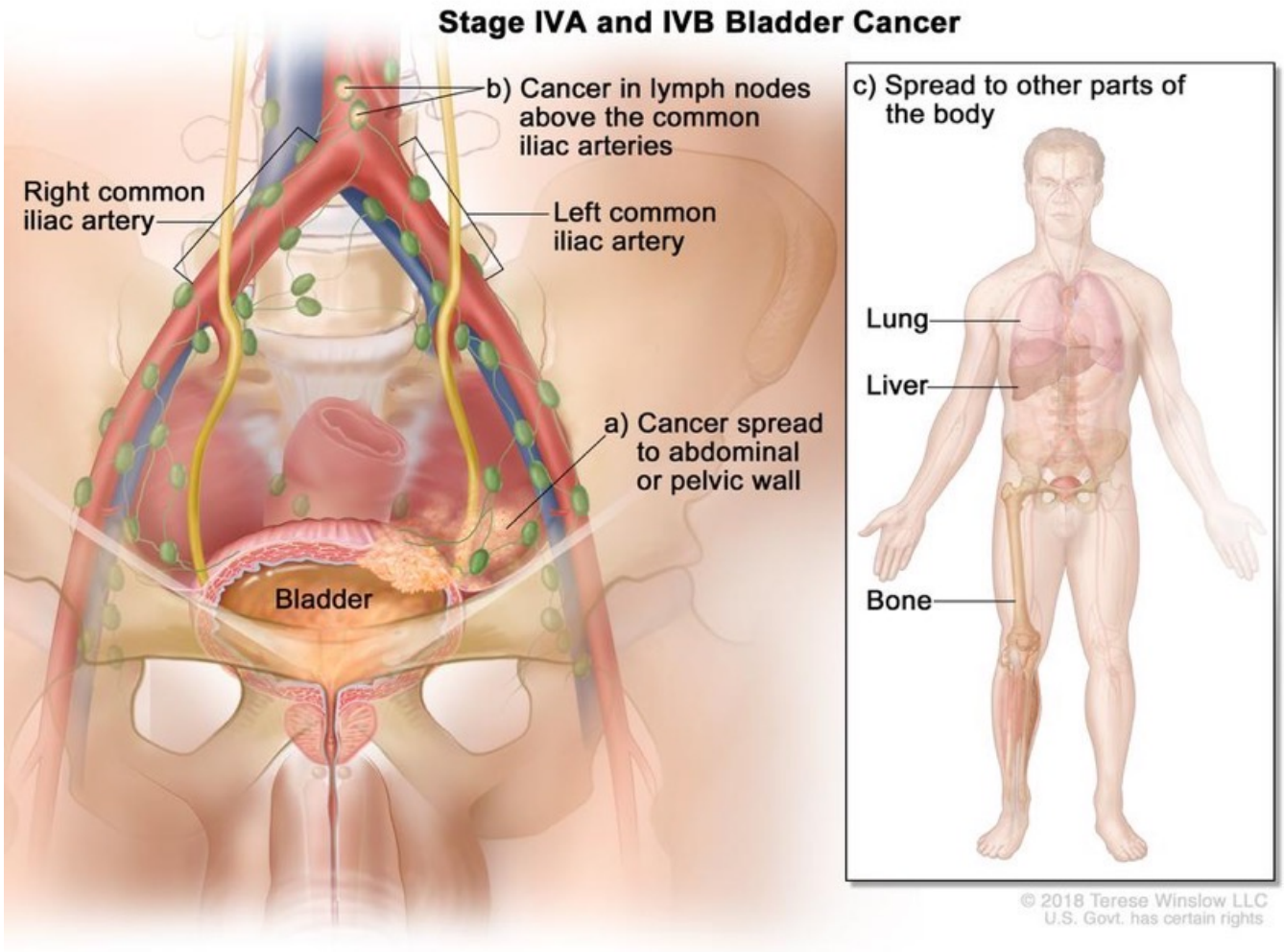
Stage IVA and IVB Bladder Cancer
b) Cancer in lymph nodes above the common iliac arteries
Right common iliac artery
Left common iliac artery
a) Cancer spread to abdominal or pelvic wall
Bladder
c) Spread to other parts of the body
Lung
Liver
Bone
© 2018 Terese Winslow LLC
U.S. Govt. has certain rights

Nectins and Nectin-like molecules (Necl) are families of cellular adhesion molecules involved in Ca2+-independent cellular adhesion.
So far four nectins have been identified in humans, namely nectin-1, nectin-2, nectin-3 and nectin-4. These four family members have also been found in most other well studied mammals. Also, five Necls have been identified, these are: Necl-1, Necl-2, Necl-3, Necl-4 and Necl-5.
All nectins and all Necls share the same overall structure defined by three extra cellular immunoglobulin domains, a single transmembrane helix and an intracellular domain. For all nectins the intracellular domain can bind a scaffold protein named afadin (the product of the MLLT4 gene).
Recently, it has been found that nectin-4 can be found in the serum of patients with lung cancer. This has led to speculations that this protein might be involved in some developing cancers and might even have a pharmaceutical potential.

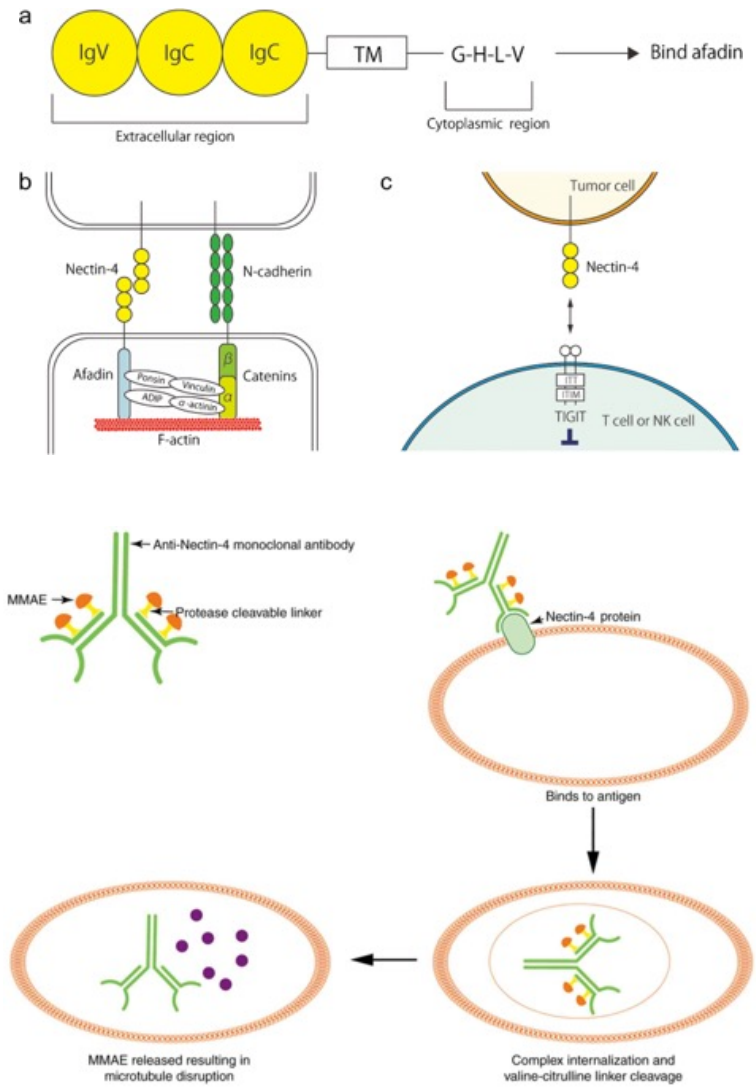

Enfortumab vedotin
Enfortumab Vedotin ist ein gegen Nectin-4 gerichtetes Antikörper-Wirkstoff-Konjugat zur Behandlung von fortgeschrittenem oder metastasiertem Urothelkarzinom. Das Antikörper-Wirkstoff-Konjugat ist mit dem Anti-Mikrotubuli-Medikament Monomethylauristatin E konjugiert. Sobald der Antikörper die Nectin-4-exprimierende Zelle bindet, wird das Konjugat internalisiert und das Chemotherapeutikum freigesetzt.

Anwendung
Enfortumab Vedotin ist als Monotherapie angezeigt zur Behandlung von erwachsenen Patienten mit lokal fortgeschrittenem oder metastasiertem Urothelkarzinom, die zuvor eine platinhaltige Chemotherapie und einen PD-1- oder PD-L1-Inhibitor erhalten haben.

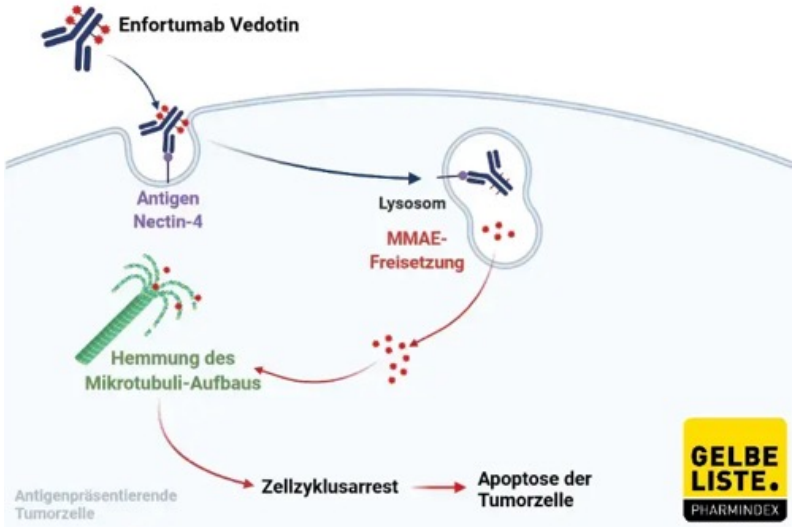

Wirkmechanismus
Enfortumab Vedotin (EV) besteht aus einem vollständig humanen monoklonalen Antikörper, der gegen Nectin-4 gerichtet ist, welches bei einer Reihe von Krebsarten überexprimiert ist (v.a. bei Urothelkarzinom, Colitis ulcerosa und Brustkrebs).
Der EV-Antikörper bindet mit hoher Affinität und Spezifität an Nectin-4-exprimierende Zellen, wodurch eine Kreuzreaktivität mit anderen Nectin-exprimierenden Zellen verhindert wird. Sobald gebundenes EV internalisiert wurde, führt dies zur intrazellulären Freisetzung des Mikrotubuli-störenden Wirkstoffs Monomethylauristatin E (MMAE), was schließlich zur Apoptose der Tumorzelle führt.

Pembrolizumab

Pembrolizumab ist ein monoklonaler Antikörper und gehört zur Wirkstoffgruppe der PD-1-Inhibitoren. Das Medikament ist zugelassen zur Behandlung des fortgeschrittenen Melanoms, des nicht kleinzelligen Bronchialkarzinoms, des Hodgkin-Lymphoms, von Urothelkarzinomen und Tumoren im Kopf- und Hals-Bereich**.**

Wirkmechanismus

Pembrolizumab ist ein humanisierter monoklonaler Antikörper, der an den PD-1 (*Programmed cell death*) Rezeptor bindet und damit die Interaktion mit seinen Liganden PD-L1 (*programmed cell death ligand*) und PD-L2 verhindert. Der PD-1-Rezeptor ist ein negativer Regulator der T-Zell-Aktivität, der an der Kontrolle der T-Zell-Immunreaktion beteiligt ist. Der Rezeptor wird hauptsächlich auf der Oberfläche aktivierter T-Zellen exprimiert . Binden an ihn die Liganden PD-L1 und PD-L2, wird die zytotoxische T-Zell-Immunantwort gehemmt und so überschießende Immunreaktionen verhindert. Diesen negativen Rückkopplungsmechanismus missbrauchen allerdings Tumorzellen, indem sie ebenfalls die beiden Liganden exprimieren. In der Folge wird das Immunsystem ausgebremst und daran gehindert, die Krebszellen zu attackieren.

Durch die Hemmung der Bindung des PD-1-Rezeptors an seine Liganden PD-L1 und PD-L2 verstärkt Pembrolizumab so die T-Zell-Reaktion einschließlich der Immunreaktion gegen den Tumor.

Pembrolizumab wird auch als **Checkpoint-Inhibitor** bezeichnet, da das Immuntherapeutikum das körpereigene Immunsystem wieder in die Lage versetzt, selbst verstärkt gegen den Krebs zu kämpfen, indem es wichtige Schaltstellen, sogenannte *Checkpoints*, blockiert.

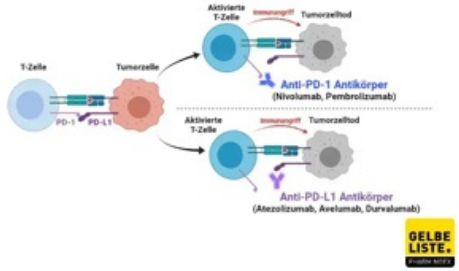

ORIGINAL ARTICLE

Enfortumab Vedotin and Pembrolizumab in Untreated Advanced Urothelial Cancer

No treatment has surpassed platinum-based chemotherapy in improving overall survival in patients with previously untreated locally advanced or metastatic urothelial carcinoma. We conducted a phase 3, global, open-label, randomized trial to compare the efficacy and safety of enfortumab vedotin and pembrolizumab with the efficacy and safety of platinum-based chemotherapy in patients with previously untreated locally advanced or metastatic urothelial carcinoma. Patients were randomly assigned in a 1:1 ratio to receive 3-week cycles of enfortumab vedotin (at a dose of 1.25 mg per kilogram of body weight intravenously on days 1 and 8) and pembrolizumab (at a dose of 200 mg intravenously on day 1) (enfortumab vedotin–pembrolizumab group) or gemcitabine and either cisplatin or carboplatin (determined on the basis of eligibility to receive cisplatin) (chemotherapy group). The primary end points were progression-free survival as assessed by blinded independent central review and overall survival.

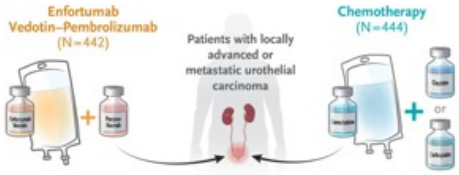

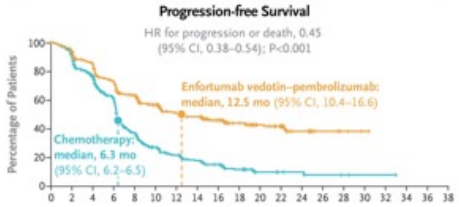

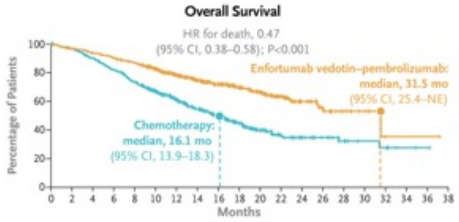

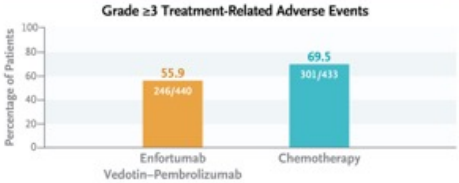

CONCLUSIONS

In patients with previously untreated locally advanced or metastatic urothelial carcinoma, treatment with enfortumab vedotin and pembrolizumab led to longer progression-free and overall survival than platinum-based chemotherapy.

Methods

Patients

Eligible adult patients had radiologically documented, histologically confirmed, unresectable locally advanced or metastatic urothelial carcinoma (including differentiation in squamous cells or in multiple cell types); there was no preselection for biomarkers, including nectin-4 and programmed death ligand 1 (PD-L1) expression.

Trial Design and Treatment

Enrolled patients were randomly assigned in a 1:1 ratio to receive enfortumab vedotin and pembrolizumab (enfortumab vedotin–pembrolizumab group) or chemotherapy (gemcitabine and either cisplatin or carboplatin; chemotherapy group). Patients assigned to the enfortumab vedotin–pembrolizumab group received enfortumab vedotin as an intravenous infusion (at a dose of 1.25 mg per kilogram of body weight with a maximum of 125 mg per dose) on days 1 and 8 and pembrolizumab as an intravenous infusion (at a dose of 200 mg) after the enfortumab vedotin infusion on day 1 of each 3-week cycle.

End Points

The trial had two primary end points: progression-free survival, which was defined as the time from randomization to the first occurrence of disease progression (as assessed by blinded independent central review according to the Response Evaluation Criteria in Solid Tumors [RECIST], version 1.1) or death from any cause (whichever occurred first), and overall survival.

Characteristic	Enfortumab Vedotin–Pembrolizumab (N=442)	Chemotherapy (N=444)
Median age (range) — yr	69 (37–87)	69 (22–91)
Age ≥75 yr — no. (%)	102 (23.1)	108 (24.3)
Sex — no. (%)		
Male	344 (77.8)	336 (75.7)
Female	98 (22.2)	108 (24.3)
Race or ethnic group — no. (%)†		
Asian	99 (22.4)	92 (20.7)
Black	3 (0.7)	7 (1.6)
White	308 (69.7)	290 (65.3)
Other‡	5 (1.1)	8 (1.8)
Unknown or not reported	27 (6.1)	47 (10.6)
Geographic region — no. (%)		
North America	103 (23.3)	85 (19.1)
Europe	172 (38.9)	197 (44.4)
Rest of the world	167 (37.8)	162 (36.5)
ECOG performance-status score — no. (%)§		
0	223 (50.5)	215 (48.4)
1	204 (46.2)	216 (48.6)
2	15 (3.4)	11 (2.5)
Data missing	0	2 (0.5)
Body-mass index — no. (%)¶		
<25	206 (46.6)	185 (41.7)
25 to <30	144 (32.6)	155 (34.9)
≥30	89 (20.1)	101 (22.7)
Data missing	3 (0.7)	3 (0.7)
Creatinine clearance — no. (%)‖		
≥60 ml/min	249 (56.3)	257 (57.9)
<60 ml/min	193 (43.7)	187 (42.1)
No. of Bajorin risk factors — no. (%)**		
0	179 (40.5)	183 (41.2)
1	263 (59.5)	259 (58.3)
Data missing	0	2 (0.5)
H score of nectin-4 expression††		
No. of patients tested	394	406
Median score (range)	280 (0–300)	270 (0–300)
Disease status at randomization — no. (%)		
Locally advanced	21 (4.8)	24 (5.4)
Metastatic	421 (95.2)	420 (94.6)
Primary site of origin of disease — no. (%)		
Upper tract	135 (30.5)	104 (23.4)
Lower tract	305 (69.0)	339 (76.4)
Unknown	2 (0.5)	1 (0.2)
Histologic type — no. (%)		
Urothelial carcinoma	379 (85.7)	373 (84.0)
Urothelial carcinoma, mixed types‡‡	50 (11.3)	53 (11.9)
Variant urothelial carcinoma only	4 (0.9)	7 (1.6)
Unknown	9 (2.0)	11 (2.5)
Sites of metastasis — no. (%)		
Lymph node only	103 (23.3)	104 (23.4)
Visceral site	318 (71.9)	318 (71.6)
Bone	81 (18.3)	102 (23.0)
Liver	100 (22.6)	99 (22.3)
Lung	170 (38.5)	157 (35.4)
Cisplatin eligibility status — no. (%)		
Eligible	240 (54.3)	242 (54.5)
Ineligible	202 (45.7)	202 (45.5)
PD-L1 expression — no./total no. (%)§§		
High, CPS ≥10	254/438 (58.0)	254/439 (57.9)
Low, CPS <10	184/438 (42.0)	185/439 (42.1)

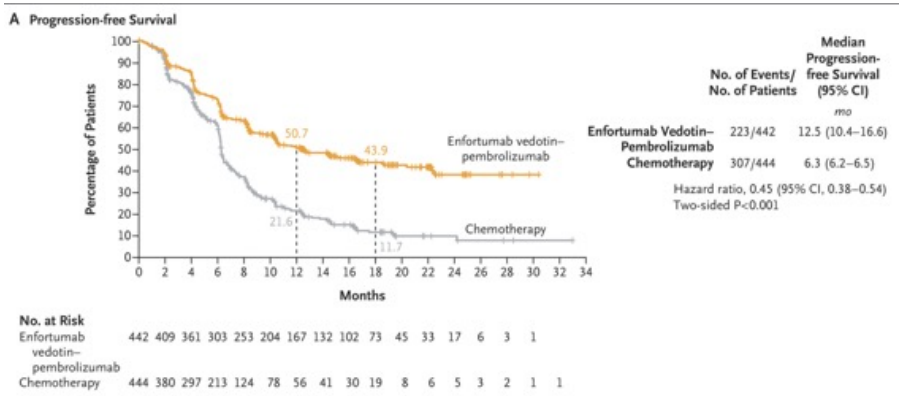

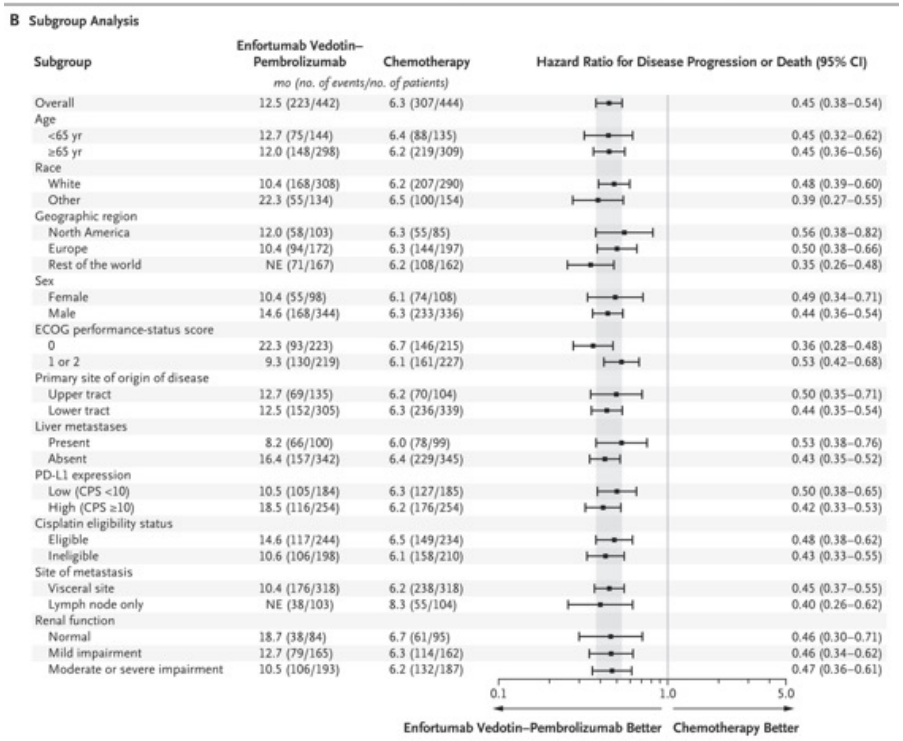

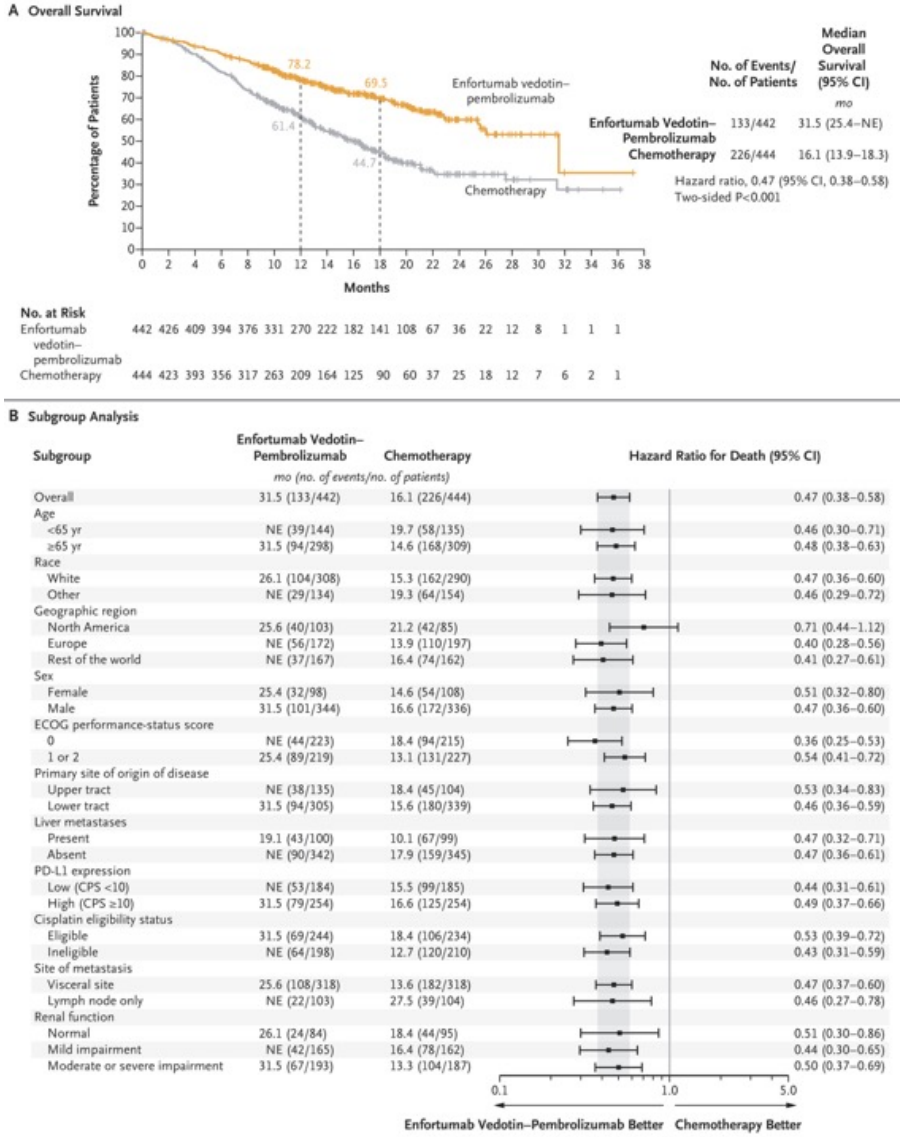

Analysis of Overall Survival in Overall Population and in Prespecified Subgroups.

Panel A shows Kaplan–Meier estimates of overall survival according to treatment group in the intention-to-treat population. The dashed lines indicate overall survival at 12 and 18 months.

Panel B shows a forest plot of the analyses of overall survival in all prespecified subgroups. Because the results of the interim analysis of overall survival were significant, the interim analysis was considered to be the final analysis.

Overall Response and Duration of Response.

Variable	Enfortumab Vedotin–Pembrolizumab (N = 437)	Chemotherapy (N = 441)
Confirmed best overall response — no. (%)		
Complete response	127 (29.1)	55 (12.5)
Partial response	169 (38.7)	141 (32.0)
Stable disease	82 (18.8)	149 (33.8)
Progressive disease	38 (8.7)	60 (13.6)
Could not be evaluated†	0	4 (0.9)
No assessment‡	21 (4.8)	32 (7.3)
Confirmed overall response (95% CI) — %§	67.7 (63.1–72.1)	44.4 (39.7–49.2)
Median time to response (range) — mo	2.1 (1.3–12.3)	2.1 (1.6–8.3)
Median duration of response (95% CI) — mo	Not reached (20.2–NE)	7.0 (6.2–10.2)

Treatment-Related Adverse Events.

Adverse Event	Enfortumab Vedotin–Pembrolizumab (N = 440)		Chemotherapy (N = 433)	
	Any Grade	Grade ≥3	Any Grade	Grade ≥3
	Number of patients (percent)			
Any adverse event	427 (97.0)	246 (55.9)	414 (95.6)	301 (69.5)
Peripheral sensory neuropathy	220 (50.0)	16 (3.6)	43 (9.9)	0
Pruritus	175 (39.8)	5 (1.1)	21 (4.8)	0
Alopecia	146 (33.2)	2 (0.5)	34 (7.9)	1 (0.2)
Maculopapular rash	144 (32.7)	34 (7.7)	14 (3.2)	0
Fatigue	129 (29.3)	13 (3.0)	156 (36.0)	18 (4.2)
Diarrhea	121 (27.5)	16 (3.6)	48 (11.1)	3 (0.7)
Decreased appetite	118 (26.8)	5 (1.1)	98 (22.6)	6 (1.4)
Nausea	89 (20.2)	5 (1.1)	168 (38.8)	12 (2.8)
Anemia	61 (13.9)	15 (3.4)	245 (56.6)	136 (31.4)
Hyperglycemia	48 (10.9)	22 (5.0)	3 (0.7)	0
Neutropenia	40 (9.1)	21 (4.8)	180 (41.6)	130 (30.0)
Neutrophil count decreased	16 (3.6)	11 (2.5)	54 (12.5)	39 (9.0)
Thrombocytopenia	15 (3.4)	2 (0.5)	148 (34.2)	84 (19.4)
Platelet count decreased	3 (0.7)	0	63 (14.5)	28 (6.5)

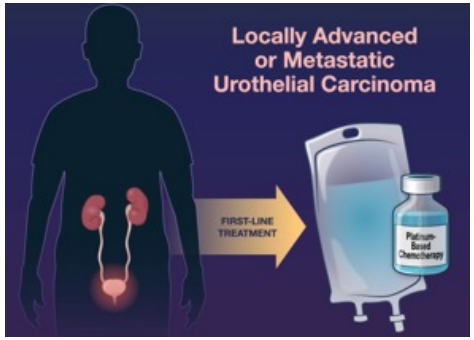
Locally Advanced
or Metastatic
Urothelial Carcinoma
FIRST-LINE
TREATMENT
Platinum-
Based
Chemotherapy

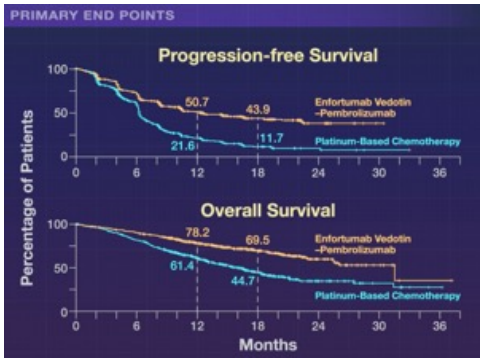
PRIMARY END POINTS
Progression-free Survival
Percentage of Patients
100
50
0
50.7
43.9
21.6
11.7
Enfortumab Vedotin
–Pembrolizumab
Platinum-Based Chemotherapy
0
6
12
18
24
30
36
Overall Survival
78.2
69.5
61.4
44.7
Enfortumab Vedotin
–Pembrolizumab
Platinum-Based Chemotherapy
Months

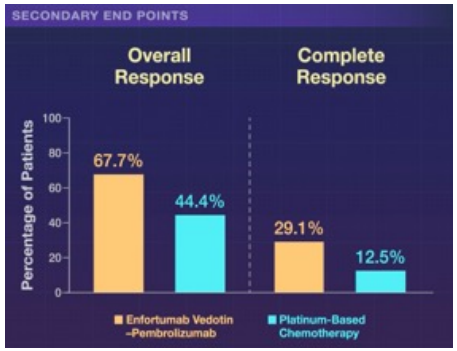
SECONDARY END POINTS
Overall
Response
Complete
Response
Percentage of Patients
100
80
60
40
20
0
67.7%
44.4%
29.1%
12.5%
Enfortumab Vedotin
–Pembrolizumab
Platinum-Based
Chemotherapy


Efficacy
and Safety
Enfortumab
Vedotin
Pembro-
lizumab
• Programmed
death 1 inhibitor

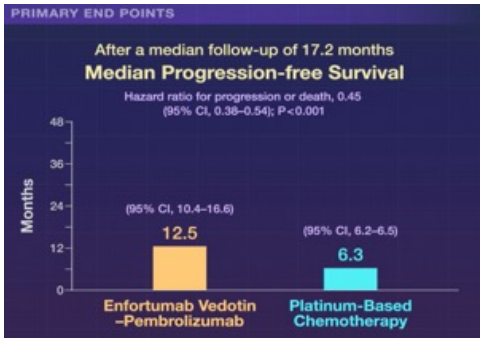
PRIMARY END POINTS
After a median follow-up of 17.2 months
Median Progression-free Survival
Hazard ratio for progression or death, 0.45
(95% CI, 0.38–0.54); P<0.001
Months
48
36
24
12
0
(95% CI, 10.4–16.6)
12.5
(95% CI, 6.2–6.5)
6.3
Enfortumab Vedotin
–Pembrolizumab
Platinum-Based
Chemotherapy

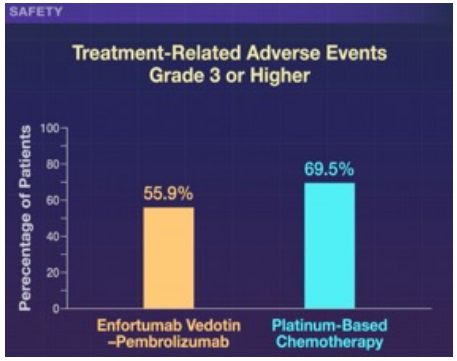
SAFETY
Treatment-Related Adverse Events
Grade 3 or Higher
Percentage of Patients
100
80
60
40
20
0
55.9%
69.5%
Enfortumab Vedotin
–Pembrolizumab
Platinum-Based
Chemotherapy

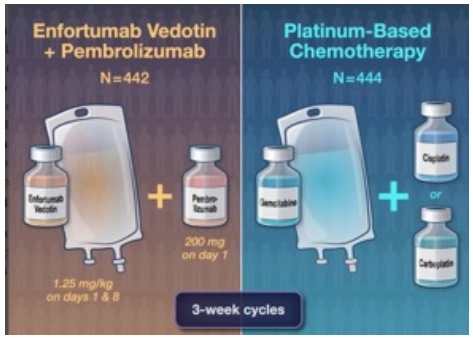
Enfortumab Vedotin
+ Pembrolizumab
N=442
Platinum-Based
Chemotherapy
N=444
Enfortumab
Vedotin
Pembro-
lizumab
200 mg
on day 1
1.25 mg/kg
on days 1 & 8
Gemcitabine
Cisplatin
or
Carboplatin
3-week cycles

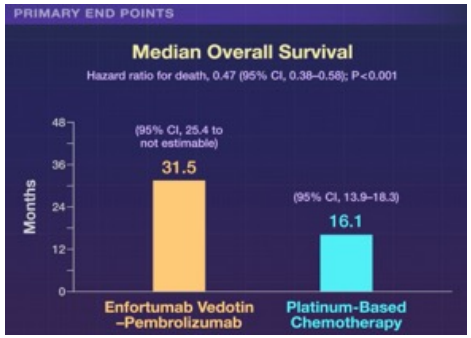
PRIMARY END POINTS
Median Overall Survival
Hazard ratio for death, 0.47 (95% CI, 0.38–0.58); P<0.001
Months
48
36
24
12
0
(95% CI, 25.4 to
not estimable)
31.5
(95% CI, 13.9–18.3)
16.1
Enfortumab Vedotin
–Pembrolizumab
Platinum-Based
Chemotherapy


Enfortumab
Vedotin
Pembro-
lizumab
• Longer progression-
free survival
• And overall survival
Than platinum-based
chemotherapy
Gemcitabine
Cisplatin
or
Carboplatin

Multiple Food Allergies ‘Remarkably Common,’ Study Finds

Omalizumab ist ein monoklonaler Antikörper, der gegen Immunglobulin E (IgE) gerichtet ist und zur Behandlung von Asthma, schwerer chronischer Rhinosinusitis mit Nasenpolypen und chronischer Urtikaria angewendet wird.

Wirkung

Omalizumab hemmt die Bindung von IgE an den hochaffinen IgE-Rezeptor (FcεRI) auf der Oberfläche von Mastzellen und Basophilen. Die Verringerung des oberflächengebundenen IgE auf FcεRI-tragenden Zellen begrenzt das Ausmaß der Freisetzung von Mediatoren der typischen allergischen Reaktion. Die Behandlung mit Omalizumab reduziert auch die Anzahl der FcεRI-Rezeptoren auf Basophilen bei Atopikern.

Omalizumab bindet an freies IgE mit einer höheren Affinität als IgE selbst an hochaffine FcεRI-Rezeptoren bindet, die auf Basophilen gefunden werden. Daher verringert es die Verfügbarkeit von freiem IgE für die Bindung.

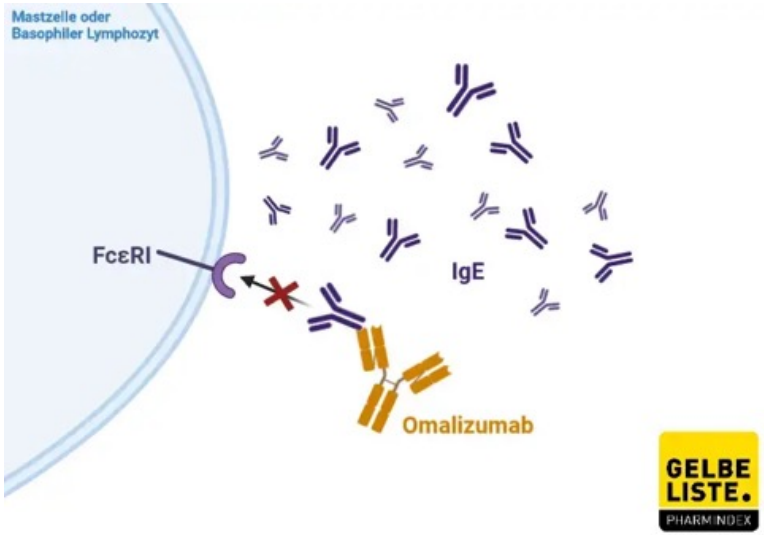

ORIGINAL ARTICLE

Omalizumab for the Treatment of Multiple Food Allergies

Food allergies are common and are associated with substantial morbidity; the only approved treatment is oral immunotherapy for peanut allergy. In this trial, we assessed whether omalizumab, a monoclonal anti-IgE antibody, would be effective and safe as monotherapy in patients with multiple food allergies. Persons 1 to 55 years of age who were allergic to peanuts and at least two other trial-specified foods (cashew, milk, egg, walnut, wheat, and hazelnut) were screened. Inclusion required a reaction to a food challenge of 100 mg or less of peanut protein and 300 mg or less of the two other foods. Participants were randomly assigned, in a 2:1 ratio, to receive omalizumab or placebo administered subcutaneously (with the dose based on weight and IgE levels) every 2 to 4 weeks for 16 to 20 weeks, after which the challenges were repeated. The primary end point was ingestion of peanut protein in a single dose of 600 mg or more without dose-limiting symptoms. The three key secondary end points were the consumption of cashew, of milk, and of egg in single doses of at least 1000 mg each without dose-limiting symptoms. The first 60 participants (59 of whom were children or adolescents) who completed this first stage were enrolled in a 24-week open-label extension.

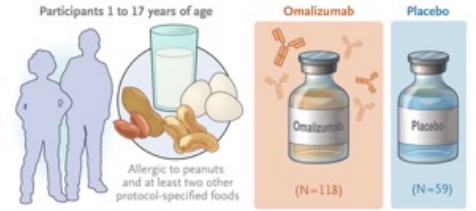

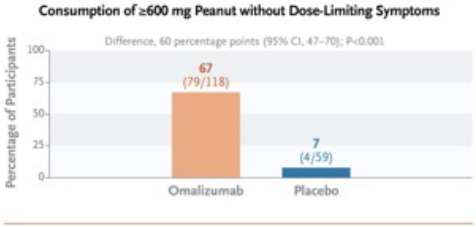

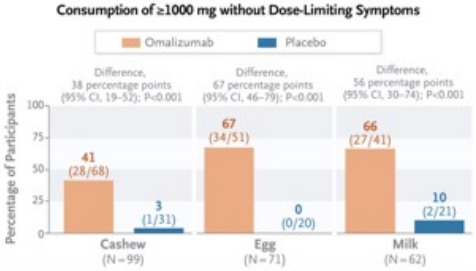

CONCLUSIONS

In children as young as 1 year of age with multiple food allergies, including peanut allergy, omalizumab was superior to placebo in increasing the reaction threshold for peanut and other common food allergens.

Methods

Trial Design and Oversight

OUtMATCH is a double-blind, randomized, placebo-controlled trial that is being conducted at 10 centers in the United States. The trial methods have been published, and the protocol and statistical analysis plan are available with the full text of this article at NEJM.org. The trial includes three stages, but only the first stage, a direct comparison of omalizumab with placebo, has been completed and is reported here. The second stage will compare longer-term (52 weeks) treatment with omalizumab with oral immunotherapy for multiple food allergies, and the third stage will assess the introduction of allergenic foods into the diet for ongoing consumption (minimum, 52 weeks) at home after discontinuation of treatment with omalizumab or oral immunotherapy.

Trial Participants

Persons 1 to 55 years of age with a history of allergy to peanut and at least two other foods in the protocol-specified list (cashew, milk, egg, walnut, wheat, and hazelnut) were screened. If the results of skin-prick and laboratory testing confirmed the food allergies, double-blind, placebo-controlled oral food challenges followed. Each food challenge was given in gradually increasing doses administered at 15-to-30-minute intervals. Eligibility required dose-limiting symptoms, as defined by the Consortium for Food Allergy Research grading scale for acute allergic reactions, after a single dose of 100 mg or less of peanut protein (cumulative amount ingested, 144 mg) and 300 mg or less of the other allergens in the list (cumulative, 444 mg).

End Points

The primary end point was consumption of a single dose of at least 600 mg of peanut protein without dose-limiting symptoms at the completion of the first stage of the trial.

Variable	Omalizumab N=118	Placebo N=59
Male sex — no. (%)	69 (58%)	31 (53%)
Age — yr	6.5 (4.0–11.0)	7.0 (3.5–11.0)
Median total IgE level (IQR) — IU/ml	700 (441–954)	712 (446–1035)
Allergy to peanut — no. of participants	118	59
Median skin-prick test (IQR) — mm†	13.5 (9.0–18.5)	16.0 (10.8–20.5)
Median allergen-specific IgE level (IQR) — kUA/liter‡	72 (23–170)	88 (27–198)
Median maximum tolerated dose (IQR) — mg	30 (10–30)	30 (10–30)
Allergy to cashew — no. of participants	68	31
Median skin-prick test (IQR) — mm	15.0 (10.5–20.0)	16.0 (10.0–22.5)
Median allergen-specific IgE level (IQR) — kUA/liter	31 (16–72)	31 (11–55)
Median maximum tolerated dose (IQR) — mg	10 (3–10)	3 (2–30)
Allergy to egg — no. of participants	51	20
Median skin-prick test (IQR) — mm	12.5 (9.0–18.0)	14.3 (10.0–16.1)
Median allergen-specific IgE level (IQR) — kUA/liter	28 (16–54)	38 (22–97)
Median maximum tolerated dose (IQR) — mg	10 (10–30)	10 (3–30)
Allergy to milk — no. of participants	41	21
Median skin-prick test (IQR) — mm	14.5 (11.0–16.5)	16.5 (10.5–18.0)
Median allergen-specific IgE level (IQR) — kUA/liter	37 (25–93)	32 (15–61)
Median maximum tolerated dose (IQR) — mg	30 (10–100)	10 (10–30)
Allergy to walnut — no. of participants	47	31
Median skin-prick test (IQR) — mm	14.0 (9.5–17.0)	11.5 (7.0–15.5)
Median allergen-specific IgE level (IQR) — kUA/liter	24 (11–63)	25 (9–39)
Median maximum tolerated dose (IQR) — mg	30 (10–100)	30 (10–100)
Allergy to hazelnut — no. of participants	17	7
Median skin-prick test (IQR) — mm	12.0 (9.5–19.5)	4.5 (4.3–9.5)
Median allergen-specific IgE level (IQR) — kUA/liter	18 (10–57)	12 (7–18)
Median maximum tolerated dose (IQR) — mg	3 (3–10)	30 (6–65)
Allergy to wheat — no. of participants	12	8
Median skin-prick test (IQR) — mm	9.3 (8.4–13.0)	11.3 (10.0–13.0)
Median allergen-specific IgE level (IQR) — kUA/liter	38 (22–96)	38 (20–79)
Median maximum tolerated dose (IQR) — mg	100 (25–100)	20 (8–100)

Successful Consumption of Prespecified Threshold Dose at Week 16.

End Point and Food Challenge	No. of Participants	Omalizumab	Placebo	Difference (95% CI)	P Value
		no./total no. (%)		*percentage points*	
Primary end point†					
Peanut	177	79/118 (67)	4/59 (7)	60 (47 to 70)	<0.001
Key secondary end points‡					
Cashew	99	28/68 (41)	1/31 (3)	38 (19 to 52)	<0.001
Egg	71	34/51 (67)	0/20 (0)	67 (46 to 79)	<0.001
Milk	62	27/41 (66)	2/21 (10)	56 (30 to 74)	<0.001
Other secondary end points‡					
Walnut	78	30/47 (64)	4/31 (13)	51 (27 to 68)	—
Hazelnut	24	11/17 (65)	1/7 (14)	50 (−2 to 78)	—
Wheat	20	9/12 (75)	1/8 (13)	63 (13 to 88)	—

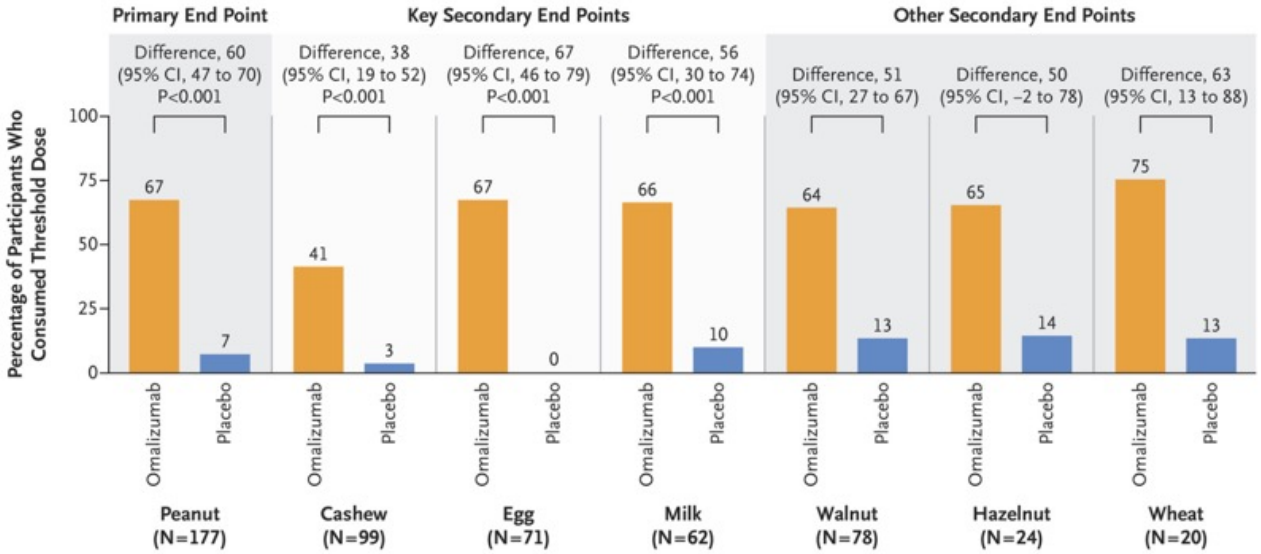

Successful Consumption of Prespecified Threshold Dose at Week 16.
Shown are the percentages of participants in the two groups who consumed the prespecified threshold doses without dose-limiting symptoms during food challenges at the end of the first stage of the trial; these food challenges were started at week 16 and were conducted during separate visits spanning up to a 4-week period. The prespecified threshold dose of peanut protein was a single dose of at least 600 mg; for cashew, egg, milk, walnut, hazelnut, and wheat protein, the prespecified threshold was a single dose of at least 1000 mg. The 95% confidence intervals for the differences were calculated with the use of exact unconditional confidence limits. The P values for the primary and key secondary end points are unadjusted, two-sided values derived from Fisher's exact test.

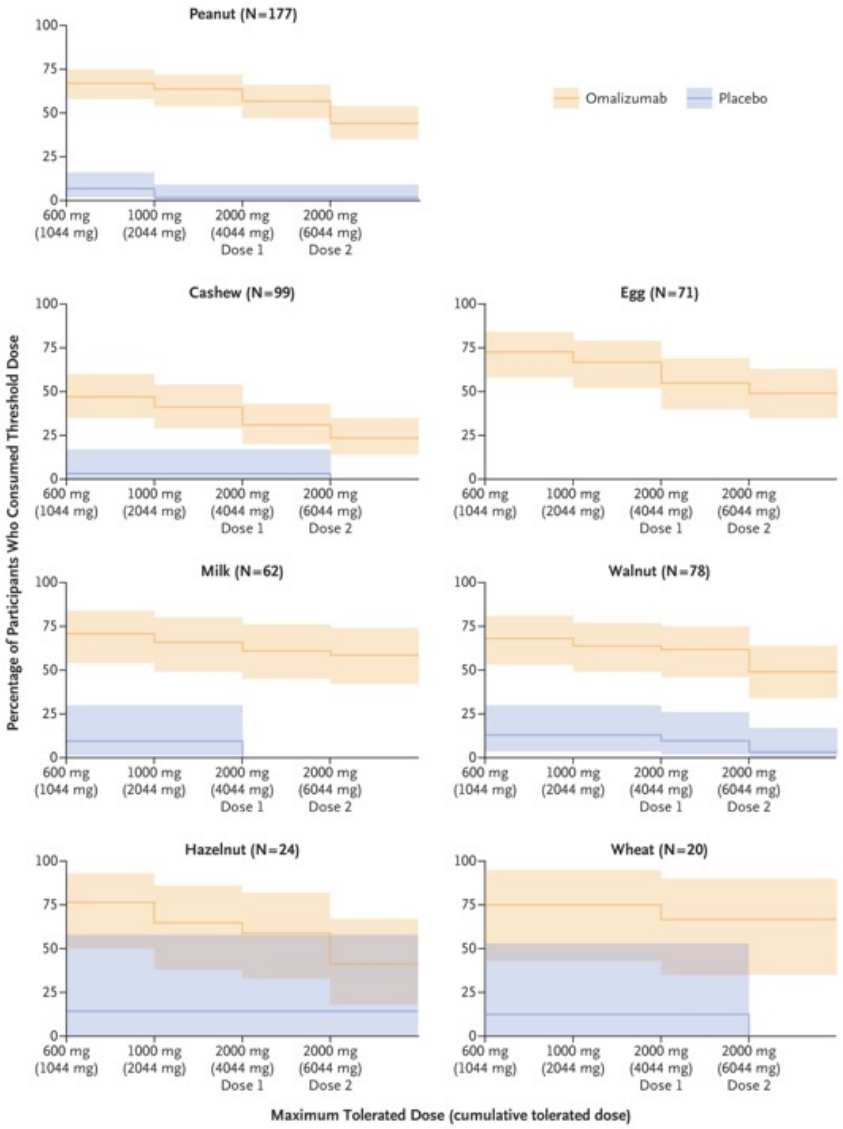

Successful Consumption of Prespecified Secondary End-Point Doses at Week 16.

Shown are the percentages of participants in the two groups who consumed the prespecified threshold doses and the cumulative doses without dose-limiting symptoms. The 95% confidence intervals for each group were calculated with the use of exact confidence limits, which are based on a score statistic. The food challenges at the end of the first stage of the trial were started at week 16 and were conducted during separate visits spanning up to a 4-week period.

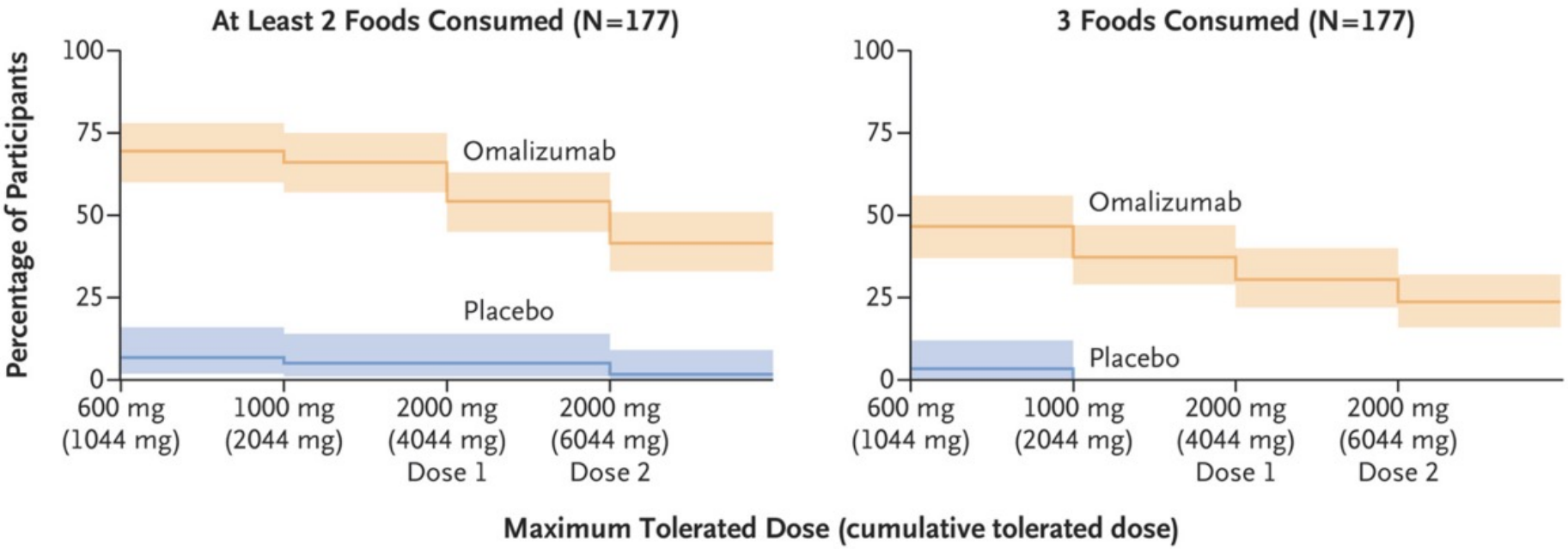

Successful Consumption of Multiple Foods at Prespecified Secondary End-Point Doses at Week 16.
Shown are the percentages of participants who consumed prespecified doses and cumulative doses of at least two foods and of all three foods without dose-limiting symptoms. The 95% confidence intervals for each group were calculated with the use of exact confidence limits, which are based on a score statistic. The food challenges at the end of the first stage of the trial were started at week 16 and were conducted during separate visits spanning up to a 4-week period.

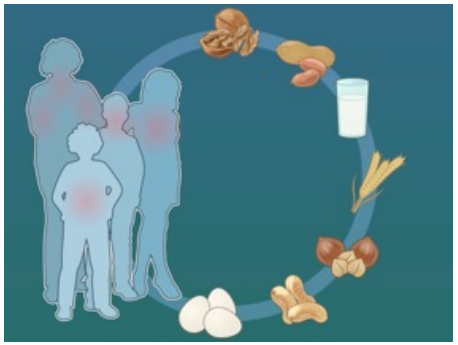

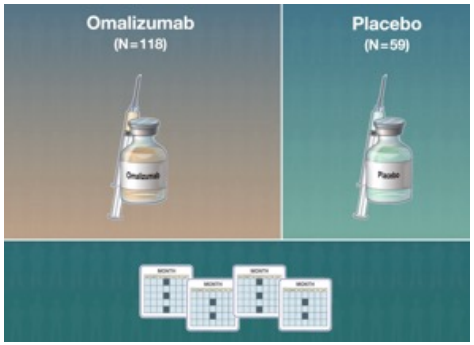

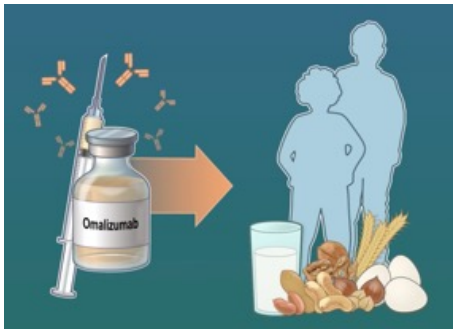

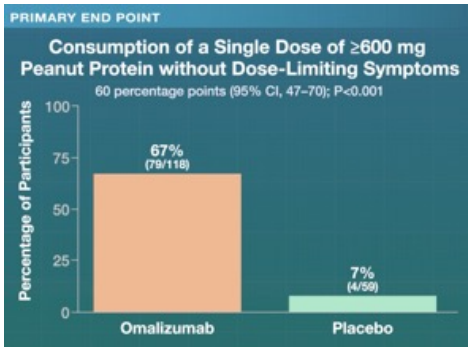

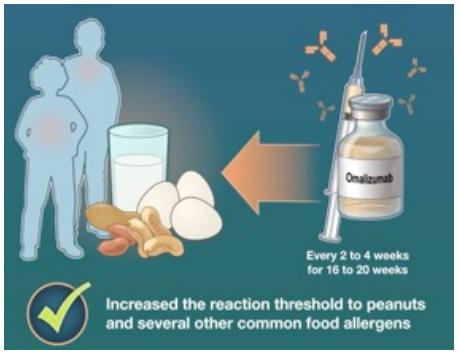

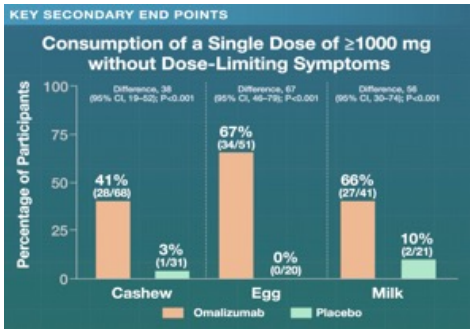

LIMITATIONS AND REMAINING QUESTIONS

- The cohort comprised mostly non-Hispanic and White children, which limits the generalizability of the findings.
- Patients with high baseline IgE levels were excluded.

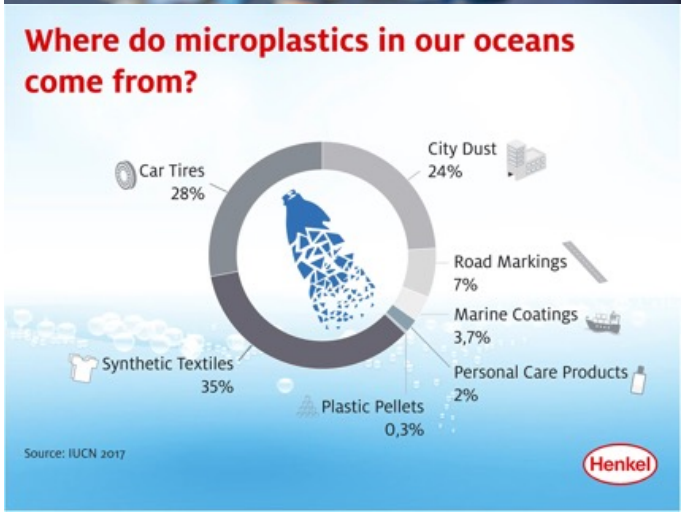
Where do microplastics in our oceans come from?
Car Tires 28%
City Dust 24%
Road Markings 7%
Marine Coatings 3,7%
Personal Care Products 2%
Plastic Pellets 0,3%
Synthetic Textiles 35%
Source: IUCN 2017
Henkel

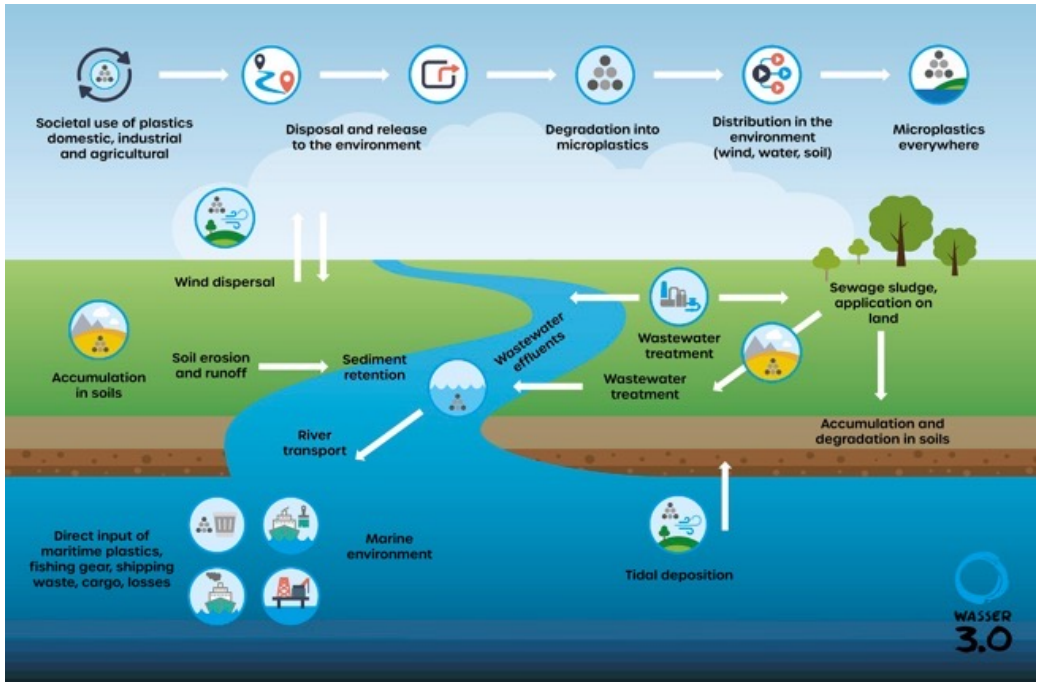
Societal use of plastics domestic, industrial and agricultural
Disposal and release to the environment
Degradation into microplastics
Distribution in the environment (wind, water, soil)
Microplastics everywhere
Wind dispersal
Accumulation in soils
Soil erosion and runoff
Sediment retention
Wastewater effluents
Wastewater treatment
Wastewater treatment
Sewage sludge, application on land
River transport
Accumulation and degradation in soils
Direct input of maritime plastics, fishing gear, shipping waste, cargo, losses
Marine environment
Tidal deposition
WASSER 3.0

ORIGINAL ARTICLE

Microplastics and Nanoplastics in Atheromas and Cardiovascular Events

Background

Microplastics and nanoplastics (MNPs) are emerging as a potential risk factor for cardiovascular disease in preclinical studies. Direct evidence that this risk extends to humans is lacking.

Methods

We conducted a prospective, multicenter, observational study involving patients who were undergoing carotid endarterectomy for asymptomatic carotid artery disease. The excised carotid plaque specimens were analyzed for the presence of MNPs with the use of pyrolysis–gas chromatography–mass spectrometry, stable isotope analysis, and electron microscopy. Inflammatory biomarkers were assessed with enzyme-linked immunosorbent assay and immunohistochemical assay. The primary end point was a composite of myocardial infarction, stroke, or death from any cause among patients who had evidence of MNPs in plaque as compared with patients with plaque that showed no evidence of MNPs.

Conclusions

In this study, patients with carotid artery plaque in which MNPs were detected had a higher risk of a composite of myocardial infarction, stroke, or death from any cause at 34 months of follow-up than those in whom MNPs were not detected.

Several studies have shown that microplastics and nanoplastics (MNPs) enter the human body through ingestion, inhalation, and skin exposure, where they interact with tissues and organs. MNPs have been found in selected human tissues, such as the placenta, lungs, and liver, as well as in breast milk, urine, and blood. Recent studies performed in preclinical models have led to the suggestion of MNPs as a new risk factor for cardiovascular diseases. Data from in vitro studies suggest that specific MNPs promote oxidative stress, inflammation, and apoptosis in endothelial and other vascular cells; animal models support a role for MNPs in altered heart rate, cardiac-function impairment, myocardial fibrosis, and endothelial dysfunction. However, the clinical relevance of these findings is unknown. Evidence is lacking to show that MNPs infiltrate vascular lesions in humans or to support an association between the burden of MNPs and cardiovascular disease.

To explore whether MNPs are detectable within atherosclerotic plaque and whether the burden of MNPs is associated with cardiovascular disease, we assessed the presence of these substances in surgically excised carotid artery plaque by means of pyrolysis–gas chromatography–mass spectrometry, stable isotope analysis, and electronic microscopy. We then determined whether the presence of MNPs was associated with a composite end point of myocardial infarction, stroke, or death from any cause.

Methods

Study Design

We performed a prospective, multicenter, observational study in which patients were assigned to groups (one group with plaque in which MNPs were detected and one group with plaque in which MNPs were not detected) after enrollment. Patients were recruited from Hospital Cardarelli, Ospedale del Mare, and the University of Salerno from August 1, 2019, to July 31, 2020. Consecutive patients with asymptomatic carotid artery stenosis (as classified by the North American Symptomatic Carotid Endarterectomy Trial) for whom intervention was indicated were screened for this study. A total of 447 consecutive patients were approached to participate, and 312 agreed to undergo screening.

Patients

Patients were eligible if they were 18 to 75 years of age, had asymptomatic extracranial high-grade (>70%) internal carotid artery stenosis, and were scheduled to undergo carotid endarterectomy. Exclusion criteria were evidence of heart failure, valvular defects, malignant neoplasms, or secondary causes of hypertension. Patients with complications in the postoperative period before discharge, who had incomplete data, or who were lost during follow-up were excluded from the analysis.

End Points

The primary end point was a composite of nonfatal myocardial infarction, nonfatal stroke, or death from any cause among patients with plaque containing MNPs and patients with plaque that did not contain those substances. Secondary end points included levels of tissue biomarkers interleukin-18, interleukin-1β, tumor necrosis factor α (TNF-α), interleukin-6, CD68, CD3, and collagen in patients with evidence of MNPs as compared with those without.

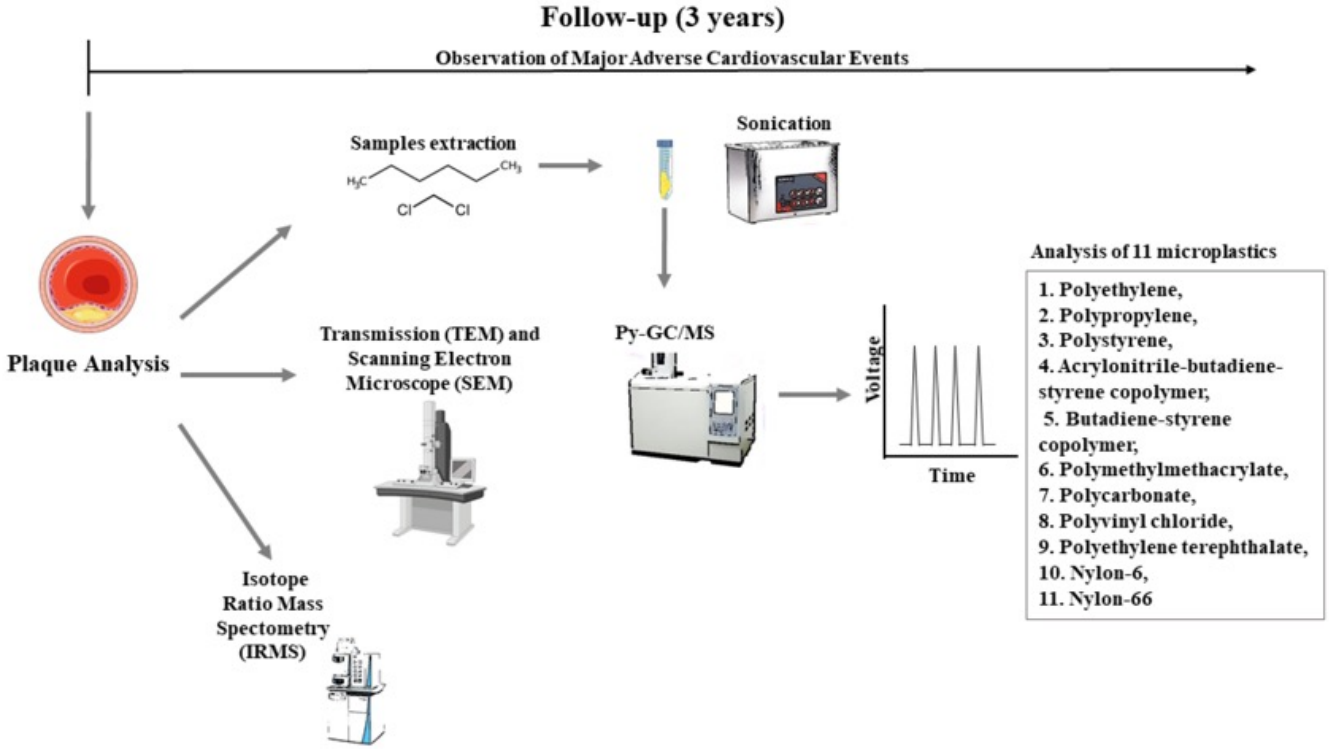

Consecutive patients unergoing carotid endarterectomy were enrolled in the study. After enrollment and during follow-up, specimens of the carotid bifurcation region were studied through Py-GC/MS to quantify 11 different microplastics. Samples from 10 patients were also analyzed by electron microscopy (SEM and TEM) while 26 specimens were analyzed by stable isotope analysis. Patients included in the study were followed to monitor the incidence of non-fatal myocardial infarction, non-fatal stroke, and all-cause mortality for 3 years. Patients were divided into two groups for analysis of clinical outcomes: those with or without evidence of MNPs within the plaque.

A

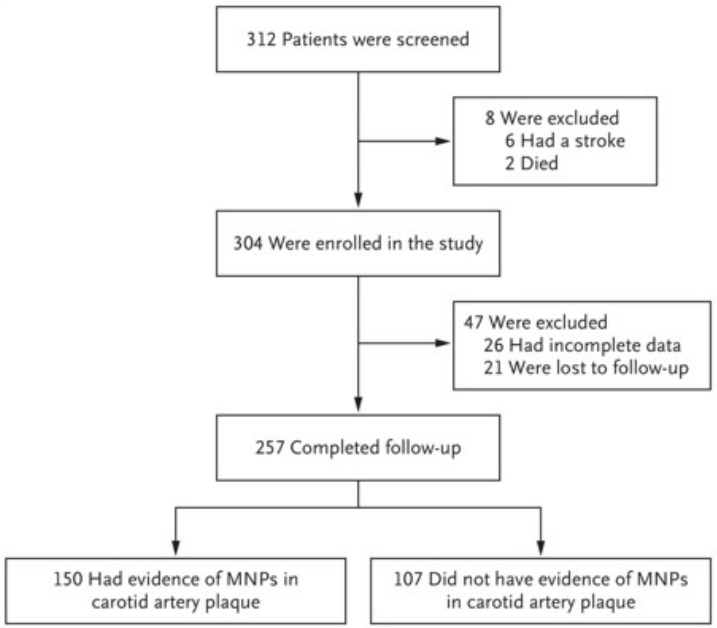

B

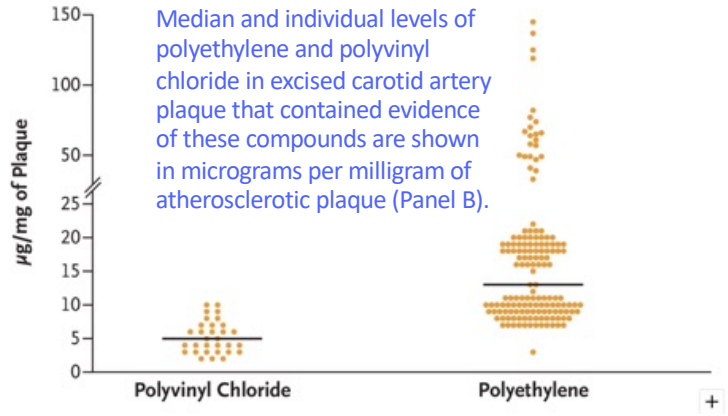

Median and individual levels of polyethylene and polyvinyl chloride in excised carotid artery plaque that contained evidence of these compounds are shown in micrograms per milligram of atherosclerotic plaque (Panel B).

Variable	MNPs Present (N=150)	MNPs Not Present (N=107)
Age (IQR) — yr	71 (65–75)	73 (67–77)
Male sex — no. (%)	116 (77.3)	79 (73.8)
Body-mass index (IQR)†	28 (27–29)	28 (26–29)
Hypertension — no. (%)	78 (52.0)	69 (64.5)
Systolic blood pressure (IQR) — mm Hg	124 (118–130)	127 (118–129)
Diastolic blood pressure (IQR) — mm Hg	78 (75–83)	77 (75–85)
Heart rate (IQR) — beats/min	85 (79–91)	81 (76–86)
Stenosis severity (IQR) — %	77 (73–83)	78 (73–83)
Diabetes — no. (%)	36 (24.0)	32 (29.9)
Cardiovascular disease — no. (%)‡	50 (33.3)	35 (32.7)
Dyslipidemia — no. (%)	55 (36.7)	40 (37.4)
Total cholesterol (IQR) — mg/dl	150 (145–158)	147 (139–158)
LDL cholesterol (IQR) — mg/dl	77 (69–84)	74 (69–82)
HDL cholesterol (IQR) — mg/dl	42 (40–43)	42 (40–44)
Triglycerides (IQR) — mg/dl	178 (165–192)	182 (163–193)
Creatinine (IQR) — mg/dl	1.00 (0.90–1.10)	0.96 (0.96–1.06)
Smoker — no. (%)	24 (16.0)	17 (15.9)
Medication use — no. (%)		
Beta-blockers	48 (32.0)	35 (32.7)
ACE inhibitors	75 (50)	53 (49.5)
ARBs	35 (23.3)	31 (29.0)
Calcium-channel blockers	13 (8.7)	8 (7.5)
Diuretics	17 (11.3)	16 (15.0)
Heparin	12 (8.0)	10 (9.3)
Antiplatelet drugs	146 (97.3)	105 (98.1)
Statin	143 (95.3)	101 (94.4)
Ezetimibe	26 (17.3)	20 (18.7)

Proportion of individuals with MNPs among different centers of recruitment (A) and areas of living (B). Histograms

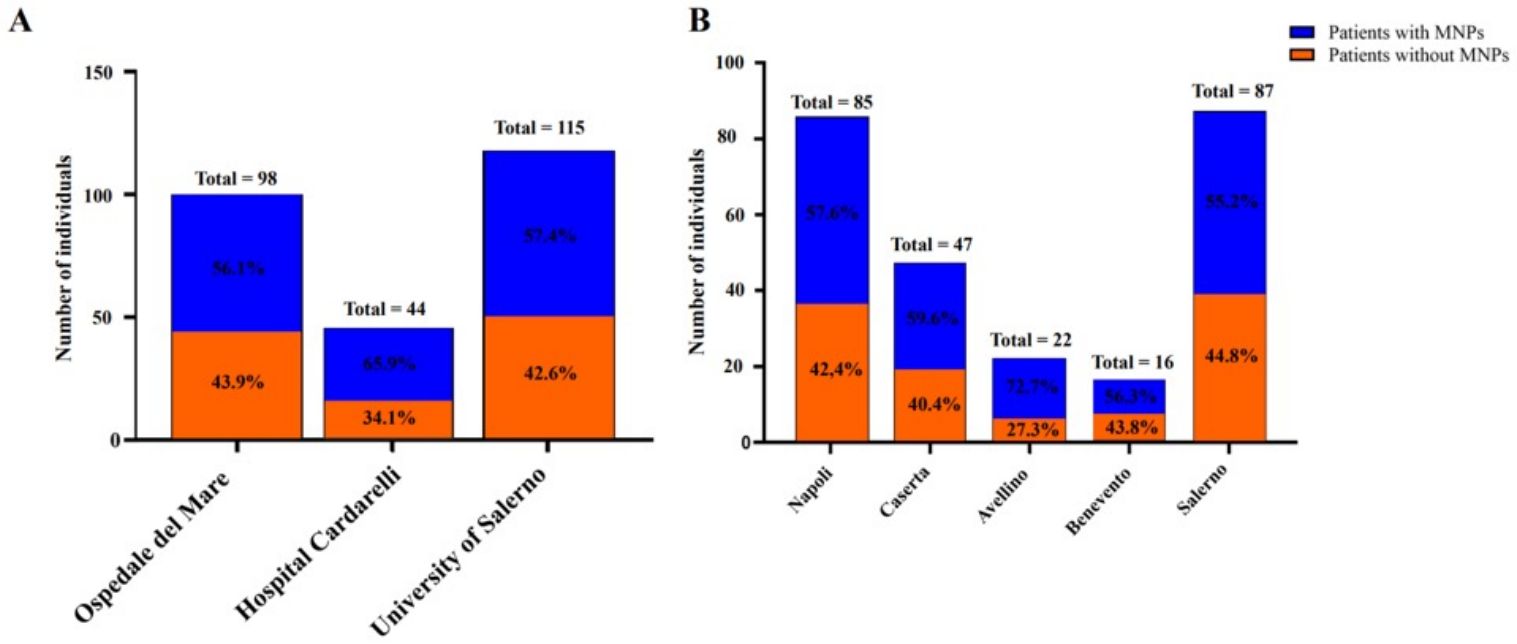

Histograms shows the number and percentage of patients with our without evidence of micronanoplastics (MNP)s within the plaque among the 3 centers that recruited patients for the study (A) or according to the patients' area of living (B). No apparent differences between the groups were observed for either the recruitment center or the patient's area of living according to Fisher's exact test.

Lower magnification of the trasmission electron microscopy (TEM) image of the atheroma showing living cells with vacuoles dispersed in the plaque.

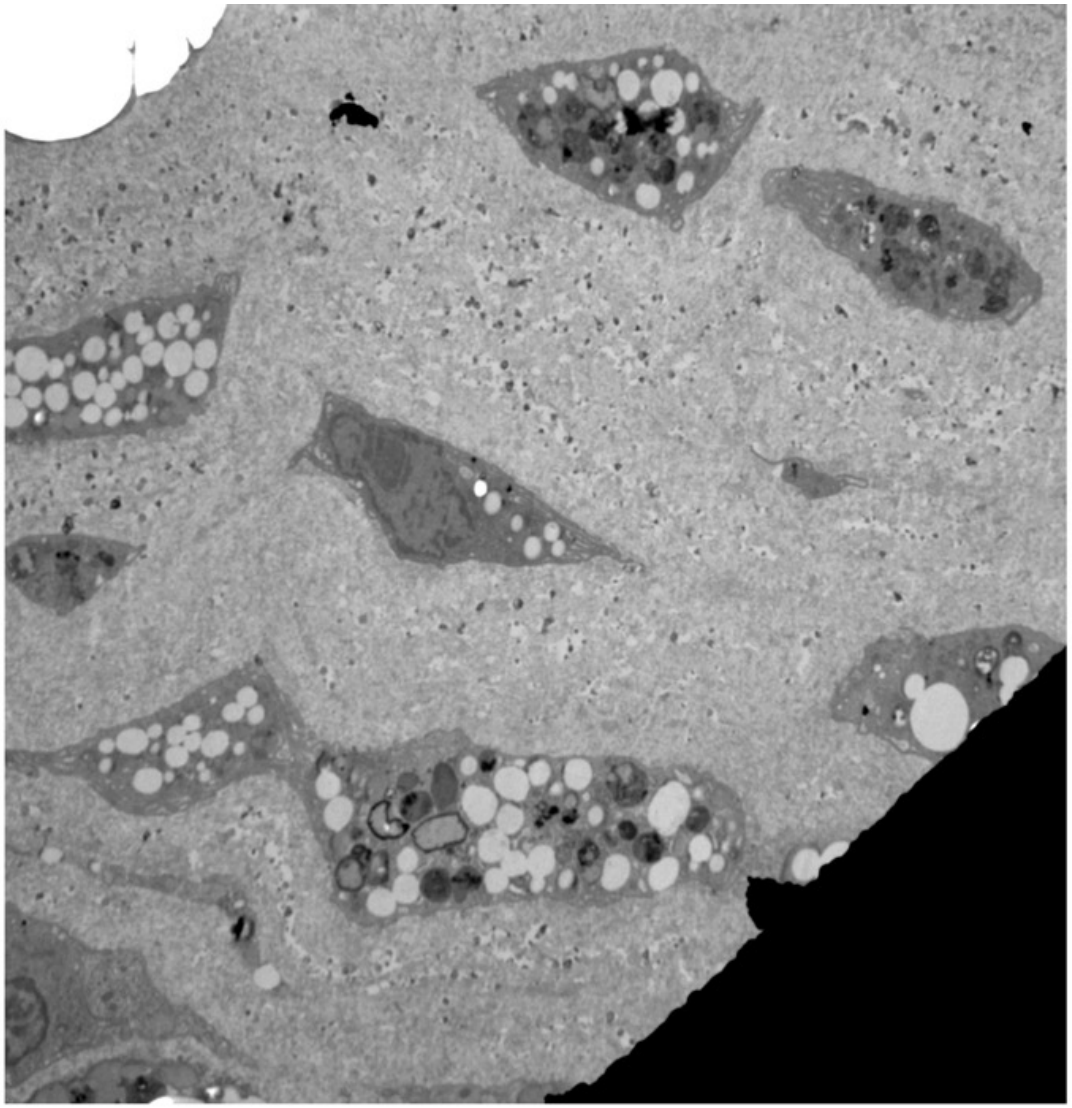

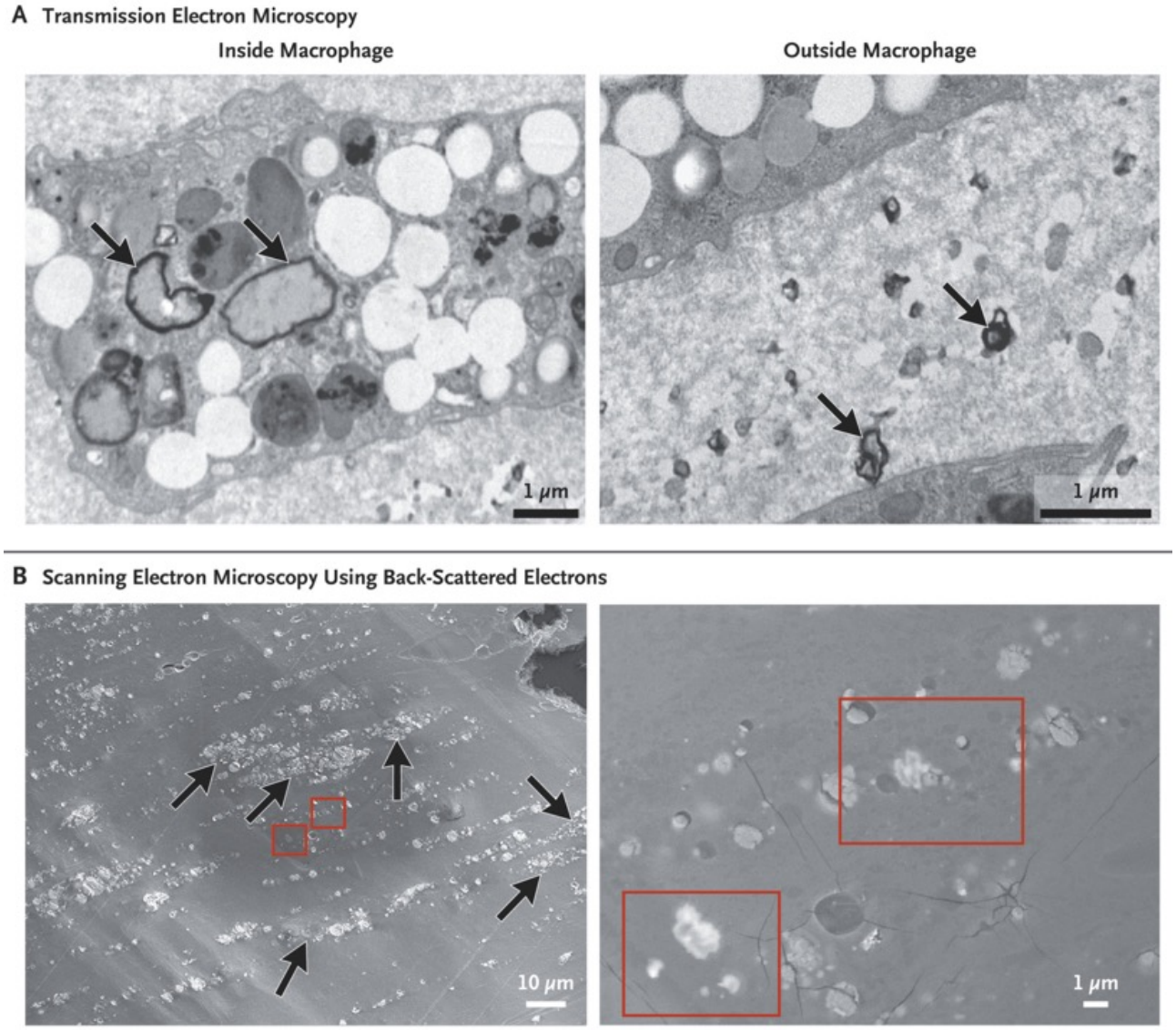

Electron Microscopy Analysis of Atheromatous Plaque.
Panel A shows transmission electron microscopy images of particles of high internal electron transparency contoured by a very thin electron opaque line. These particles do not resemble usual organic material owing to their particularly irregular shape. These particles (arrows) were detected inside living macrophages and outside in the amorphous material of the plaque (arrows). Panel B shows images of the same specimen obtained with scanning electron microscopy using back-scattered electrons, which showed macrophages dispersed in the amorphous plaque material (arrows) and small particles of low-reflecting material contoured by a thin line of high-reflecting material identified in the plaque (red boxes).

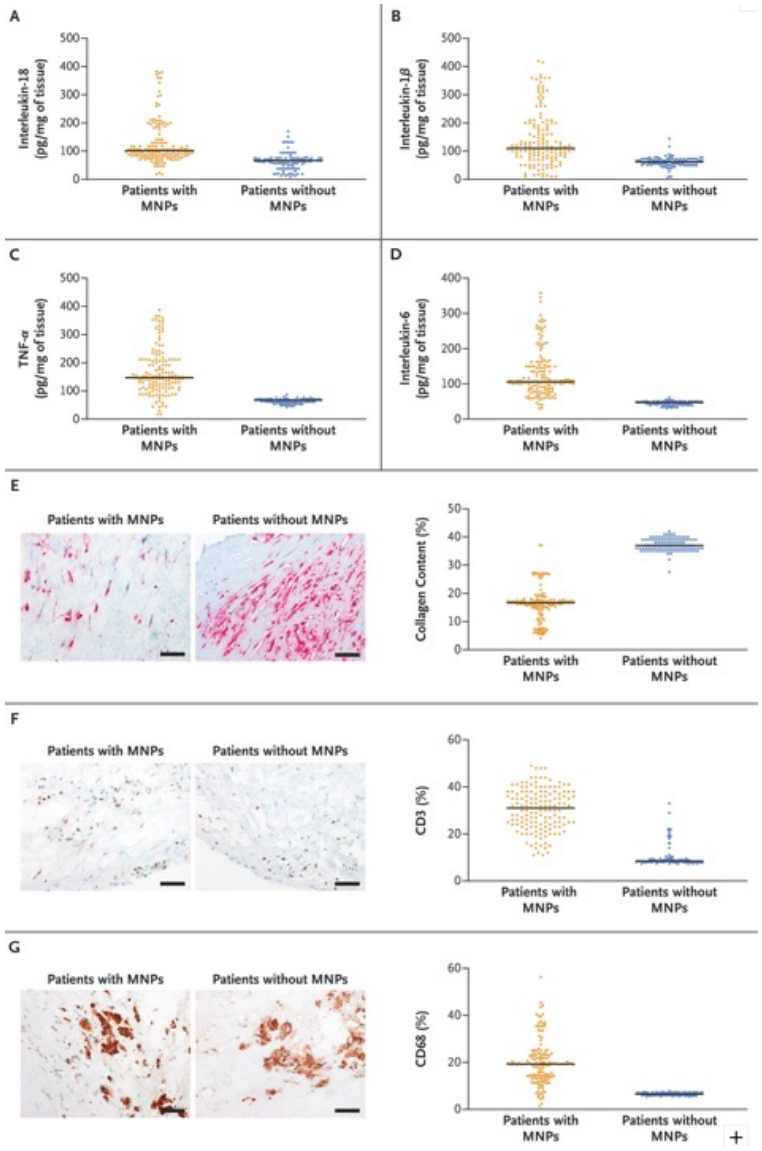

Inflammatory Markers in Plaque Samples.
Panels A through D show the abundance of interleukin-18, interleukin-1β, tumor necrosis factor α (TNF-α), and interleukin-6, respectively, assessed by means of enzyme-linked immunosorbent assay. Panels E, F, and G show the abundance of collagen, CD3, and CD68, respectively, measured by immunohistochemical assay in the group of patients with evidence of MNPs within the plaque and the group with no evidence of MNPs. Medians and individual values are shown.

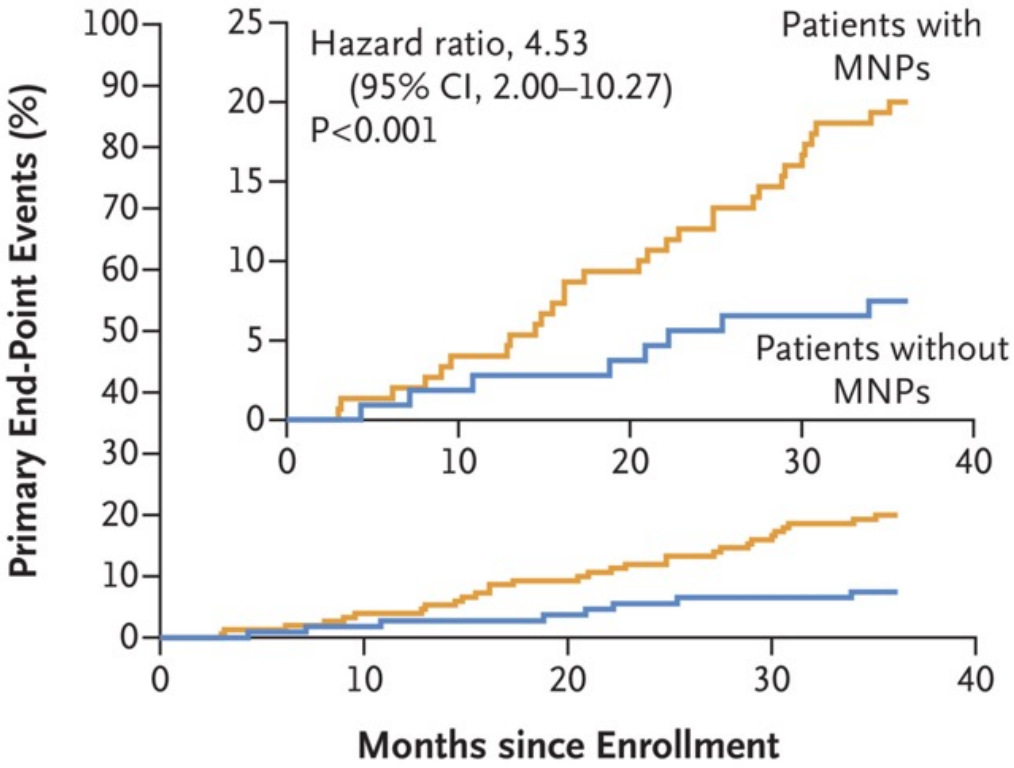

Associations between the Presence of MNPs and Cardiovascular Events.
Shown is the cumulative incidence curve of the composite outcome — nonfatal stroke, nonfatal myocardial infarction, or death from any cause. The results were estimated with the use of Cox regression analysis with adjustment for age, sex, body-mass index, total cholesterol, high-density lipoprotein cholesterol, low-density lipoprotein cholesterol, triglycerides, creatinine, diabetes, hypertension, and previous cardiovascular events in the group of patients with evidence of MNPs in plaque and the group of patients with no evidence of MNPs in plaque. The inset shows the same data on an expanded y axis.

Discussion

Among patients with asymptomatic high-grade (>70%) carotid artery stenosis who were undergoing carotid endarterectomy, those with evidence of MNPs within the carotid plaque had a greater incidence of a composite of myocardial infarction, stroke, or death from any cause than patients who did not have evidence of MNPs within the atheroma. Observational data from occupational-exposure studies suggest an increased risk of cardiovascular disease among persons who are exposed to plastics-related pollution, including polyvinyl chloride, than that seen in the general population. Mechanistic data from preclinical models has proposed both direct translocation of MNPs into the circulation and indirect mechanisms as possible underpinnings of the cardiovascular toxic effects observed with MNPs, as has been noted with other nanoparticles such as inhaled gold nanoparticles of similar size to MNPs. A range of studies in mice and rats showed a wide distribution of MNPs after both inhalation and ingestion, with consistent accumulations in highly vascularized organs and the heart. Particle size influences the ability of MNPs to reach multiple tissues. According to a World Health Organization statement, MNPs larger than 150 µm or 10 µm in diameter, respectively, are not absorbed into blood and do not penetrate blood vessels. Our findings suggest that nanoplastics, rather than microplastics, might accumulate in sites of atherosclerosis. Indeed, the large majority of particles detected in the current study were also below the 200-nm threshold suggested for gut and other barriers and were visible in the extracellular space as scattered debris, which aligns with the notion that the absorption and distribution of MNPs increase as particle size decreases. Data from studies in humans have shown that MNPs of up to 30 µm in size have been detected in liver samples, up to 10 µm in placenta samples, up to 88 µm in lung samples, up to 12 to 15 µm in breast milk and urine, and more than 700 nm in whole blood.

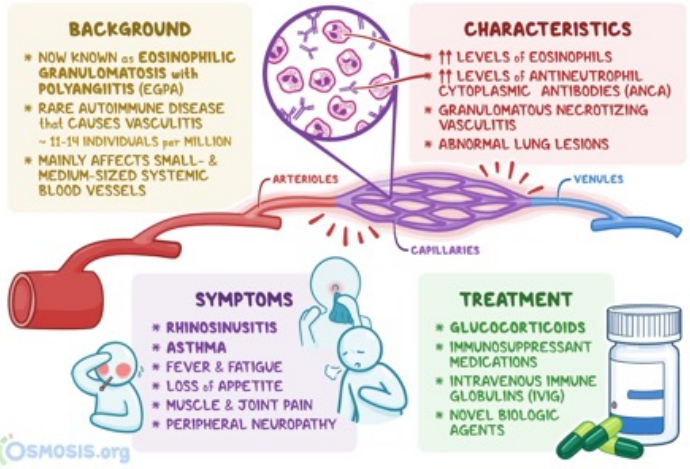
BACKGROUND
* NOW KNOWN as EOSINOPHILIC GRANULOMATOSIS with POLYANGIITIS (EGPA)
* RARE AUTOIMMUNE DISEASE that CAUSES VASCULITIS
~ 11-14 INDIVIDUALS per MILLION
* MAINLY AFFECTS SMALL- & MEDIUM-SIZED SYSTEMIC BLOOD VESSELS
CHARACTERISTICS
↑↑ LEVELS of EOSINOPHILS
↑↑ LEVELS of ANTINEUTROPHIL CYTOPLASMIC ANTIBODIES (ANCA)
* GRANULOMATOUS NECROTIZING VASCULITIS
* ABNORMAL LUNG LESIONS
ARTERIOLES
VENULES
CAPILLARIES
SYMPTOMS
* RHINOSINUSITIS
* ASTHMA
* FEVER & FATIGUE
* LOSS of APPETITE
* MUSCLE & JOINT PAIN
* PERIPHERAL NEUROPATHY
TREATMENT
* GLUCOCORTICOIDS
* IMMUNOSUPPRESSANT MEDICATIONS
* INTRAVENOUS IMMUNE GLOBULINS (IVIG)
* NOVEL BIOLOGIC AGENTS
OSMOSIS.org

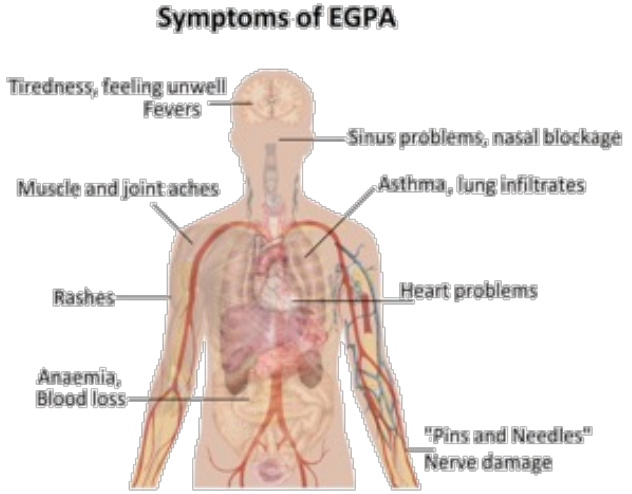
Symptoms of EGPA
Tiredness, feeling unwell
Fevers
Sinus problems, nasal blockage
Muscle and joint aches
Asthma, lung infiltrates
Rashes
Heart problems
Anaemia,
Blood loss
"Pins and Needles"
Nerve damage

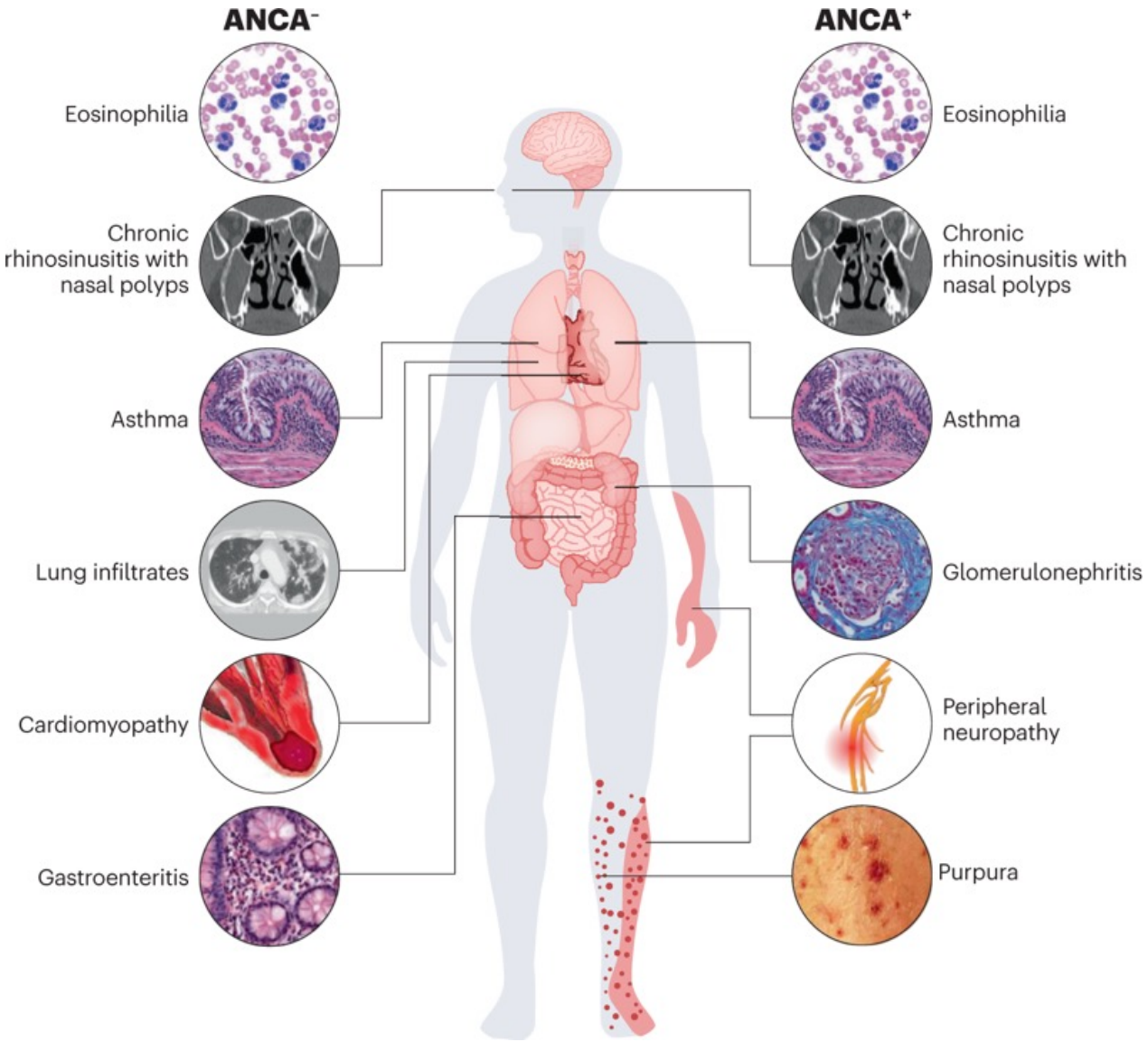
ANCA⁻
ANCA⁺
Eosinophilia
Chronic rhinosinusitis with nasal polyps
Asthma
Lung infiltrates
Cardiomyopathy
Gastroenteritis
Eosinophilia
Chronic rhinosinusitis with nasal polyps
Asthma
Glomerulonephritis
Peripheral neuropathy
Purpura

Benralizumab ist ein humanisierter monoklonaler Antikörper zur Behandlung von schwerem eosinophilem Asthma.

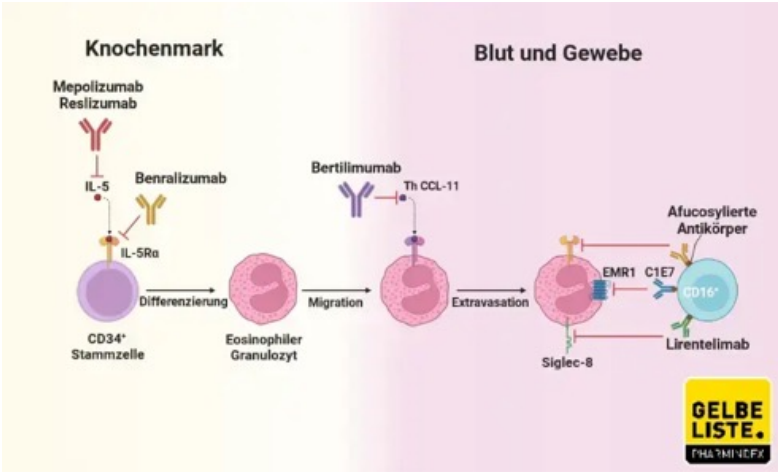

Wirkmechanismus

Benralizumab ist ein anti-eosinophiler, humanisierter, afucosylierter, monoklonaler Immunglobulin G1 (IgG1)-Antikörper, der hochaffin und spezifisch an die Alpha-Untereinheit des menschlichen Interleukin-5-Rezeptors (IL-5Rα) bindet. IL-5R wird spezifisch auf der Oberfläche von Eosinophilen und Basophilen exprimiert. Durch das Fehlen von Fucose im Fc-Bereich von Benralizumab hat der Arzneistoff eine hohe Affinität zu FcγRIII-Rezeptoren auf Immuneffektorzellen. Dazu gehören die natürlichen Killerzellen (NK-Zellen). Eine dadurch verstärkte antikörperabhängige zellvermittelte Zytotoxizität (ADCC) führt zur Apoptose von Eosinophilen und Basophilen und folglich zu einer Reduktion der eosinophilen Entzündung.

Mepolizumab

Mepolizumab ist ein humanisierter monoklonaler Antikörper, der mit hoher Affinität und Spezifität an humanes Interleukin 5 (IL-5) bindet.

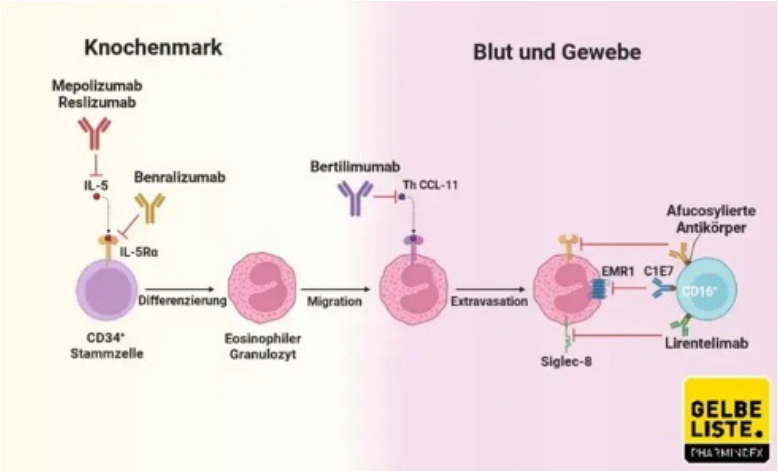

Wirkmechanismus

Mepolizumab bindet spezifisch an das Zytokin Interleukin-5 (IL-5) und neutralisiert dieses. Infolgedessen wird die Interaktion zwischen IL-5 und dem IL-5-Rezeptor (IL-5Rα) unterbunden, die für die Differenzierung, Reifung, Rekrutierung und Aktivierung von humanen Eosinophilen elementar ist. Dadurch wird die Überlebensrate und Aktivität von Eosinophilen reduziert.

In der Pathogenese von eosinophilem Asthma spielen Th2-Zellen eine Schlüsselrolle. Diese differenzieren sich aus naiven T-Helferzellen unter IL-4-Einfluss und produzieren neben IL-5 unter anderem auch die Zytokine IL-4 und IL-13. Während die Zytokine IL-4 und IL-13 in B-Zellen die Bildung von IgE-Antikörpern stimulieren, vermittelt IL-5 die Differenzierung, Reifung, Rekrutierung und Aktivierung von humanen Eosinophilen. Aus diesem Grund stellt die IL-5/IL-5R-Interaktion ein vielversprechendes Target bei eosinophilem Asthma dar.

ORIGINAL ARTICLE

Benralizumab versus Mepolizumab for Eosinophilic Granulomatosis with Polyangiitis

Eosinophilic granulomatosis with polyangiitis (EGPA) is a vasculitis characterized by eosinophilic inflammation. Benralizumab, a monoclonal antibody against the interleukin-5α receptor expressed on eosinophils, may be an option for treating EGPA. We conducted a multicenter, double-blind, phase 3, randomized, active-controlled noninferiority trial to evaluate the efficacy and safety of benralizumab as compared with mepolizumab. Adults with relapsing or refractory EGPA who were receiving standard care were randomly assigned in a 1:1 ratio to receive benralizumab (30 mg) or mepolizumab (300 mg) subcutaneously every 4 weeks for 52 weeks. The primary end point was remission at weeks 36 and 48 (prespecified noninferiority margin, –25 percentage points). Secondary end points included the accrued duration of remission, time to first relapse, oral glucocorticoid use, eosinophil count, and safety.

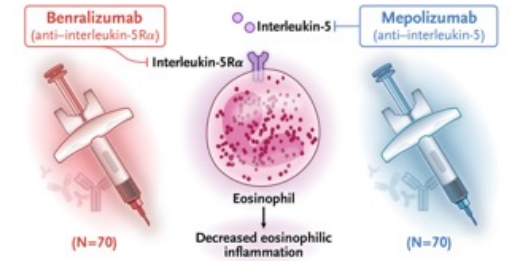

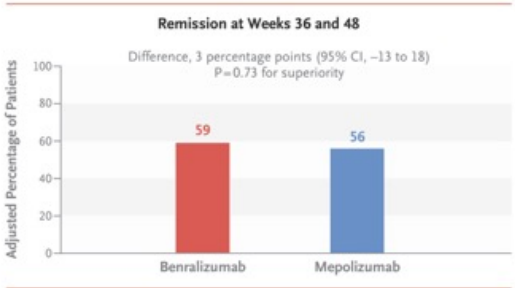

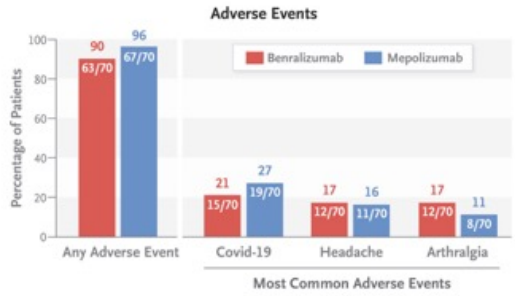

CONCLUSIONS

Benralizumab was noninferior to mepolizumab for the induction of remission in patients with relapsing or refractory EGPA who were receiving standard care.

Eosinophilic granulomatosis with polyangiitis (EGPA) is a rare inflammatory disorder characterized by asthma, necrotizing vasculitis, extravascular granulomas, and blood and tissue eosinophilia. Oral glucocorticoids and immunosuppressive drugs have long been the cornerstone of treatment for EGPA, despite burdensome side effects. Although not formally approved for EGPA, treatment with either cyclophosphamide or rituximab has been recommended to induce remission in severe cases, and azathioprine, methotrexate, and mycophenolate mofetil help to maintain remission. However, although prolonged treatment with oral glucocorticoids reduces the risk of relapse, it is associated with progressive toxic effects. Relapse is also common during oral glucocorticoid tapering, and patients are often unable to fully discontinue treatment.

Benralizumab is a humanized, afucosylated monoclonal antibody with high affinity and specificity for the human interleukin-5 receptor α subunit (interleukin-5Rα) expressed on eosinophil, and is approved for the treatment of severe eosinophilic asthma.

Methods

Trial Design

We conducted the MANDARA trial, a double-blind, 52-week, phase 3, randomized, active-controlled, noninferiority head-to-head trial with an open-label extension of at least 1 year in duration, at 50 sites across nine countries. Eligible patients were randomly assigned in a 1:1 ratio to receive benralizumab (30 mg in one injection) or mepolizumab (300 mg in three injections of 100 mg each) administered subcutaneously every 4 weeks for 52 weeks.

Participants and Eligibility Criteria

Adults (≥18 years of age) were eligible to participate if they had an EGPA diagnosis based on medical history or the presence of asthma and blood eosinophilia (eosinophil count of $>1.0\times10^9$ per liter, >10%, or both) plus at least two additional features of EGPA and a history of relapsing or refractory disease despite therapy with oral glucocorticoids at a dose of 7.5 to 50.0 mg of prednisolone per day or equivalent (a stable dose for ≥4 weeks before baseline), with or without stable immunosuppressive therapy.

End Points

The primary end point was remission (defined as a BVAS of 0 and an oral glucocorticoid dose of ≤4 mg per day) at weeks 36 and 48. European League against Rheumatism (EULAR)–defined remission (BVAS of 0 and oral glucocorticoid dose of ≤7.5 mg per day) was examined in a supportive analysis, and an indirect, per-protocol comparison with a historic placebo group from the previous trial of mepolizumab in EGPA was also performed.

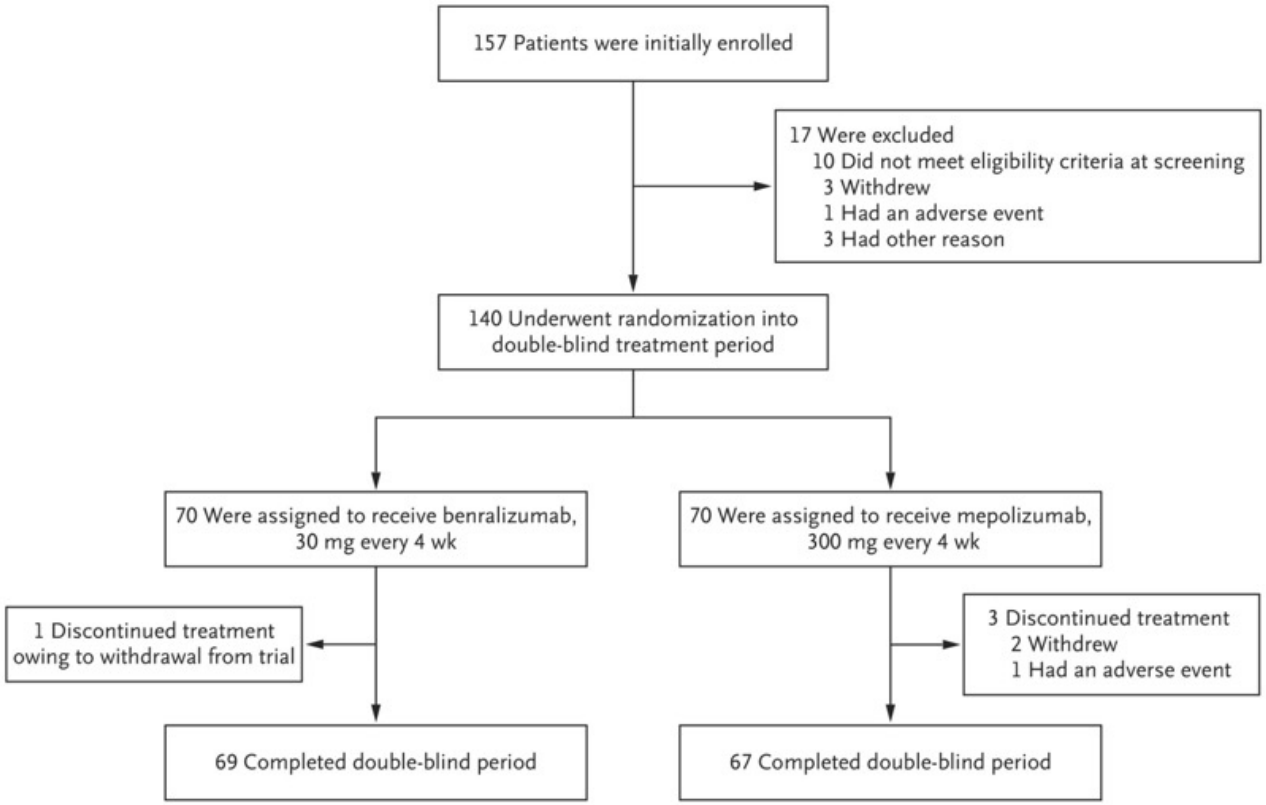

Characteristic	Benralizumab (N=70)	Mepolizumab (N=70)	Total (N=140)
Age — yr	52.0±13.9	52.7±14.4	52.3±14.1
Median (range)	55.0 (20–76)	55.0 (19–79)	55.0 (19–79)
Female sex — no. (%)	45 (64)	39 (56)	84 (60)
Region — no. (%)			
North America	16 (23)	16 (23)	32 (23)
Japan	4 (6)	4 (6)	8 (6)
Rest of the world	50 (71)	50 (71)	100 (71)
EGPA disease type — no. (%)			
Relapsing	45 (64)	48 (69)	93 (66)
Refractory	42 (60)	42 (60)	84 (60)
Relapsing and refractory	18 (26)	20 (29)	38 (27)
Time since diagnosis of EGPA — yr	5.39±5.38	4.93±5.92	5.16±5.64
Range	0.6–24.0	0.1–38.0	0.1–38.0
ANCA-positive status — no. (%)			
At screening†	7 (10)	7 (10)	14 (10)
At screening or historic	18 (26)	22 (31)	40 (29)
Blood eosinophil count/μl‡	306.0±225.0	384.9±563.6	345.4±429.4
Median (range)	240 (30–920)	225 (0–3830)	230 (0–3830)
EGPA disease characteristics — no. (%)			
Asthma	70 (100)	70 (100)	140 (100)
Blood eosinophilia	70 (100)	70 (100)	140 (100)
Biopsy evidence of eosinophilic vasculitis inflammation§	20 (29)	33 (47)	53 (38)
Neuropathy¶	38 (54)	45 (64)	83 (59)
Nonfixed pulmonary infiltrates	49 (70)	43 (61)	92 (66)
Sinonasal abnormality	63 (90)	66 (94)	129 (92)
Cardiomyopathy‖	17 (24)	13 (19)	30 (21)
Glomerulonephritis	4 (6)	2 (3)	6 (4)
Palpable purpura	7 (10)	10 (14)	17 (12)
Dose of oral glucocorticoid — mg/day**	11.09±4.58	10.95±5.88	11.02±5.25
Median (range)	10.0 (5.0–30.0)	10.0 (7.5–40.0)	10.0 (5.0–40.0)
Oral glucocorticoid dose stratum — no. (%)**			
≥12 mg/day	18 (26)	14 (20)	32 (23)
<12 mg/day	52 (74)	56 (80)	108 (77)
Nonoral glucocorticoid immunosuppressive therapy — no. (%)	26 (37)	24 (34)	50 (36)
Azathioprine	15 (21)	13 (19)	28 (20)
Methotrexate	7 (10)	5 (7)	12 (9)
Mycophenolate mofetil	4 (6)	3 (4)	7 (5)
Methotrexate sodium	1 (1)	1 (1)	2 (1)
Hydroxychloroquine	0	1 (1)	1 (1)
BVAS††	2.3±3.5	1.9±2.9	2.1±3.2
BVAS >0 — no. (%)††	34 (49)	33 (47)	67 (48)
VDI score‡‡	4.0±1.8	4.0±1.8	4.0±1.8
VDI score ≥5 — no. (%)‡‡	23 (33)	21 (30)	44 (31)
Prebronchodilator FEV_1 — liters	2.520±0.925	2.622±0.873	2.570±0.898

Primary and Secondary Outcomes.

End Point	Benralizumab (N=70)	Mepolizumab (N=70)	Difference or Odds Ratio (95% CI)
Primary end point: remission at weeks 36 and 48 — adjusted % of patients	59	56	3 (−13 to 18)†‡
Secondary end points*			
Accrued duration of remission — no. (%)			1.36 (0.75 to 2.48)§
0 wk	9 (13)	15 (21)	
0 to <12 wk	12 (17)	10 (14)	
12 to <24 wk	8 (11)	8 (11)	
24 to <36 wk	21 (30)	19 (27)	
≥36 wk	20 (29)	18 (26)	
Mean daily dose of oral glucocorticoid during weeks 48 through 52 — no. (%)¶			1.42 (0.77 to 2.62)§
0 mg	29 (41)	19 (27)	
>0 to ≤4 mg	20 (29)	30 (43)	
>4 to ≤7.5 mg	14 (20)	13 (19)	
>7.5 mg	7 (10)	8 (11)	
Reduction in oral glucocorticoid dose — adjusted % of patients¶			
≥50% reduction	86	74	12 (−1 to 25)‡
100% reduction	41	26	16 (1 to 31)‡

Time to First Relapse.

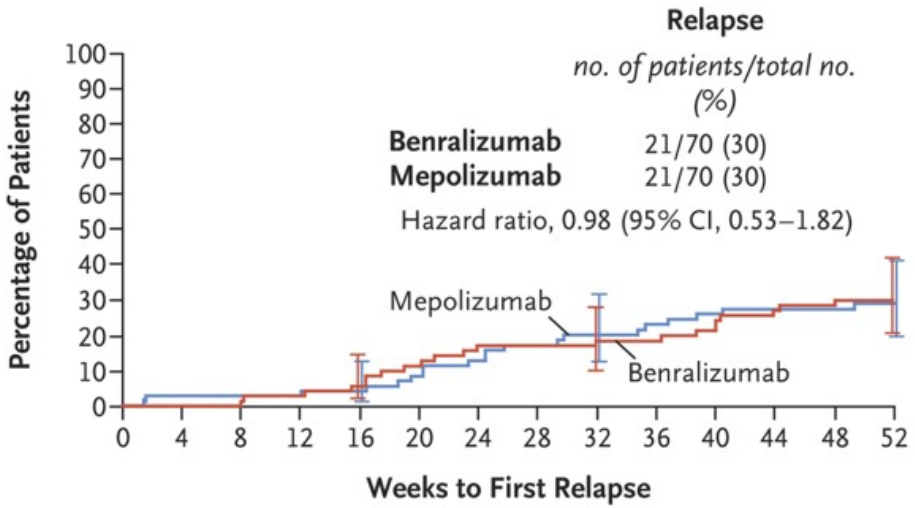

Adverse events were reported in 90% of the patients who received benralizumab and 96% of those who received mepolizumab. The most often reported adverse events were coronavirus disease 2019 (Covid-19) (in 21% of the patients in the benralizumab group and 27% of those in the mepolizumab group), headache (17% and 16%), and arthralgia (17% and 11%).

Event	Benralizumab (N=70)	Mepolizumab (N=70)
	no. of patients (%)	
Any adverse event	63 (90)	67 (96)
Most common adverse events†		
Covid-19	15 (21)	19 (27)
Headache	12 (17)	11 (16)
Arthralgia	12 (17)	8 (11)
Nasopharyngitis	6 (9)	10 (14)
Sinusitis	5 (7)	8 (11)
Any serious adverse event	4 (6)	9 (13)
Serious adverse events		
Covid-19	1 (1)	1 (1)
Appendicitis	0	1 (1)
Bronchitis	1 (1)	0
Urinary tract infection	0	1 (1)
Wound infection	0	1 (1)
Cholangitis	0	1 (1)
Eosinophilic hepatic infiltration	0	1 (1)
Prostate cancer	0	2 (3)
Peripheral neuropathy	1 (1)	0
Syncope	1 (1)	0
Acute respiratory failure	0	1 (1)
Any adverse event leading to discontinuation of treatment	0	2 (3)
Adverse events leading to discontinuation		
Prostate cancer	0	2 (3)
Any adverse event with outcome of death	0	0

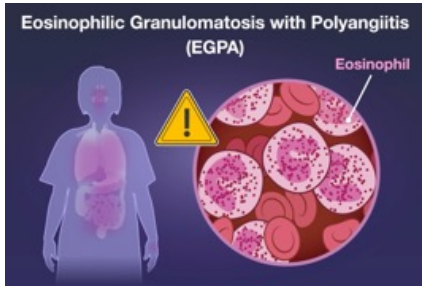

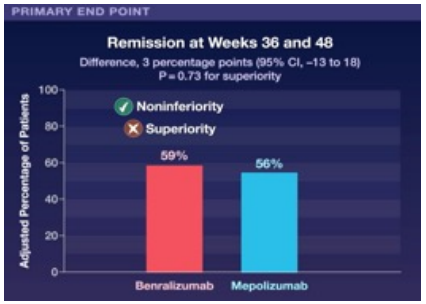

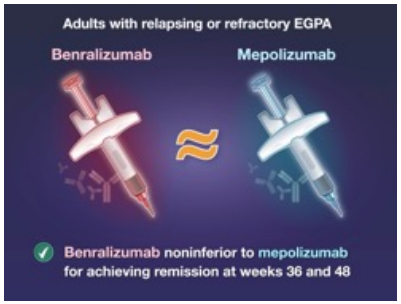

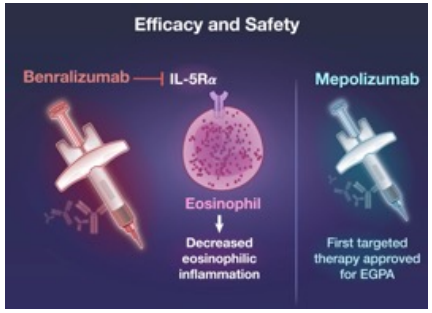

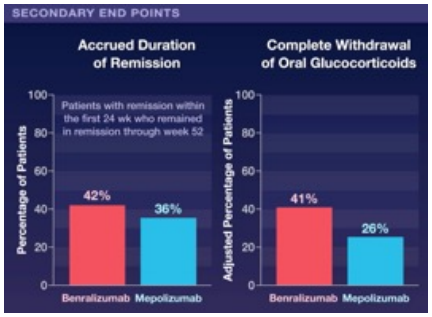

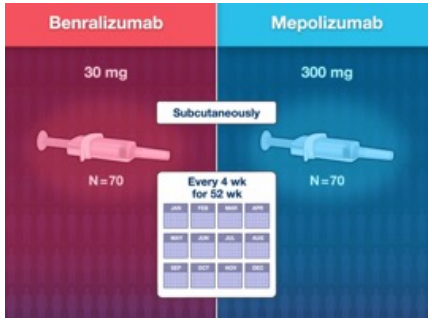

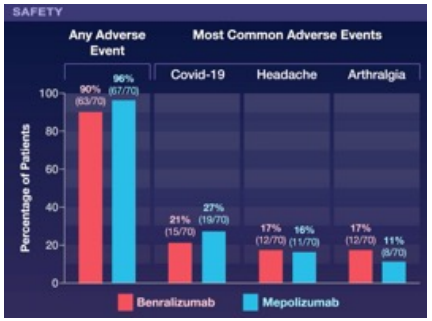

LIMITATIONS AND REMAINING QUESTIONS

- The small sample size due to the rarity of the disease precludes conclusions based on subgroup analyses or the exploration of alternative dosing strategies.
- The duration of the double-blind period and the different starting doses of oral glucocorticoids at baseline may not have allowed all patients to discontinue oral glucocorticoids.
- Future trials are needed to assess whether eosinophil depletion in patients with EGPA is associated with complete discontinuation of oral glucocorticoids.

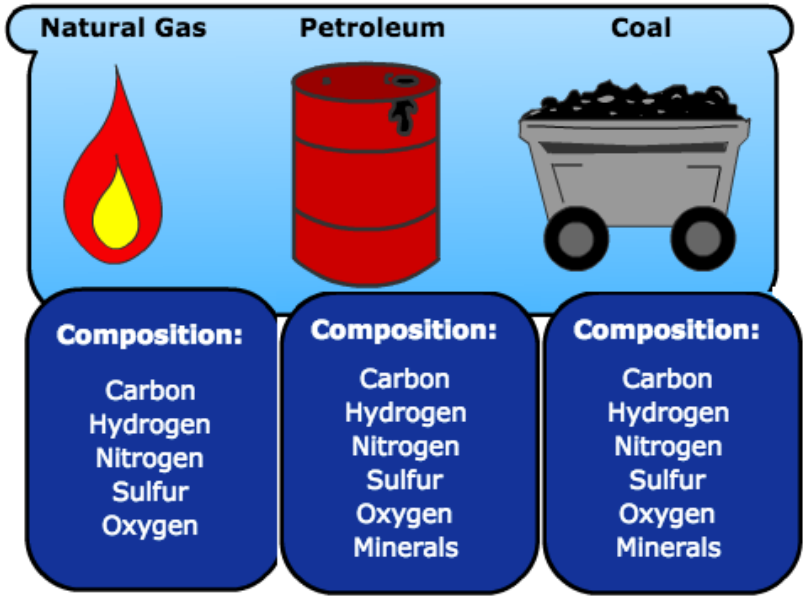
Natural Gas
Petroleum
Coal
Composition:
Carbon
Hydrogen
Nitrogen
Sulfur
Oxygen
Composition:
Carbon
Hydrogen
Nitrogen
Sulfur
Oxygen
Minerals
Composition:
Carbon
Hydrogen
Nitrogen
Sulfur
Oxygen
Minerals

REVIEW ARTICLE FOSSIL-FUEL POLLUTION AND CLIMATE CHANGE

Health Effects of Fossil Fuel–Derived Endocrine Disruptors

Pollution, including air pollution, water pollution, pollution from lead and other chemicals, and toxic occupational exposures, is the leading cause of premature death globally, with more than 90% of pollution-related deaths occurring in low- and middle-income countries. Chemical pollution is estimated to be responsible for at least 1.8 million deaths each year. This number is probably an underestimate, since less than 5% of approximately 350,000 chemicals registered for use globally have been adequately studied; most countries do not require testing for chemical health harms or disclosure of use.

Chemical pollution is driven by the extraction, production, and use of fossil fuels (coal, oil, and gas), and fossil fuels are also the primary driver of climate change. Many fossil fuel–derived chemicals (petrochemicals) interfere with the function of the endocrine system. These endocrine-disrupting chemicals (EDCs) are present in many industrial and everyday products (e.g., plastics, building materials, children's toys, fabrics and dyes, detergents, cosmetics, and pesticides). Exposures have been linked to multiple adverse human health conditions, including cancer, neurodevelopmental harm, and infertility.

Trends in Global Fossil-Fuel Consumption and Primary Plastic Production.

Panel A shows global fossil-fuel consumption from 1800 to 2022. Panel B shows historical and projected global primary plastic production. The shaded area indicates the period known as the “shale revolution” in the United States (2000 through 2010). Data are from Geyer, the Energy Institute, and Smil.

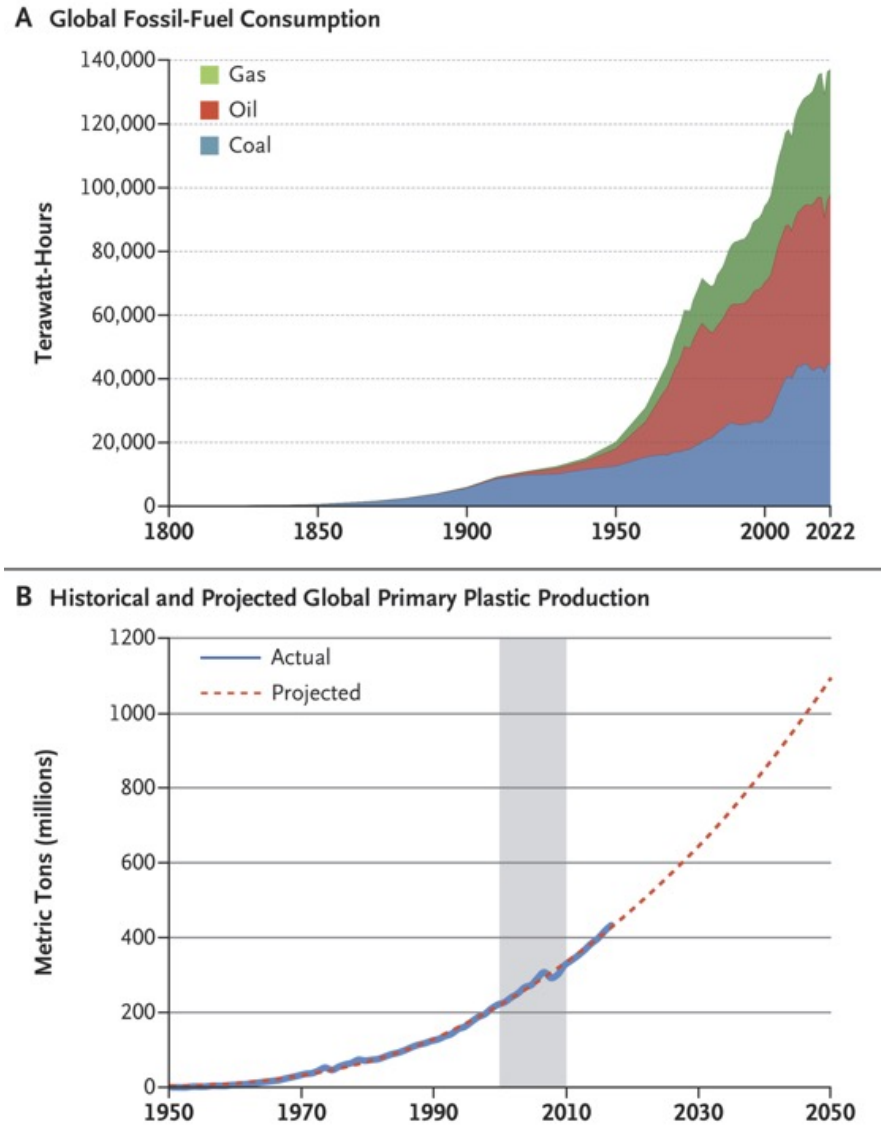

KEY POINTS

Health Effects of Fossil Fuel–Derived Endocrine Disruptors

- Pollution is the leading cause of premature death globally.
- Fossil fuels contribute to chemical pollution through production of petrochemicals, many of which interfere with hormonal function (endocrine-disrupting chemicals [EDCs]). Examples include perfluoroalkyl and polyfluoroalkyl substances in food packaging and fabrics and phthalates in plastics and consumer products.
- Petrochemical production is increasing, and people are exposed through contaminated air, water, food, and manufactured products (e.g., plastics, pesticides, building materials, and cosmetics).
- EDCs can increase several health risks, including cancer, neurodevelopmental harm, and infertility.
- Risks are higher with exposures during fetal and child development and with exposure to multiple EDCs and occur at low exposure levels. Exposures are higher in communities of color and low-income communities and contribute to health inequities.
- Clinicians can provide advice to patients toward reducing some exposures, but policy change is needed to establish legal requirements for comprehensive safety testing and to reduce health threats from petrochemicals. Clinicians are important advocates for these changes.

Adverse Effects of Chemical Exposures on Health Outcomes.
Chemical exposures from the plastics life cycle (from fossil-fuel extraction and processing to product manufacturing, distribution, and disposal) interact with social vulnerabilities and biologic susceptibilities, resulting in adverse health outcomes. These lists are not exhaustive.

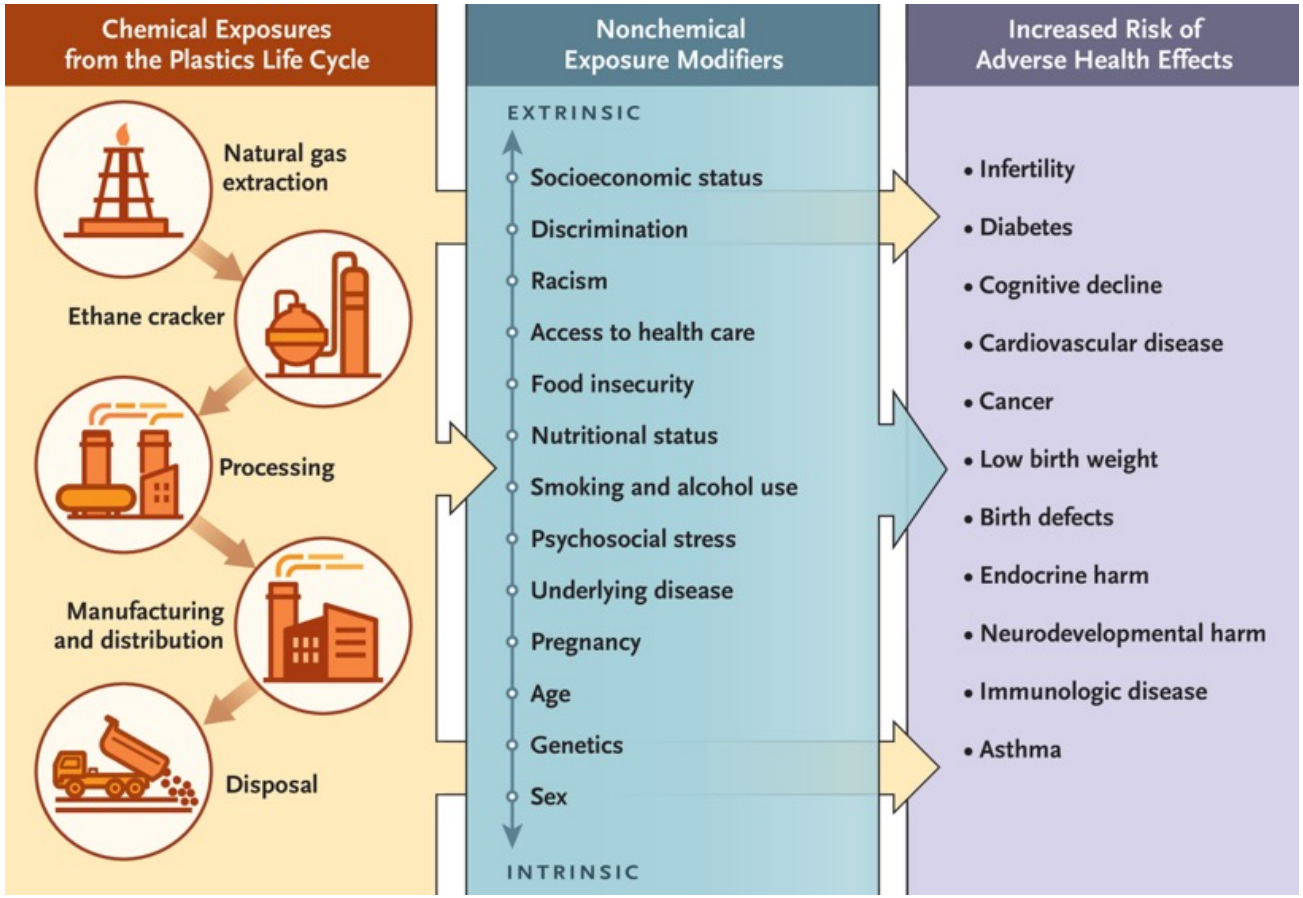

Examples of Fossil Fuel–Derived Chemicals with Known, Likely, or Suspected Endocrine Effects.

Chemical Class and Examples	Major Exposure Sources	Health Effects		Specific Effects
		Known or Likely	Suspected	
PFASs: PFOA, PFOS, PFHxS, PFBS, PFBA†	Consumer products (e.g., nonstick cookware, stain-resistant clothing), building materials (e.g., stain-resistant carpeting), personal care products (e.g., cosmetics, menstrual products), food packaging materials, drinking water, industrial facility releases, legacy environmental exposures	Decreased infant and fetal growth, dyslipidemia, decreased antibody response to vaccines in children and adults[9]	Kidney cancer, testicular and breast cancer, gestational hypertension and preeclampsia, thyroid disease and dysfunction[9]	A meta-analysis of 24 studies showed a 10.5-g decrement in birth weight per 1-ng increase in PFOA/ml, and an analysis of 29 studies showed a 3-g decrement in birth weight per 1 ng PFOS/ml increase.[45] EPA's proposed new standard to reduce drinking water levels of PFOA and PFOS to 4.0 ppt is projected to result in savings of $175 million annually because of increased birth weight and reduced deaths attributed to low birth weight.
Ortho-phthalates: DEHP, DBP, BBP, DEP, DINP	Food, personal care products (e.g., fragrances), food packaging materials, building materials (e.g., PVC flooring), industrial facility releases	Male reproductive toxicity (e.g., sperm effects), decreased anogenital distance,[10,44] preterm birth,[44] metabolic disorders (e.g., insulin resistance, diabetes)[44]	Spontaneous abortion,[44] neurodevelopmental harms (e.g., ADHD)[46]	A meta-analysis of 5 studies showed that a log increase in gestational DEHP levels was associated with a 4% reduction in anogenital distance in human male offspring, reflecting reduced fetal testosterone production.[30]
Flame retardants: PBDEs, organophosphate ester flame retardants (OPFRs)	Consumer products (e.g., electronics, furniture, mattresses, children's products), personal care products (e.g., nail polish), plastics, industrial facility releases, legacy environmental exposures	Impaired neurodevelopment[47]	Altered thyroid function in newborns,[33] reproductive toxicity[4,23]	A meta-analysis of 4 U.S. and European studies showed that an increase by a factor of 10 in PBDE exposure during pregnancy was associated with a decrement of 3.7 IQ points in the offspring.[47]
Bisphenols: BPA, BPS	Polycarbonate plastic products (e.g., water bottles, food-storage containers and packaging, eyeglasses), epoxy resin liners of aluminum cans, and other consumer goods such as thermal paper receipts[36]	Adverse effects on ovarian development and function,[48] female reproductive toxicity, impaired neurodevelopment, metabolic abnormalities, immune system abnormalities[10]		A study of 700 couples from China showed that an increase of 1 ln unit in urinary concentrations of BPA in women was associated with a longer time to pregnancy (OR, 0.87; 95% CI, 0.78–0.98) and an increased risk of infertility (OR, 1.23; 95% CI, 1.00–1.50).[49]‡
Heavy metals: lead, cadmium, mercury, arsenic[2]	Consumer products (e.g., dishware, ceramics, jewelry, children's products), spices, personal care products (e.g., skin lighteners), tobacco smoke, industrial facility releases, legacy environmental exposures	Impaired neurodevelopment, male reproductive toxicity (e.g., impaired semen quality, fertility effects), female reproductive toxic effects, cancer, immunosuppression[36,50]		A pooled analysis with a total of 1333 children from 7 longitudinal cohort studies showed a 6.9-point reduction in IQ with an increase in blood lead levels by a factor of approximately 10.[51]
Pesticides: organophosphate pesticides, neonicotinoids, pyrethroids, DDT[2]	Food and drinking water, insecticides, rodenticides, herbicides, spray drift from use in agricultural fields	Impaired neurodevelopment (e.g., lowered IQ),[36] reduced sperm quality[52]	Increased susceptibility to childhood cancers (e.g., leukemia and brain tumors), increased susceptibility to testicular cancer, impaired fetal growth[3,4,23]	A birth cohort study of 329 children showed an average 7-point IQ deficit for children in the highest quintile of exposure to organophosphate pesticides during pregnancy, as compared with those in the lowest quintile of exposure.[53]
Volatile organic compounds: benzene, formaldehyde, toluene	Consumer products (furniture, textiles, glues, paints, detergents, disinfectants), personal care products (cosmetics, fragrances, nail polish), tobacco smoke, gas-stove emissions, fireplace emissions, industrial facility releases	Respiratory toxicity, lung cancer, nasopharyngeal cancer, leukemia, acute neurologic harm (e.g., dizziness, vomiting), female reproductive toxicity (e.g., increased time to pregnancy, spontaneous abortion risk), altered male reproductive system, reduced fetal growth[3,4,23,54]		A meta-analysis of 15 studies showed an elevated risk of leukemia (RR, 1.54; 95% CI, 1.18–2.00) among workers exposed to high levels of formaldehyde.[55]

Examples of Recommendations for Reducing Exposure to Toxic Chemicals.

Recommendation Category	Examples
Diet and food preparation and storage	Consume less meat and more fruits, vegetables, and whole grains, because certain chemicals can concentrate in animal fat. Eat fresh (and if accessible and feasible, organic) produce whenever possible; always wash raw produce to decrease exposure to pesticides. Avoid or minimize intake of foods with a high risk of contamination (e.g., fish containing high levels of mercury, such as swordfish and bluefin tuna). Avoid fatty foods, because persistent chemicals concentrate in fats. Avoid packaged and highly processed foods (e.g., fast food) when possible, to decrease exposures to chemicals such as phthalates and PFAS. Store food in nonplastic containers, such as glass, ceramic, or stainless steel containers (if accessible and feasible), instead of plastic containers, and avoid microwaving food or drinks in plastic containers. Substitute cookware made from nontoxic materials (e.g., cast iron, stainless steel, and ceramic cookware) for nonstick cookware.
Cleaning and other products	Use nontoxic cleaning products (e.g., baking soda, vinegar, and lemon). Use a wet mop or wet cloth to clean floors and surfaces in order to avoid distributing dust containing chemicals in the air. Remove shoes before entering the house to avoid tracking in contaminants. Minimize use of toxic insect control methods; prioritize alternative control methods (e.g., eliminate standing water, which provides an insect breeding ground; use screens on doors and windows; protect skin with clothing as much as possible). Substitute professional wet cleaning for chemical dry cleaning. Use volatile organic compound–free or water-based home improvement materials. Select flame retardant–free foam products. Use less-toxic personal care products (e.g., those that are paraben-free and unscented). Avoid synthetic turf fields. (If synthetic turf must be used for sports, do not eat or place water bottles on field; on returning home, keep sneakers or cleats outside, shower, and wash clothes separately.)
Work	Pregnant people or those planning a pregnancy who are exposed to toxic chemicals at work should request a change in duties to avoid these exposures. (Guidance can be obtained from an occupational health specialist or union representative.) Request information and training about hazardous substances in the workplace. Employers are required by law to provide such information and training, including access to handouts about toxic substances, called Safety Data Sheets. Request information about substitutes for toxic substances and other ways to prevent harmful exposures, such as use of personal protective gear (which should be provided by employers). People who work with toxic chemicals should shower and change clothing immediately after returning home from work and should keep work tools and clothing away from other people and living areas in the home.
Advocacy	Engage in partnerships and advocacy to support policies that reduce exposure to toxic chemicals and promote decarbonization and detoxification through reductions in fossil-fuel dependence and production of harmful EDCs.

Conclusions

There is an urgent need for the clinical community to address the growing burden of exposure to EDCs, largely derived from petrochemicals, in order to prevent a broad range of associated health harms. With projected increases in fossil-fuel production in the United States and globally, despite the recommendations of the United Nations Intergovernmental Panel on Climate Change and other groups to rapidly reduce production, the problem will continue to grow. In addition to counseling their patients, clinicians can be critical advocates for policy changes to both decarbonize and detoxify the economy in order to address the combined health threats of petrochemical-derived EDCs and climate change.

Syphilitic Pharyngitis

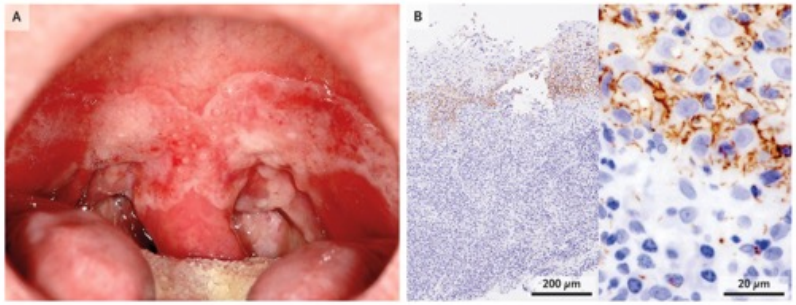

A 40-year-old man was referred to the otorhinolaryngology clinic with a 1-month history of a sore throat. He reported no upper respiratory symptoms, fever, rash, or genital lesions. He had a family history of Behçet's disease (in his brother). The physical examination was notable for nonulcerated white plaques that formed a butterfly shape across the posterior oropharynx, upper uvula, and tonsils (Panel A). No lymphadenopathy or skin or genital lesions were present. A bacterial throat culture grew normal flora. A biopsy of the plaques showed dense lymphoplasmacytic infiltration. A *Treponema pallidum* hemagglutination assay was positive, and the rapid plasma reagin level was 122.4 U (reference range, 0 to 0.9). Further history was obtained, and the patient reported having had sexual intercourse with a commercial sex worker 2 months before the onset of symptoms. Subsequent immunohistochemical staining for *T. pallidum* performed on the biopsy specimen was positive (Panel B). Testing for human immunodeficiency virus infection was negative. A diagnosis of syphilitic pharyngitis — a manifestation of secondary syphilis — was made. Owing to the lack of availability of benzathine penicillin G, treatment with amoxicillin was given in accordance with local guidelines. At follow-up 1 month after the start of treatment, the patient's symptoms had abated.

IMAGES IN CLINICAL MEDICINE

Gastric Syphilis

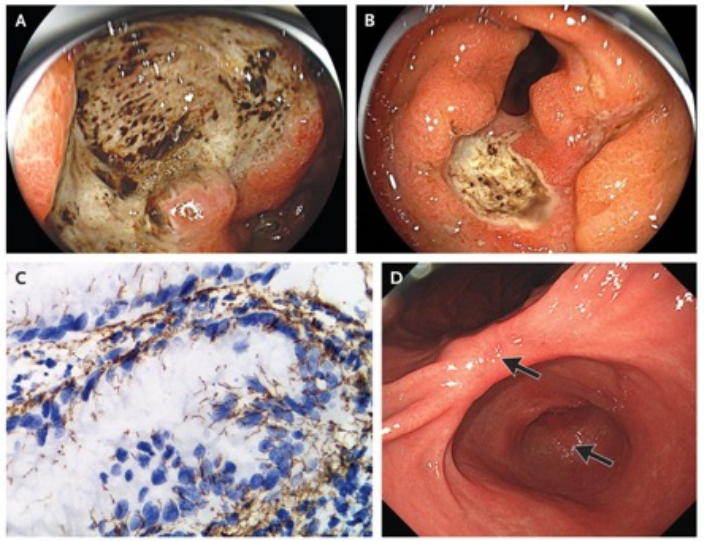

A 32-year-old man presented to the internal medicine clinic with a 2-week history of epigastric pain, nausea, anorexia, and weight loss. Physical examination was notable for epigastric tenderness. A computed tomographic scan of the abdomen showed mural thickening of the gastric antrum. Endoscopy revealed an ulcer measuring 4.0 cm by 5.0 cm in the gastric antrum (Panel A) and an ulcer measuring 1.2 cm by 1.2 cm on the greater antral curvature (Panel B). Biopsy samples of the ulcers showed infiltration of lymphocytes, neutrophils, and plasma cells. There were no malignant features. Further history taking revealed that the patient had had a genital ulcer 1 month before presentation. A subsequent serum *Treponema pallidum* particle agglutination test was positive, and the rapid plasma reagin (RPR) titer was 1:128. Immunohistochemical staining of the ulcer-biopsy specimens for *T. pallidum* was positive (Panel C). Testing for the human immunodeficiency virus was negative. A diagnosis of gastric syphilis was made. Once-weekly injections of penicillin G benzathine were given for 3 weeks. Two weeks after the patient began treatment, his symptoms had abated. Four months after the completion of treatment, repeat testing showed that the RPR titer had decreased to 1:4, and a repeat endoscopy showed that the ulcers had resolved (Panel D, arrows).

CLINICAL PROBLEM-SOLVING

Peeling and Plummeting

A 20-year-old Guatemalan woman who had immigrated to Maryland 6 years earlier presented to an urgent care facility with a 6-month history of progressive joint pain and malaise. The patient described symmetric joint pain and swelling affecting the small joints of the hands, wrists, and ankles. She reported 1 hour of morning stiffness accompanied by notable hair thinning, night sweats, and unintentional weight loss. Eating and dressing were compromised by impaired dexterity. She noted no recent interaction with children. She had last traveled to Guatemala 5 years previously. Given limited English proficiency, a qualified language interpreter was used. The white-cell count was 4750 per microliter, hemoglobin level 12.6 g per deciliter, and platelet count 273,000 per microliter. The serum creatinine level was 0.4 mg per deciliter (35 µmol per liter). Urinalysis did not show blood or protein. The thyrotropin level was 5.32 IU per milliliter (normal range, 0.30 to 4.00). A test for antinuclear antibodies was positive (1:80 titer); a test for rheumatoid factor was negative. At the urgent care facility, hydroxychloroquine and levothyroxine were prescribed, and the patient was referred to a rheumatology clinic for further evaluation and care management. The patient lacked health insurance and had no primary care physician. With the onset of the coronavirus disease 2019 (Covid-19) pandemic, she found it difficult to obtain insurance coverage or to access care, and she ran out of the 2-month hydroxychloroquine supply that had been issued at the urgent care facility.

Ten months after initial symptom onset, she presented to the emergency department with a 30-lb (14-kg) unintentional weight loss (corresponding to 25% of her body weight), a diffuse hyperpigmented rash, and an inability to ambulate independently. She reported having had persistence of painful, swollen, and stiff joints since her initial urgent care evaluation, without abatement while she was taking hydroxychloroquine. She also noted continued fatigue and malaise, with subsequent development of generalized weakness. She attributed her difficulty walking to her fatigue and weakness and reported that it took her several minutes to walk as little as 8 ft (approximately 2.5 m). For the preceding 4 months, she had also been having early satiety, without abdominal pain or a change in bowel habits. In addition, she noted darkening of her skin over the trunk, arms, and legs and menstrual irregularity, as well as continued hair thinning.

On physical examination, the patient appeared chronically ill. The temperature was 38.4°C, heart rate 120 beats per minute, blood pressure 110/70 mm Hg, and respiratory rate 16 breaths per minute. The oxygen saturation was 95% while she was breathing ambient air. The weight was 79 lb (36 kg) and the height 59 in. (150 cm); the body-mass index (BMI, the weight in kilograms divided by the square of the height in meters) was 16.0. She had a diffuse dry, fish scale–like rash, with hyperkeratosis over hands and feet, and hyperpigmented plaques on her face, chest, abdomen, arms, and legs.

Photographs of the Patient.
Shown are diffuse ichthyosis and hyperkeratosis with hyperpigmented plaques affecting the face (Panel A), hand dorsal surface (Panel B), and distal legs and dorsal aspect of both feet (Panel C).

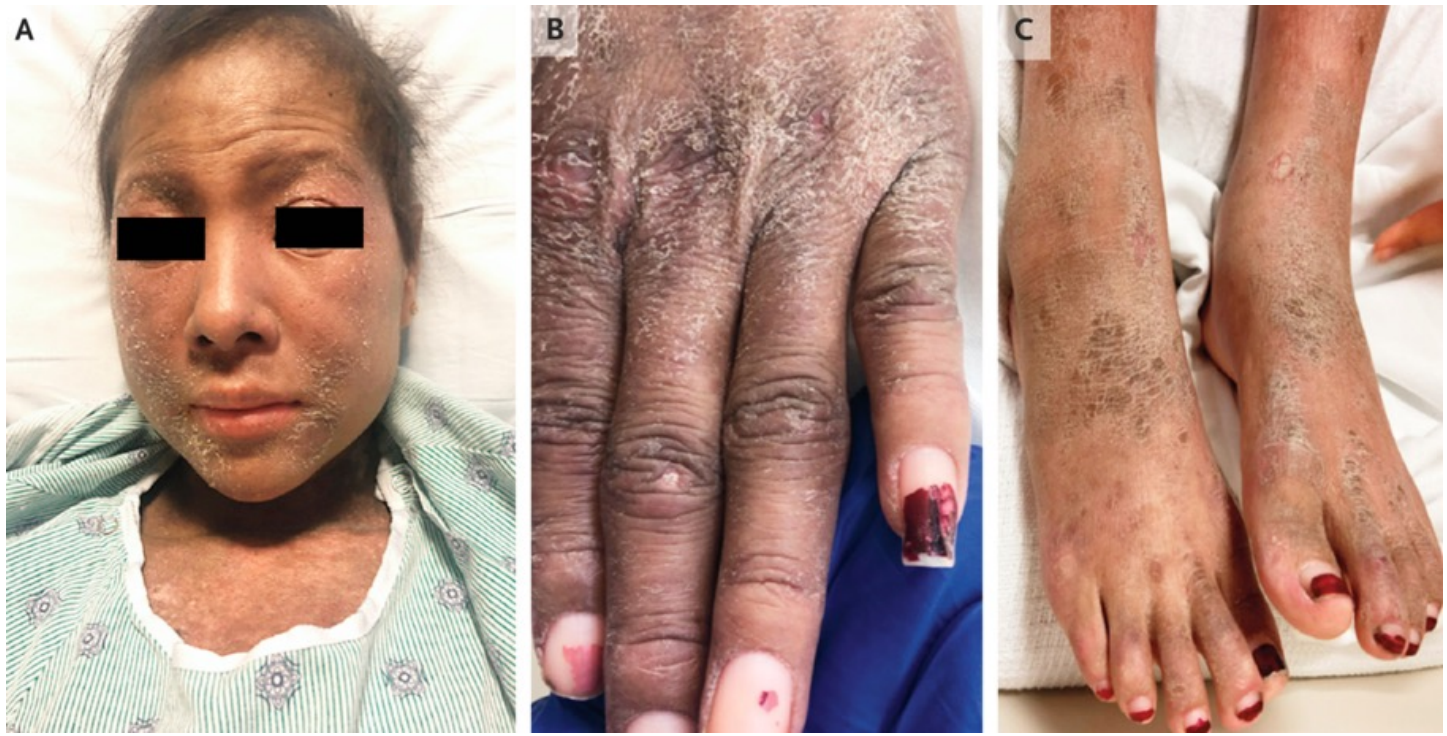

“Peeling paint” or “flaky paint” dermatosis in a malnourished child or adult strongly suggests kwashiorkor. Evaluation for nutritional deficiencies is warranted, as is treatment of the underlying insult causing severe malnutrition — that is, dysphagia presumed to result from myositis associated with the patient’s SLE.

The white-cell count was 6.23 per microliter, with 73% neutrophils, 1% immature neutrophils, 15% lymphocytes, 7% monocytes, and 4% eosinophils; the hemoglobin level was 9 g per deciliter, mean corpuscular volume 94 fl, and platelet count 212,000 per microliter. The serum creatinine level was 0.3 mg per deciliter (27 µmol per liter). The ferritin level was 767 ng per milliliter (normal range, 13 to 150), and the erythrocyte sediment rate was 88 mm per hour (normal range, 4 to 25). The C-reactive protein level was 0.4 mg per deciliter (normal value, <0.5). The aspartate aminotransferase level was 650 U per liter (normal range, 0 to 31), alanine aminotransferase level 426 U per liter (normal range, 0 to 31), alkaline phosphatase level 443 U per liter (normal range, 30 to 120), total protein level 5.2 g per deciliter (normal range, 6.0 to 8.2), and albumin level 0.7 g per deciliter (normal range, 3.5 to 5.3); the total bilirubin level was normal. The thyrotropin level was 7.92 IU per milliliter, and the free thyroxine level was 1.0 ng per deciliter (12.9 pmol per liter) (normal range, 0.8 to 1.8 ng per deciliter [10.3 to 23.2 pmol per liter]). Urinalysis was negative for leukocytes, red cells, and bacteria but showed 2+ protein. Sputum, urine, and blood cultures were without growth.

A test for antinuclear antibodies was positive at a titer of 1:160, a test for anti–double-stranded DNA (dsDNA) antibodies was positive at a titer of 1:160, and the level of anti-Smith antibodies was 21 U (normal value, <20). The level of C3 was 71 mg per deciliter (normal range, 82 to 167), and the C4 level was 18 mg per deciliter (normal range, 12 to 38); a Coombs' test was positive, without hemolysis on a peripheral smear. The creatine kinase level was 58 U per liter (normal range, 32 to 182), and the aldolase level was 16.4 U per liter (normal value, <8.1). The urinary protein:creatinine ratio was 2.27 (normal value, <0.19). Tests for IgA and IgG antibodies against tissue transglutaminase were negative. Measurement of 24-hour stool alpha$_1$-antitrypsin and fecal fat was normal.

Additional history taking was negative for toxin exposure or alcohol use. Within 6 hours after the initiation of intravenous fluid repletion and antibiotic therapy, tachycardia and fever resolved. Hepatitis A, B, and C serologic tests were nonreactive. Tests for CMV, EBV, and HIV viral loads were negative. Computed tomography of the abdomen revealed hepatomegaly measuring 25 cm craniocaudally (upper limit of the normal range, <13 cm) with the appearance of diffuse fatty liver; there was no lymphadenopathy or splenomegaly. Edema in the abdominal wall and paraspinal subcutaneous tissue was noted. Blood, sputum, and urine cultures remained negative for bacterial growth at 48 hours; antimicrobial therapy was stopped. Magnetic resonance imaging of thigh muscles identified proximal muscle and fascial edema in both thighs. Electromyography (EMG) showed fibrillations and positive sharp waves consistent with an inflammatory myopathy. On further questioning, the patient noted a 4-month history of difficulty with swallowing, initially limited to liquids but then also involving solid foods.

A videofluoroscopic swallowing study indicated impaired pharyngeal constriction, absent epiglottic inversion, and substantial pharyngeal retention of swallowed liquids, which did not clear with additional swallows. This retention resulted in laryngeal penetration and aspiration.

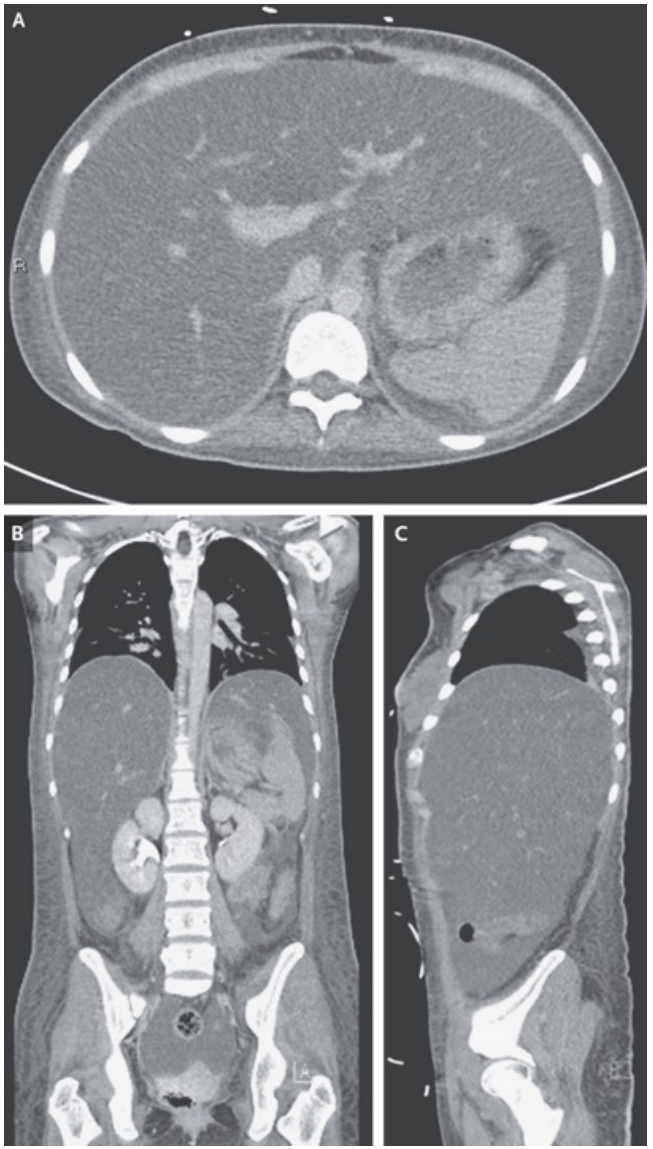

Renal biopsy demonstrates diffuse capillary wall thickening with orangeophilic deposits on Masson trichrome stain [Panels A, B]. On direct immunofluorescence, there was a diffuse fine granular capillary wall and mesangial staining for IgG, IgA, IgM, kappa and lambda light chains, C3 and C1q [Panel C]. There were numerous subepithelial and mesangial electron-dense deposits on electron microscopy [Panel D] and endothelial tubuloreticular inclusions [Panel D inset].

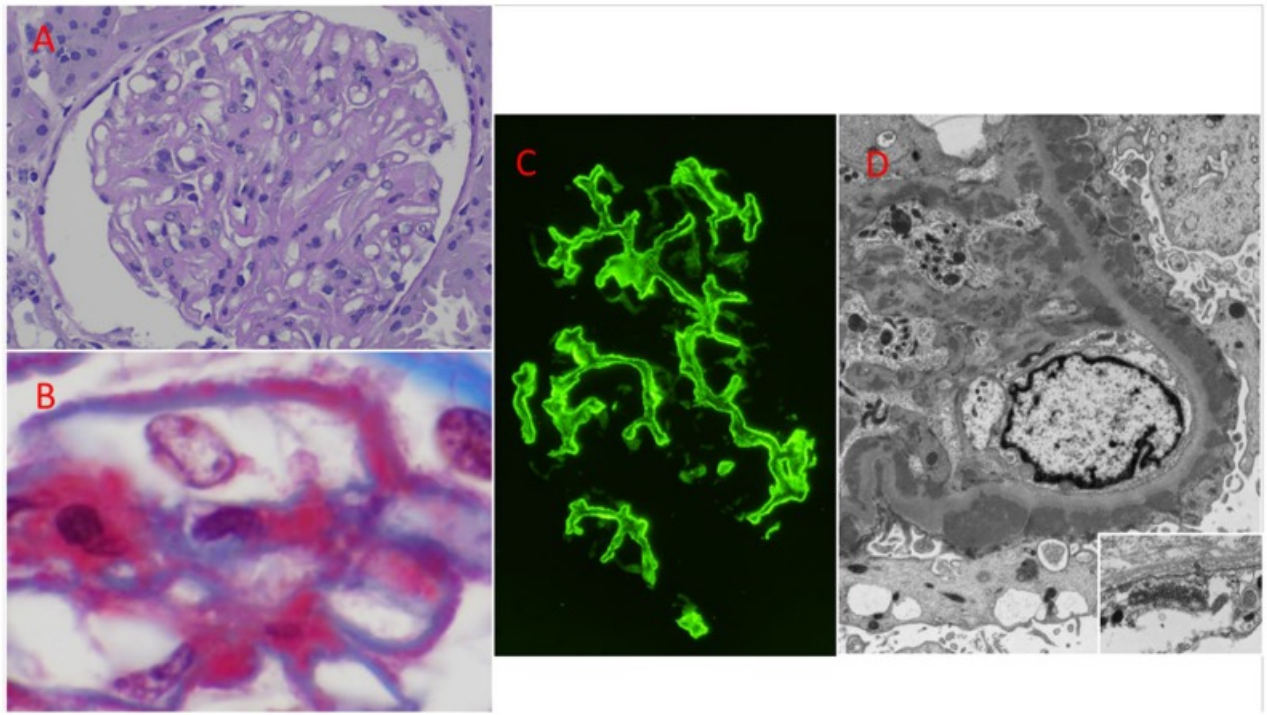

Liver Biopsy demonstrating severe large droplet macrovesicular steatosis with bands of fibrosis and focal nodule formation, shown at high magnification (H&E, 200X). (A) The areas of fibrosis are highlighted by a trichrome stain (100X). (B)

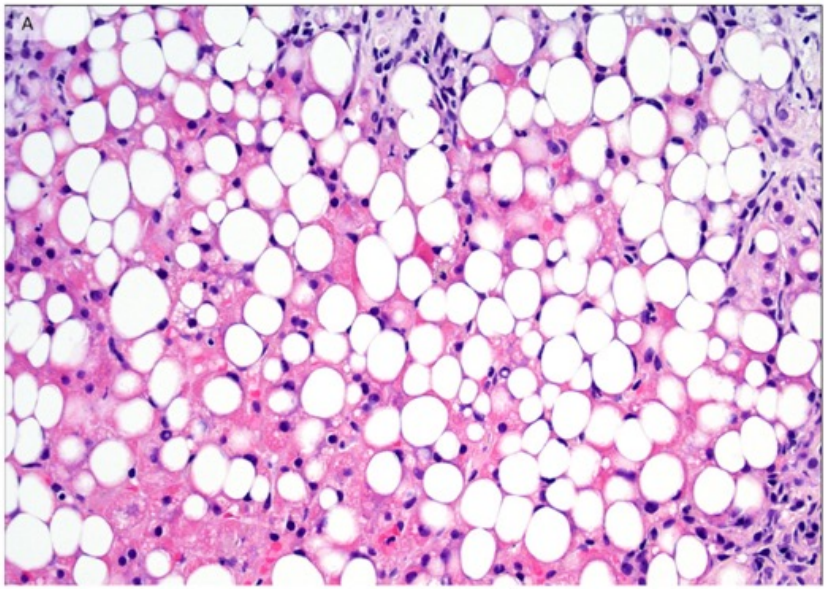

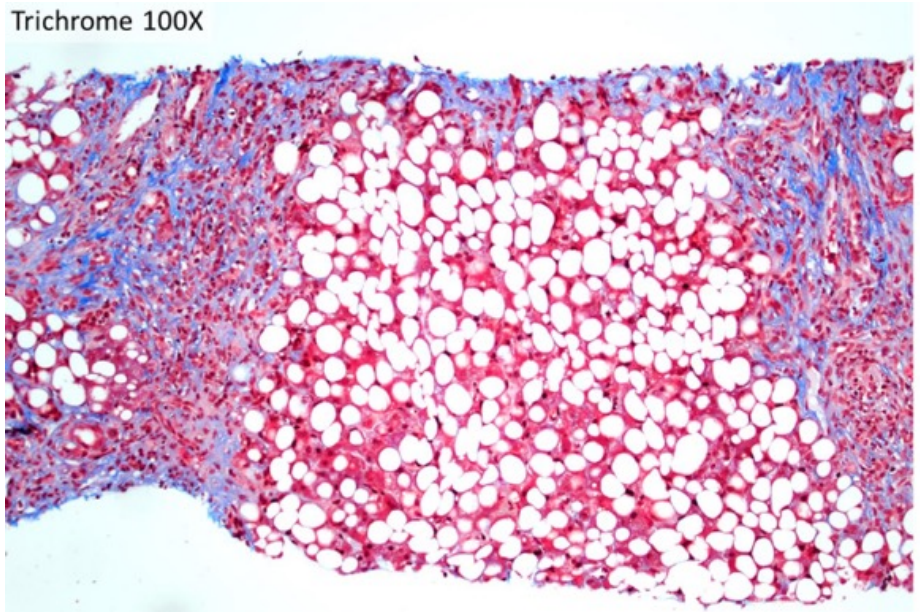

The vitamin A level was 17 µg per deciliter (normal range, 38 to 98), 25-hydroxyvitamin D level 10 ng per milliliter (normal range, 30 to 100), and zinc level 16 µg per deciliter (normal range, 60 to 130). Levels of vitamins B_{12}, C, E, and K and selenium were normal. The patient was treated with pulse-dose glucocorticoids, mycophenolate mofetil, intravenous immune globulin, and intensive nutritional support, including intravenous vitamin repletion and caloric supplements. Electrolyte levels were monitored closely for potential refeeding syndrome. On the basis of consultation with a speech and language therapist, she was started on a pureed diet, which was advanced to regular consistency as her dysphagia abated with treatment. Physical and occupational therapy provided inpatient care and a home rehabilitation plan. She was discharged while receiving treatment with methylprednisolone, mycophenolate, hydroxychloroquine, a topical glucocorticoid, levothyroxine, ergocalciferol, and both multivitamin and nutritional supplements, with shakes thickened to improve safe swallowing.

At 6-month follow-up, she had regained 35 lb (16 kg), with normalization of her albumin level and liver indexes and resolution of proteinuria, dysphagia, weakness, and generalized ichthyosis. At 1-year follow-up, she had regained her independence in all activities of daily living and resumed working.

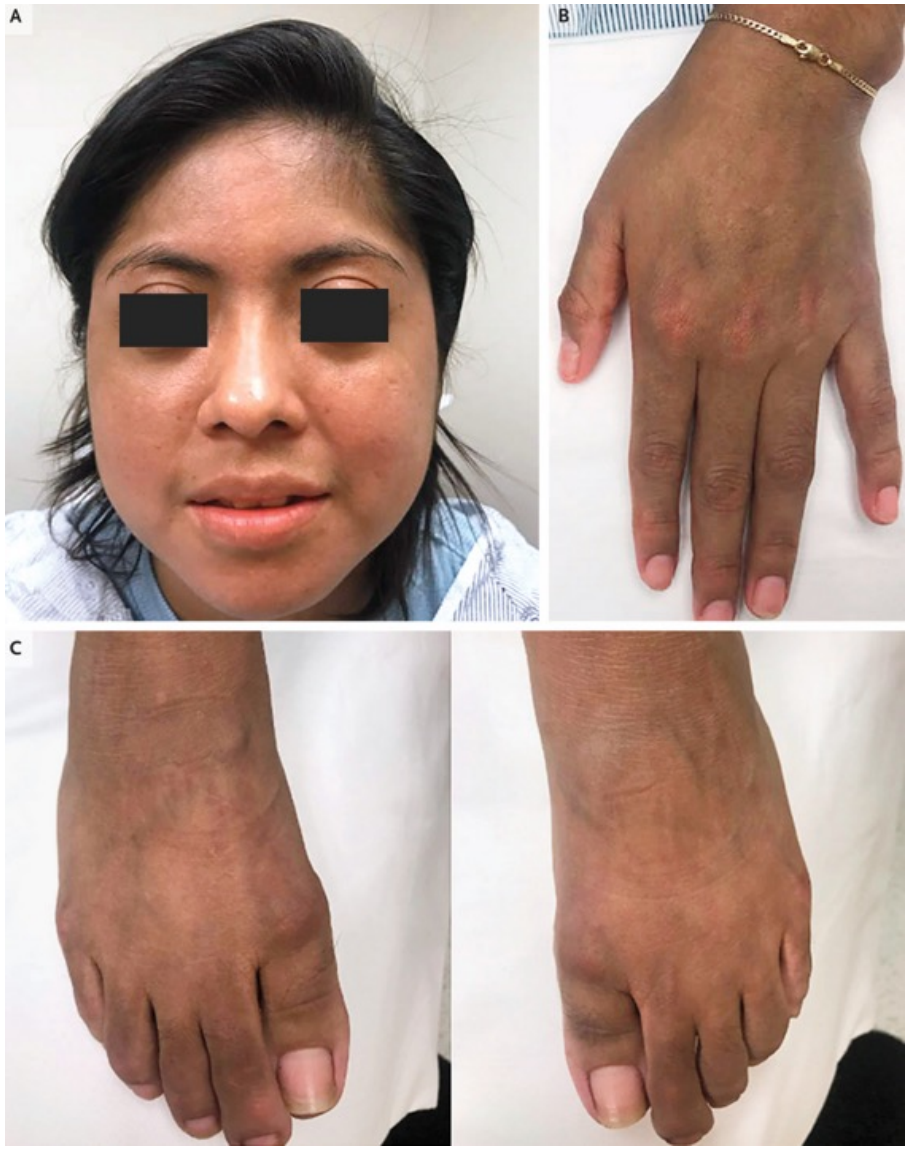

Commentary

This 20-year-old woman presented with inflammatory arthritis, alopecia, and proteinuria, with subsequent serologic and pathological findings indicative of SLE; however, this diagnosis did not account for all her phenotypic features. After an interruption in care in the context of the Covid-19 pandemic, she returned to the emergency department unable to walk or swallow, with substantial weight loss and malnutrition. Ultimately, her profound hypoalbuminemia, hepatomegaly, peeling-paint dermatosis, and liver histopathological findings led to a diagnosis of kwashiorkor.

Kwashiorkor is a consequence of severe protein malnutrition that results in marked muscle loss, hepatic enlargement, and hypoalbuminemia. A hyperpigmented, ichthyotic, and peeling rash, as affected this patient's face, trunk, and limbs, is a characteristic finding. Protein deficiency results in a reduction in plasma triglyceride and phospholipid levels, a rise in free fatty acid levels, and subsequent liver enlargement attributed to accumulation of triglycerides. Her liver biopsy revealed severe large-droplet macrovesicular steatosis compatible with kwashiorkor.

The root cause of our patient's severe malnutrition was her inability to properly swallow. Her elevated aldolase levels and EMG findings supported an active myositis that was presumed to be caused by SLE. Myositis in SLE can lead to dysphagia, arm and leg weakness, and (less commonly) myocarditis. Our patient's impaired oropharyngeal and esophageal swallowing mechanisms were identified at bedside by speech and language pathology evaluation and confirmed by a videofluoroscopic swallow study.

Digital health tools can promote disease self-management, but the association of smartphone app engagement and medication adherence is unclear. We assessed the relationship between objective smartphone app engagement and controller medication use in adults with asthma and COPD.

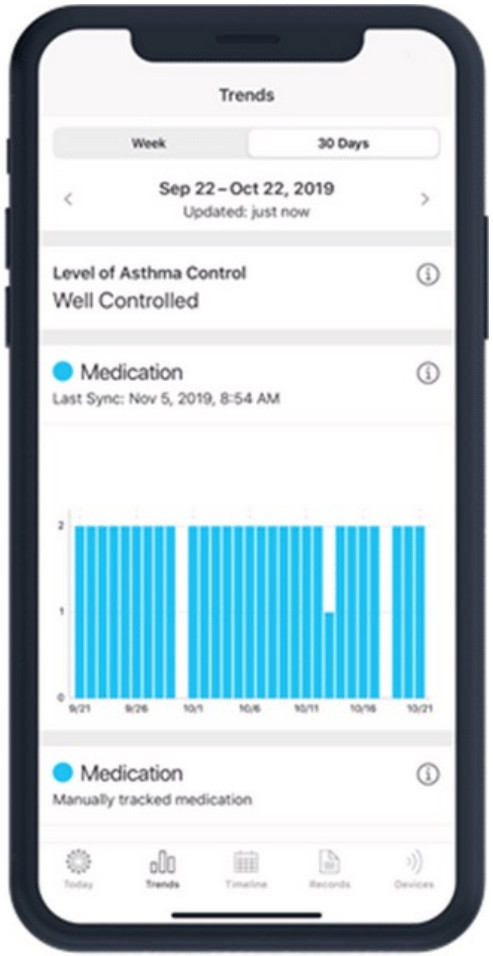

Summary

Background WHO recommends that electronic medication monitors, a form of digital adherence technology, be used as a complement to directly observed treatment (DOT) for tuberculosis, as DOT is inconvenient and costly. However, existing evidence about the effectiveness of these monitors is inconclusive. Therefore, we evaluated the effectiveness of a comprehensive package based on electronic medication monitors among patients with tuberculosis in Tibet Autonomous Region (hereafter Tibet), China.

Methods This multicentre, randomised controlled trial recruited patients from six counties in Shigatse, Tibet. Eligible participants had drug-susceptible tuberculosis and were aged 15 years or older when starting standard tuberculosis treatment. Tuberculosis doctors recruited patients from the public tuberculosis dispensary in each county and the study statistician randomly assigned them to the intervention or control group based on the predetermined randomised allocation sequence. Intervention patients received an electronic medication monitor box. The box included audio medication-adherence reminders and recorded box-opening data, which were transmitted to a cloud-based server and were accessible to health-care providers to allow remote adherence monitoring. A linked smartphone app enabled text, audio, and video communication between patients and health-care providers. Patients were also provided with a free data plan. Patients selected a treatment supporter (often a family member) who was trained to support patients with using the electronic medication monitor and app. Patients in the control group received usual care plus a deactivated electronic medication monitor, which only recorded and transmitted box-opening data that was not made available to health-care providers. The control group also had no access to the app or trained treatment supporters. The primary outcome was a binary indicator of poor monthly adherence, defined as missing 20% or more of planned doses in the treatment month, measured using electronic medication monitor opening data, and verified by counting used medication blister packages during consultations. We recorded other secondary treatment outcomes based on national tuberculosis reporting data. We analysed the primary outcome based on the intention-to-treat population. This trial is registered at ISRCTN, 52132803.

Findings Between Nov 17, 2018, and April 5, 2021, 278 patients were enrolled into the study. 143 patients were randomly assigned to the intervention group and 135 patients to the control group. Follow-up ended when the final patient completed treatment on Oct 4, 2021. In the intervention group, 87 (10%) of the 854 treatment months showed poor adherence compared with 290 (37%) of the 795 months in the control group. The corresponding adjusted risk difference for the intervention versus control was –29·2 percentage points (95% CI –35·3 to –22·2; p<0·0001). Five of the six secondary treatment outcomes also showed clear improvements, including treatment success, which was found for 133 (94%) of the 142 individuals in the intervention arm and 98 (73%) of the 134 individuals in the control arm, with an adjusted risk difference of 21 percentage points (95% CI 12·4–29·4); p<0·0001.

Interpretation The interventions were effective at improving tuberculosis treatment adherence and outcomes, and the trial suggests that a comprehensive package involving electronic medication monitors might positively affect tuberculosis programmes in high-burden and low-resource settings.

Effectiveness of a comprehensive package based on electronic medication monitors at improving treatment outcomes among tuberculosis patients in Tibet: a multicentre randomised controlled trial

Patients in the intervention group received an electronic medication monitor box to store their medications in, which had two key features. First, the monitor reminded patients to take their medication on time using human voice-based recordings. Second, the monitor recorded every time the box was opened and transmitted this information to a cloud-based server. This information could then be accessed by a patient's village doctor and their tuberculosis doctor via a computer web-based interface or a password protected WeChat-based smartphone app in real time. Patients who refused to start or continue treatment, missed more than three consecutive doses, or for whom either doctor had concerns about their adherence, received daily real-time video-observed therapy or audio calls by the village doctor until they had taken four consecutive doses.

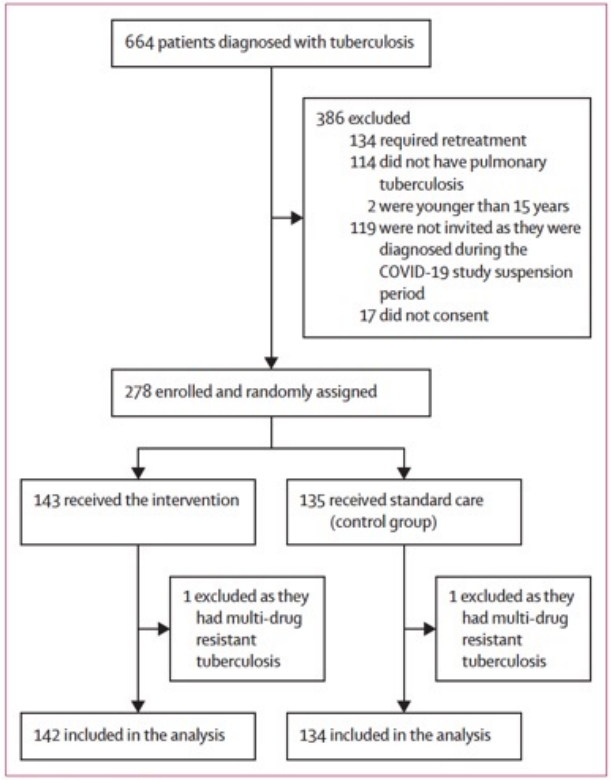

Figure 1: **Trial profile**

During the recruitment period the trial was suspended for 9 months in Samzhubze, 7 months in Sa'gya, and 3 months in Gyantse in total due to either the COVID-19 emergency response or that tuberculosis diagnosis and treatment functions were transferred from county Center for Disease Control and Prevention to county hospital according to local policy changes. During the suspension period, all patients received usual tuberculosis management but were not invited to participate in the trial. There were 50 eligible patients identified during the suspension period in Samzhubze, 46 in Sa'gya, and 23 in Gyantse. Among the 17 patients who refused consent, six were students who did not want to bring the electronic monitor into their dormitories, six were bus drivers or construction workers who did not have a place for the electronic monitor in their dormitory, and five did not provide clear reasons.

	Intervention arm (n=142)	Control arm (n=134)
County of residence		
Samzhubze	36 (25%)	34 (25%)
Sa'gya	39 (28%)	37 (28%)
Gyantse	44 (31%)	41 (31%)
Ngamring	12 (9%)	12 (9%)
Tingri	9 (6%)	5 (4%)
Bainang	2 (1%)	5 (4%)
Sex		
Male	89 (63%)	81 (60%)
Female	53 (37%)	53 (40%)
Age (years)	57·0 (40·2–64·8)	55·0 (40·0–62·8)
Education level		
Primary school or below	127 (89%)	112 (84%)
High school	12 (9%)	13 (10%)
College or above	3 (2%)	9 (7%)
Job		
Farmer	106 (75%)	107 (80%)
Other	36 (25%)	27 (20%)
Monthly income (US$*)	154·6 (0·0–309·1)	185·5 (0·0–463·7)
Number of family members in their household	5·0 (3·0–7·0)	6·0 (4·0–8·0)
Marital status		
Married	116 (82%)	110 (82%)
Single, divorced, or widowed	26 (18%)	24 (18%)
Sputum smear test at diagnosis		
Negative	102 (72%)	104 (78%)
Positive	40 (28%)	30 (22%)
Planned treatment length		
6 months	138 (97%)	128 (96%)
7 months	4 (3%)	6 (5%)

Data are n (%) or median (IQR). *Based on the exchange rate on April 30, 2021: US$ 1=6·47 RMB.

Table 1: **Baseline characteristics**

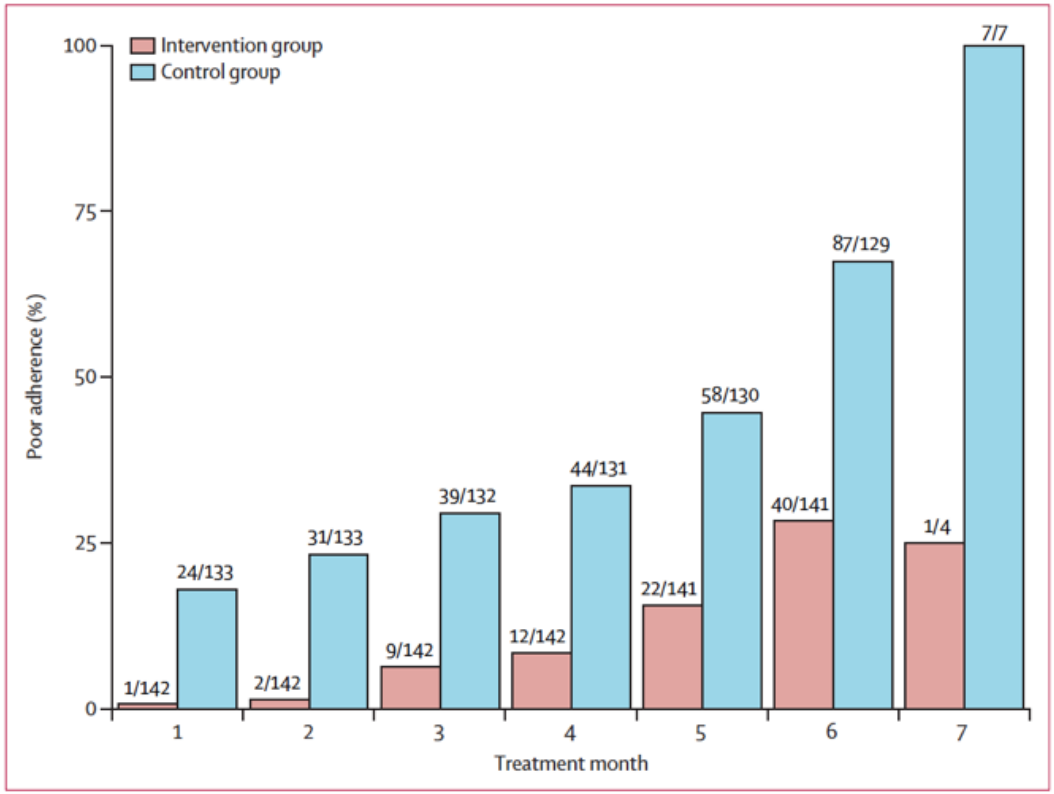

Figure 2: **Tuberculosis treatment adherence**

Poor adherence is defined as a patient missing ≥20% of their treatment doses. Patients were expected to take 30 medication doses per treatment month. Patients who died are included in the figure's results for the months up to and including the month of their death, if it was possible to determine their adherence status for that month, and are also excluded from the results for any months after their death.

	Summary values		Risk difference in percentage points (95% CI); p value		Risk ratio in percentage points (95% CI); p value	
	Intervention	Control	Adjusted	Crude	Adjusted	Crude
Primary outcome						
Monthly poor treatment adherence (ie, missing ≥20% of planned doses in the treatment month)	87/854 (10%)	290/795 (37%)	−29·2 (−35·3 to −22·2); p<0·0001	−28·7 (−34·5 to −21·8); p<0·0001	0·33 (0·23 to 0·43); p<0·0001	0·34 (0·26 to 0·45); p<0·0001
Secondary outcomes						
Treatment success (ie, cured: negative sputum or culture negative in the last month of treatment and ≥1 other month during treatment or treatment completed: completed treatment with no evidence of failure but results proving that patient was cured were not done or were unavailable)	133/142 (94%)	98/134 (73%)	21·0 (12·4 to 29·4); p<0·0001	21·4 (12·8 to 29·8); p<0·0001	1·29 (1·16 to 1·45); p<0·0001	1·30 (1·17 to 1·46); p<0·0001
Total planned doses missed during treatment	1976/25 594 (8%)	6937/23 872 (29%)	−22·4 (−28·3 to −16·9); p<0·0001	−22·2 (−27·9 to −16·8); p<0·0001	0·25 (0·18 to 0·35); p<0·0001	0·25 (0·18 to 0·35); p<0·0001
Overall poor treatment adherence (ie, missing ≥10% of all planned doses)	32/142 (23%)	72/134 (54%)	−32·7 (−43·2 to −21·8); p<0·0001	−32·2 (−42·7 to −21·4); p<0·0001	0·40 (0·28 to 0·56); p<0·0001	0·41 (0·28 to 0·57); p<0·0001
Lost to follow-up (ie, never started treatment after diagnosis or missed ≥2 consecutive months of treatment)	4/142 (3%)	29/134 (22%)	−19·3 (−26·7 to −11·8); p<0·0001	−19·7 (−27·1 to −12·2); p<0·0001	0·12 (0·03 to 0·30); p<0·0001	0·12 (0·03 to 0·29); p<0·0001
Poor treatment outcome (ie, patient death, lost to follow-up, or smear or culture positive at treatment month ≥5)	10/142 (7%)	39/134 (29%)	−23·1 (−31·6 to −14·1); p<0·0001	−23·1 (−31·5 to −14·3); p<0·0001	0·23 (0·11 to 0·42); p<0·0001	0·23 (0·11 to 0·41); p<0·0001
Sputum conversion (from positive to negative) at the end of month 2	36/40 (90%)	19/26 (73%)	13·2 (−2·5 to 41·1); p=0·20	19·2 (−3·0 to 39·5); p=0·077	1·18 (1·00 to 2·74); p=0·20	1·28 (1·00 to 1·88); p=0·077

Data are n/N (%) unless otherwise specified. For the treatment effect results, the primary outcome was derived and analysed at the patient treatment-month level (planned treatment length being 6 or 7 months), and all other outcomes were derived and analysed at the patient level. All treatment effect results calculated via a marginal standardisation approach using bootstrapping to obtain the CIs and permutation methods to obtain the p values (incorporating a clustered approach for the primary outcome). All adjusted results were adjusted for the covariates county (the stratum or centre), age (years), sex (male or female), job (farmer or other), marriage status (married or other), and the primary outcome alone was also adjusted for treatment month (treated as a continuous variable). All crude results were only adjusted for county (the stratum or centre), and the primary outcome alone was also adjusted for treatment month. All outcomes other than sputum conversion included the intention-to-treat population. Analyses for the primary outcome, and the outcomes for planned doses missed during treatment and overall poor adherence, included outcome values for patients who died during treatment that were derived only from their dose adherence data available before death. Sputum conversion analyses consisted of the subset of the intention-to-treat population who were sputum positive at diagnosis.

Table 2: **Intervention effects on all outcomes**

Research in context

Evidence before this study

Directly observed treatment short course (DOTS) is the best standard health service delivery model for tuberculosis treatment and has been widely studied across different contexts globally. Digital adherence technologies have emerged as a strategy to complement DOTS and better support patients in adhering to their tuberculosis medication. Three systematic reviews exploring a variety of digital adherence technologies (consisting of using short message service, video-observed therapy, and electronic medication monitors) used during tuberculosis treatment reported insufficient data and high variability in study quality, concluding that evidence of their beneficial effects on treatment adherence and treatment outcomes is only mixed. Although electronic medication monitors have shown potential for managing chronic conditions, such as hypertension and HIV, there appear to be no systematic reviews focusing on using electronic medication monitors to support tuberculosis treatment. Several trials of digital adherence technologies have shown their effectiveness at improving tuberculosis treatment adherence measures, but none have demonstrated clear effects on treatment outcomes. We searched MEDLINE, Embase, proceedings from major scientific meetings on tuberculosis, and the Cochrane Central Register of Controlled Trials for randomised controlled trials of digital adherence technologies, specifically electronic pill boxes or electronic medication monitors, targeting tuberculosis treatment adherence from Jan 01, 2000 (when digital adherence technologies for patients started to become widely used), to Oct 01, 2023. We also reviewed the reference lists of the included studies and have searched for subsequent publications.

Added value of this study

This pragmatic, multicentre, individually randomised, controlled trial evaluated a comprehensive intervention package including a new generation of electronic medication monitors, which use a wide range of components to support treatment, including voice reminders, real-time recording of box-opening data to facilitate adherence monitoring by health-care providers, and a smartphone app to facilitate direct follow-up communications with health-care providers (and video-observed therapy, if required). Other package components included provision of training to a family member treatment supporter. The trial showed that the intervention reduced the monthly level percentage of poor medication adherence in the intervention group compared with the control group by −29 percentage points (95% CI −35 to −22). We also observed a 21 percentage point increase (95% CI 12 to 29) in treatment completion or cure in the intervention group compared with the control group. The intervention also clearly and substantially reduced the total percentage of missed medication doses, overall poor adherence, loss to follow-up, and poor treatment, as defined in the secondary outcomes.

Implications of all the available evidence

The available evidence, including this trial, shows the potential of electronic medication monitors to improve tuberculosis treatment adherence and treatment outcomes, and to provide more patient-centred care. Importantly, this trial was done in a remote and rural area with a high burden of tuberculosis, showing that digital adherence technologies can be feasible and effective in areas with resource constraints, which often have a high burden of tuberculosis. Digital adherence technologies need to be adapted to the local context to maximise patient uptake and use, and these technologies must also improve communications between patients and their health-care providers.

Intracytoplasmic sperm injection for male infertility and consequences for offspring

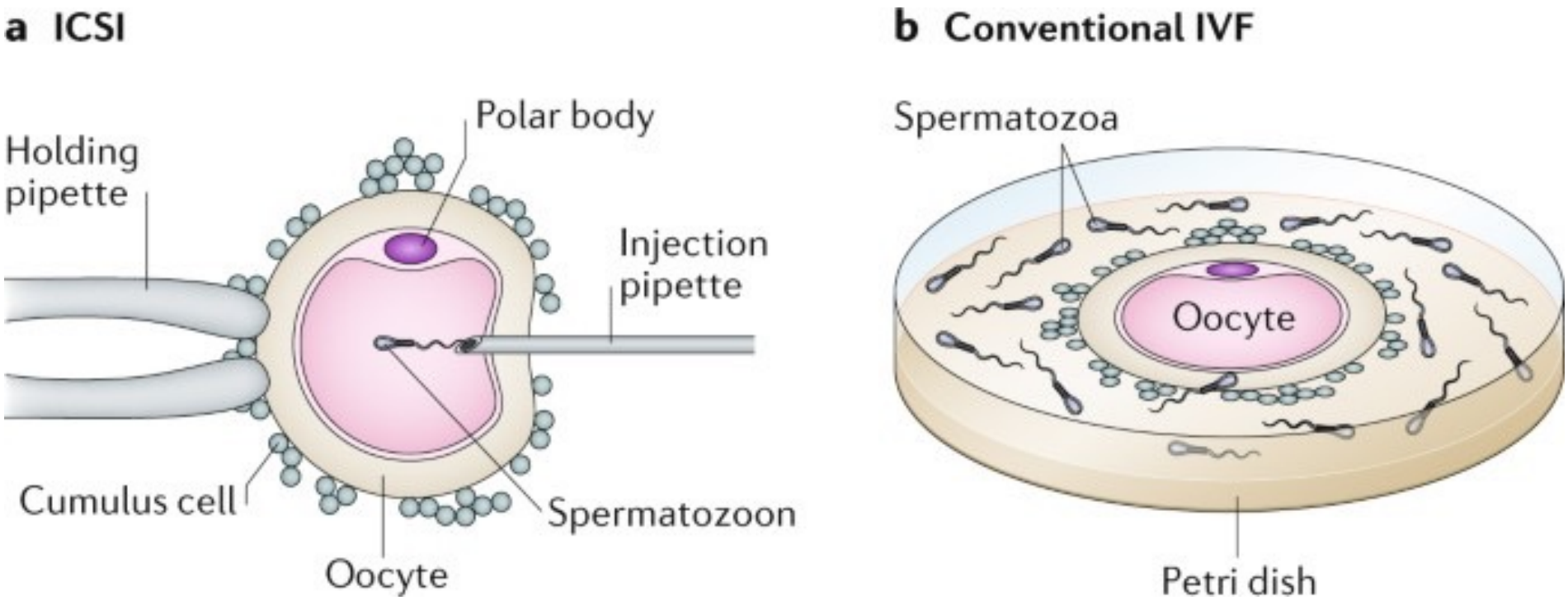

Intracytoplasmic sperm injection versus conventional in-vitro fertilisation for couples with infertility with non-severe male factor: a multicentre, open-label, randomised controlled trial

Summary

Background Introduced in 1992, intracytoplasmic sperm injection (ICSI) was initially indicated for severe male infertility; however, its use has since been expanded to non-severe male infertility. We aimed to compare the efficacy and safety of ICSI versus conventional in-vitro fertilisation (IVF) in couples with infertility with non-severe male factor.

Methods We conducted an investigator-initiated, multicentre, open-label, randomised controlled trial in ten reproductive medicine centres across China. Couples with infertility with non-severe male factor without a history of poor fertilisation were randomly assigned (1:1) to undergo either ICSI or conventional IVF. The primary outcome was live birth after first embryo transfer. We performed the primary analysis in the intention-to-treat population using log-binomial regression models for categorical outcomes or linear regression models for continuous outcomes, adjusting for centre. This trial is registered with Clinicaltrials.gov, NCT03298633, and is completed.

Findings Between April 4, 2018, and Nov 15, 2021, 3879 couples were screened, of whom 2387 (61·5%) couples were randomly assigned (1184 [49·6%] to the ICSI group and 1203 [50·4%] to the conventional IVF group). After excluding couples who were ineligible, randomised twice, or withdrew consent, 1154 (97·5%) in the ICSI group and 1175 (97·7%) in the conventional IVF group were included in the primary analysis. Live birth after first embryo transfer occurred in 390 (33·8%) couples in the ICSI group and in 430 (36·6%) couples in the conventional IVF group (adjusted risk ratio [RR] 0·92 [95% CI 0·83–1·03]; p=0·16). Two (0·2%) neonatal deaths were reported in the ICSI group and one (0·1%) in the conventional IVF group.

Interpretation In couples with infertility with non-severe male factor, ICSI did not improve live birth rate compared with conventional IVF. Given that ICSI is an invasive procedure associated with additional costs and potential increased risks to offspring health, routine use is not recommended in this population.

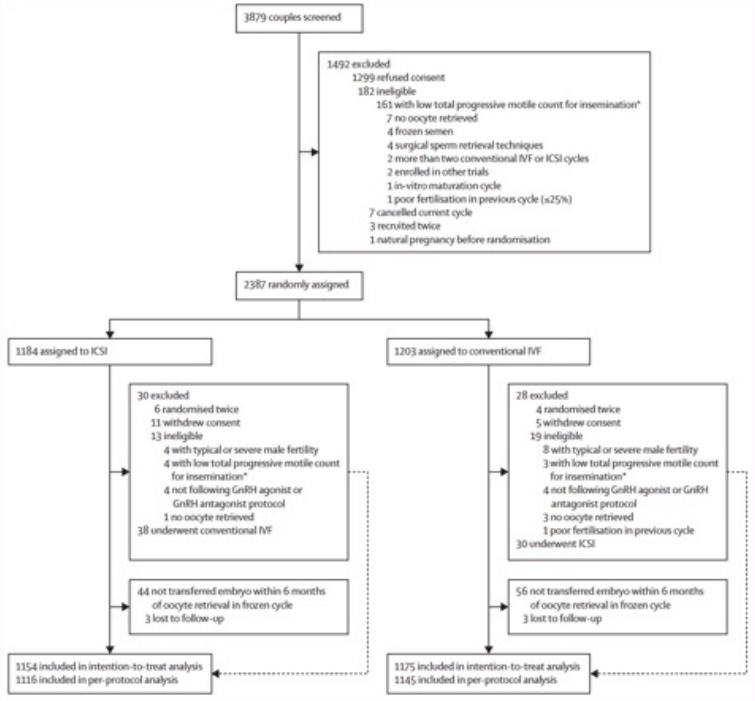

Figure 1: **Trial profile**
ICSI=intracytoplasmic sperm injection. IVF=in-vitro fertilisation. GnRH=gonadotropin-releasing hormone. *Low count considered to be <0·1 × 10⁶ sperm per mL on the day of oocyte retrieval.

	ICSI group (n=1154)	Conventional IVF group (n=1175)
Age, years		
Female	34 (31–37)	33 (30–37)
Male	34 (31–38)	34 (31–38)
Female BMI, kg/m²	22·1 (20·2–24·8)	22·0 (20·2–24·6)
Data missing	0	4 (0·3%)
Duration of infertility, years	3 (2–5)	3 (2–5)
Data missing	1 (0·1%)	0
Number of previous IVF or ICSI cycles		
0	1051 (91·1%)	1068 (90·9%)
1	103 (8·9%)	107 (9·1%)
Primary infertility	607 (52·6%)	613 (52·2%)
Indication for IVF		
Male factor (non-severe)	1154 (100%)	1175 (100%)
Female factor	939 (81·4%)	1008 (85·8%)
Tubal factor	736 (63·8%)	785 (66·8%)
Ovulatory dysfunction	131 (11·4%)	152 (12·9%)
Endometriosis	87 (7·5%)	84 (7·1%)
Diminished ovarian reserve	118 (10·2%)	101 (8·6%)
Other	70 (6·1%)	81 (6·9%)
Ultrasonographic examination		
Antral follicle count	12 (8–17)	13 (9–20)
Data missing	1 (0·1%)	2 (0·2%)
Endometrial thickness, mm	7 (5–9)	7 (5–9)
Data missing	17 (1·5%)	14 (1·2%)
Basal laboratory testing (female partner)		
Basal follicle-stimulating hormone, IU/L	6·7 (5·5–8·1)	6·5 (5·2–7·9)
Data missing	11 (1·0%)	9 (0·8%)
Basal luteinising hormone, IU/L	4·2 (2·9–5·8)	4·2 (2·8–6·2)
Data missing	9 (0·8%)	9 (0·8%)
Basal oestradiol, pmol/L	138·9 (93·2–197·1)	144·4 (93·9–194·6)
Data missing	8 (0·7%)	11 (0·9%)
Basal semen analysis before IVF*		
Sperm volume, mL	2·9 (2·0–3·8)	3·0 (2·0–3·8)
Sperm concentration, × 10⁶ sperm per mL	37·9 (17·4–69·2)	40·9 (20·0–68·8)
Progressive motility, %	22·6 (16·9–27·8)	23·5 (18·0–28·2)
Normal morphology, %	3·0 (2·0–4·2)	3·0 (2·0–4·0)
Data missing	175 (15·2%)	189 (16·1%)
Classification of basal semen analysis		
Oligoasthenozoospermia†	153 (13·3%)	126 (10·7%)
Oligozoospermia‡	84 (7·3%)	91 (7·7%)
Asthenozoospermia§	917 (79·5%)	958 (81·5%)
Teratospermia¶	590/979 (60·3%)	599/986 (60·8%)
Controlled ovarian hyperstimulation protocol		
GnRH agonist protocol	455 (39·4%)	471 (40·1%)
GnRH antagonist protocol	699 (60·6%)	704 (59·9%)
Duration of ovarian stimulation, days	10 (9–12)	10 (9–12)
Total dose of follicle-stimulating hormone, IU	2025 (1500–2700)	2025 (1500–2700)

(Table 1 continues on next page)

	ICSI group (n=1154)	Conventional IVF group (n=1175)
(Continued from previous page)		
Human chorionic gonadotropin trigger day		
Luteinising hormone, IU/L	1·5 (0·8–2·8)	1·5 (0·8–2·9)
Data missing	9 (0·8%)	4 (0·3%)
Oestradiol, pmol/L	8677·0 (5010·0–13792·0)	8613·4 (5366·2–14328·2)
Data missing	5 (0·4%)	3 (0·3%)
Progesterone, nmol/L	2·6 (1·6–4·4)	2·6 (1·6–4·3)
Data missing	14 (1·2%)	12 (1·0%)
Endometrial thickness, mm	11·0 (9·5–12·0)	11·0 (9·8–12·0)
Data missing	1 (0·1%)	0
Progressive motile sperm for insemination on day of oocyte retrieval, × 10⁶ sperm per mL	8·3 (4·5–18·0)	9·0 (5·2–21·9)
Number of oocytes retrieved	11 (7–16)	11 (7–17)
Number of metaphase II oocytes‖	8 (5–13)	9 (5–12)

Data are median (IQR), n (%), or n/N (%). The complete case population (1151 participants in the ICSI group and 1172 in the conventional IVF group) was generated from the intention-to-treat population (1154 in the ICSI group and 1175 in the conventional IVF group), with the exclusion of couples lost to follow-up (three in each group). ICSI=intracytoplasmic sperm injection. IVF=in-vitro fertilisation. GnRH=gonadotropin-releasing hormone. *Performed at the initial consultation before IVF. †Sperm concentration 5–15 × 10⁶ sperm per mL and progressive motility 10–32%. ‡Sperm concentration 5–15 × 10⁶ sperm per mL and progressive motility ≥32%. §Sperm concentration ≥15 × 10⁶ sperm per mL and progressive motility 10–32%. ¶Typical morphology <4%. ‖Calculated when the actual fertilisation method was ICSI (1116 participants in the ICSI group and 30 in the conventional IVF group).

Table 1: **Baseline characteristics in the intention-to-treat population**

	ICSI group (n=1154)	Conventional IVF group (n=1175)	Unadjusted RR* (95% CI)	Unadjusted p value	Adjusted RR† (95% CI)	Adjusted p value
Primary outcome						
Number of live births	390 (33·8%)	430 (36·6%)	0·92 (0·83–1·03)	0·16	0·92 (0·83–1·03)	0·16
Fertility outcomes						
Implantation rate‡	564/1642 (34·3%)	620/1644 (37·7%)	0·91 (0·83–1·00)	0·045	..	..
Clinical pregnancy	463 (40·1%)	498 (42·4%)	0·95 (0·86–1·04)	0·27	0·95 (0·86–1·04)	0·28
Multiple pregnancy	103 (8·9%)	124 (10·6%)	0·85 (0·66–1·08)	0·21	0·85 (0·66–1·08)§	0·21
Twin pregnancy	99 (8·6%)	121 (10·3%)	0·83 (0·65–1·07)	0·16	0·84 (0·65–1·07)§	0·16
Triplet pregnancy	4 (0·3%)	3 (0·3%)	1·36 (0·30–6·05)	0·72	..	..
Ongoing pregnancy	402 (34·8%)	442 (37·6%)	0·93 (0·83–1·03)	0·16	0·93 (0·83–1·03)	0·18
Embryological outcomes						
Number of zygotes with two pronuclei per female partner	6 (3–10)	6 (3–10)	..	0·14	..	0·12
Fertilisation per oocyte retrieved, %	59·0 (42·0–75·0)	60·0 (40·0–75·0)	..	0·64	..	0·90
Total fertilisation failure	42 (3·6%)	56 (4·8%)	0·76 (0·52–1·13)	0·18	0·77 (0·52–1·14)	0·19
Number of available embryos on day 3	4 (2–8)	5 (2–9)	..	0·0054	..	0·0009
Number of good quality embryos on day 3	2 (1–5)	3 (1–5)	..	0·13	..	0·19
Embryo transfer	1029 (89·2%)	1019 (86·7%)	1·03 (1·00–1·06)	0·070	1·03 (1·00–1·06)§	0·076
Fresh	655 (56·8%)	638 (54·3%)	1·04 (0·97–1·12)	0·23	1·04 (0·97–1·12)§	0·22
Frozen-thawed	374 (32·4%)	381 (32·4%)	1·00 (0·89–1·12)	0·99	1·00 (0·89–1·12)§	0·99
Cleavage-stage embryo transfer¶	828 (71·8%)	816 (69·4%)	1·03 (0·98–1·09)	0·22	1·03 (0·98–1·08)§	0·20
Blastocyst embryo transfer¶	203 (17·6%)	203 (17·3%)	1·02 (0·85–1·22)	0·84	1·02 (0·88–1·19)§	0·78
Single-embryo transfer	416 (36·0%)	394 (33·5%)	1·08 (0·96–1·20)	0·20	1·07 (0·97–1·18)	0·16
Double-embryo transfer	613 (53·1%)	625 (53·2%)	1·00 (0·92–1·08)	0·97	1·01 (0·95–1·08)	0·75
Number of couples with freeze-all embryos without a transfer within 6 months‖	44 (3·8%)	56 (4·8%)	0·80 (0·54–1·18)	0·26	0·81 (0·55–1·18)§	0·27
Number of rescue ICSI procedures**	2/38 (5·3%)	30/1145 (2·6%)	2·01 (0·50–8·10)	0·28	..	..

Data are median (IQR), n/N (%), or n (%). ICSI=intracytoplasmic sperm injection. IVF=in-vitro fertilisation. RR=risk ratio. *For continuous outcomes, p values were calculated with either a t test, owing to the normality of the variables, or a Wilcoxon rank-sum test, owing to the non-normality of the variables. †For continuous outcomes, p values were calculated with a linear regression model. ‡The numerator was the total number of gestational sacs and the denominator was the total number of embryos transferred. There were six (0·5%) cases of monochorionic diamniotic twins in the ICSI group and five (0·4%) in the conventional IVF group. §Calculated with a Poisson regression model with robust SEs because the log-binomial model failed to converge. ¶Two couples in the ICSI group had two fresh embryos transferred (one cleavage-stage embryo and one blastocyst embryo). ‖As of March 31, 2023, 27 (2·3%) couples in the ICSI group and 36 (3·1%) in the conventional ICF group had received frozen-thawed embryo transfer; eight (0·7%) couples in the ICSI group and 13 (1·1%) in the conventional IVF had a singleton live birth, and no couple in the ICSI group and two (0·2%) couples in the conventional IVF group had twin live births. One (0·1%) couple in the ICSI group had ongoing pregnancy but had a miscarriage in the second trimester, and one (0·1%) couple in the conventional IVF group had ongoing pregnancy but terminated the pregnancy due to fetal cardiac malformation. **The denominator was the total number of cases in which the actual fertilisation method was conventional IVF.

Table 2: **Primary and secondary outcomes after first embryo transfer in the intention-to-treat population**

	ICSI group (n=1154)	Conventional IVF group (n=1175)	RR* (95% CI)	Unadjusted p value	Adjusted RR† (95% CI)	Adjusted p value
Maternal						
Moderate or severe ovarian hyperstimulation syndrome	15 (1·3%)	17 (1·4%)	0·90 (0·45–1·79)	0·76	..	..
Ectopic pregnancy	9 (0·8%)	13 (1·1%)	0·70 (0·30–1·64)	0·42	..	..
Miscarriage	58 (5·0%)	43 (3·7%)	1·37 (0·93–2·02)	0·11	1·38 (0·94–2·02)‡	0·10
Gestational diabetes	28 (2·4%)	28 (2·4%)	1·02 (0·61–1·71)	0·95	..	..
Hypertensive disorders of pregnancy	16 (1·4%)	24 (2·0%)	0·68 (0·36–1·27)	0·22	..	..
Antepartum haemorrhage	2 (0·2%)	3 (0·3%)	0·68 (0·11–4·06)	1·00	..	..
Fetal or neonatal						
Preterm birth	62 (5·4%)	81 (6·9%)	0·78 (0·57–1·07)	0·13	0·78 (0·57–1·08)‡	0·14
Birthweight§, g	2995·5 (683·4)	2970·0 (633·7)	..	0·54	..	0·50
Singleton¶, g	3294·7 (505·0)	3265·1 (482·4)	..	0·44	..	0·44
Twin||, g	2335·0 (549·4)	2417·5 (490·7)	..	0·16	..	0·20
Triplet**, g	..	1850·0 (100·0)	..	..	..	..
Low birthweight (<2500 g)	42 (3·6%)	45 (3·8%)	0·95 (0·63–1·44)	0·81	0·96 (0·64–1·45)	0·85
Very low birthweight (<1500 g)	8 (0·7%)	8 (0·7%)	1·02 (0·38–2·70)	0·97	..	..
High birthweight (>4000 g)	19 (1·6%)	17 (1·4%)	1·14 (0·60–2·18)	0·70	..	..
Very high birthweight (>4500 g)	3 (0·3%)	3 (0·3%)	1·02 (0·21–5·03)	1·00	..	..
Large for gestational age	43 (3·7%)	60 (5·1%)	0·73 (0·50–1·07)	0·10	..	..
Small for gestational age	39 (3·4%)	42 (3·6%)	0·94 (0·62–1·45)	0·80	..	..
Congenital anomaly	7 (0·6%)	13 (1·1%)	0·55 (0·22–1·37)	0·19	..	..
Perinatal mortality	4 (0·3%)	6 (0·5%)	0·68 (0·19–2·40)	0·75	..	..
Neonatal mortality††	2 (0·2%)	1 (0·1%)	2·04 (0·18–22·43)	0·62	..	..

Data are n (%) or mean (SD). ICSI=intracytoplasmic sperm injection. IVF=in-vitro fertilisation. RR=risk ratio. *For continuous outcomes, p values were calculated with either a *t* test, owing to the normality of the variables, or a Wilcoxon rank-sum test, owing to the non-normality of the variables. †For continuous outcomes, p values were calculated with a linear regression model. ‡Calculated with a Poisson regression model with robust SEs because the log-binomial model failed to converge. §462 babies (390 couples) in the ICSI group and 520 babies (430 couples) in the conventional IVF group. ¶318 babies (318 couples) in the ICSI group and 341 babies (341 couples) in the conventional IVF group. ||144 babies (72 couples) in the ICSI group and 176 babies (88 couples) in the conventional IVF group. **No babies in the ICSI group and three babies (one couple) in the conventional IVF group. ††In the ICSI group, one baby died on the day of birth due to pneumorrhagia and one baby died 16 days after birth due to congenital heart disease. In the conventional IVF group, one baby died on the day of birth due to neonatal asphyxia.

Table 3: **Maternal and fetal or neonatal complications after first embryo transfer in the intention-to-treat population**

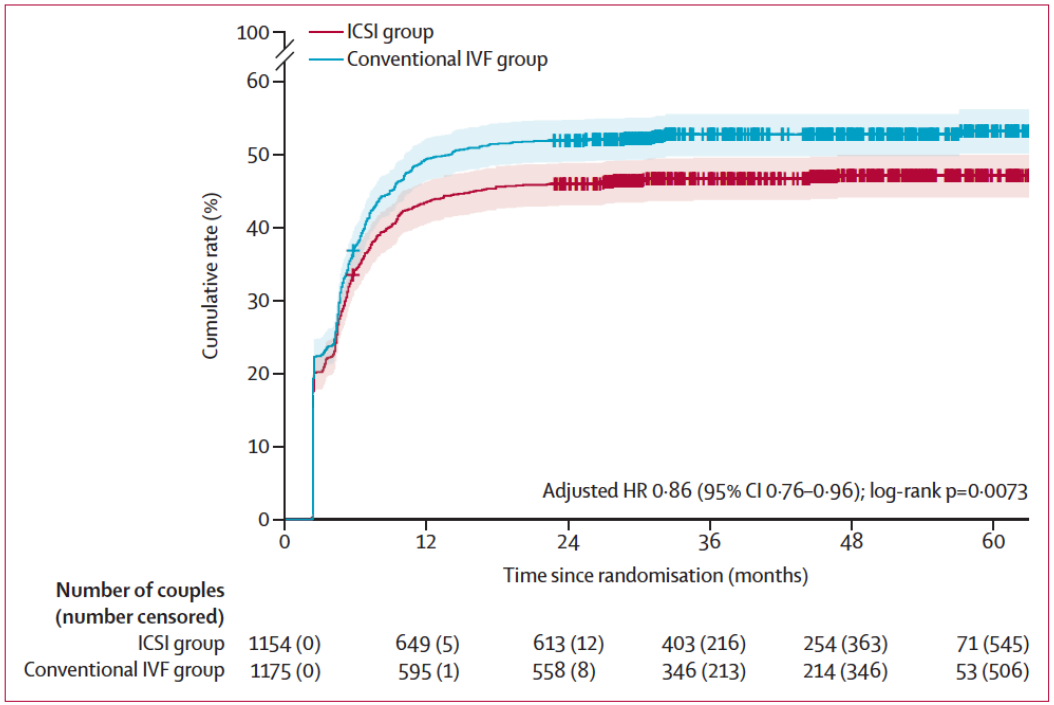

Figure 2: **Cumulative rate of ongoing pregnancy leading to live birth in the intention-to-treat population**
ICSI=intracytoplasmic sperm injection. IVF=in-vitro fertilisation. HR=hazard ratio.

Research in context

Evidence before this study

Intracytoplasmic sperm injection (ICSI), originally introduced for severe male infertility, has been used in couples with infertility with mild-to-moderate male factor. We searched PubMed and Cochrane Library for trials in English and Chinese, published from database inception to July 15, 2023, using the following search terms: "intracytoplasmic sperm injection" AND ("male subfertility" OR "male infertility" OR "oligoasthenozoospermia" OR "oligozoospermia" OR "asthenozoospermia" OR "teratozoospermia" OR "teratospermia" OR "abnormal sperm morphology"). A Cochrane review, including two multicentre randomised trials, showed no benefit of ICSI over conventional in-vitro fertilisation (IVF) in improving rates of implantation or live birth among couples with infertility with typical sperm concentration and motility. However, there is no evidence from randomised trials comparing the use of ICSI versus conventional IVF in couples with infertility with non-severe male factor. Despite this scarcity of level I evidence supporting the use of ICSI in this population, use of ICSI has steadily increased worldwide.

Added value of this study

In this investigator-initiated, multicentre, open-label, randomised controlled trial, 2329 couples with infertility with non-severe male factor were recruited from ten reproductive medicine centres across China and included in the primary intention-to-treat analysis (1154 in the ICSI group and 1175 in the conventional IVF group). Our analysis showed similar rates of live birth after first embryo transfer (the primary outcome) between both groups. Compared with the conventional IVF group, the ICSI group had fewer available embryos on day 3 and a lower implantation rate. No significant differences were found in any of the prespecified secondary outcomes for efficacy or safety.

Implications of all the available evidence

Our trial shows that, compared with conventional IVF, ICSI does not improve live birth rate in couples with infertility with non-severe male factor. Given that ICSI is an invasive procedure, associated with additional costs and a potential increased risk to offspring health, conventional IVF should be recommended as the treatment of choice for this population.

Stark racial disparities in murder victimization persist, even as overall murder rate declines

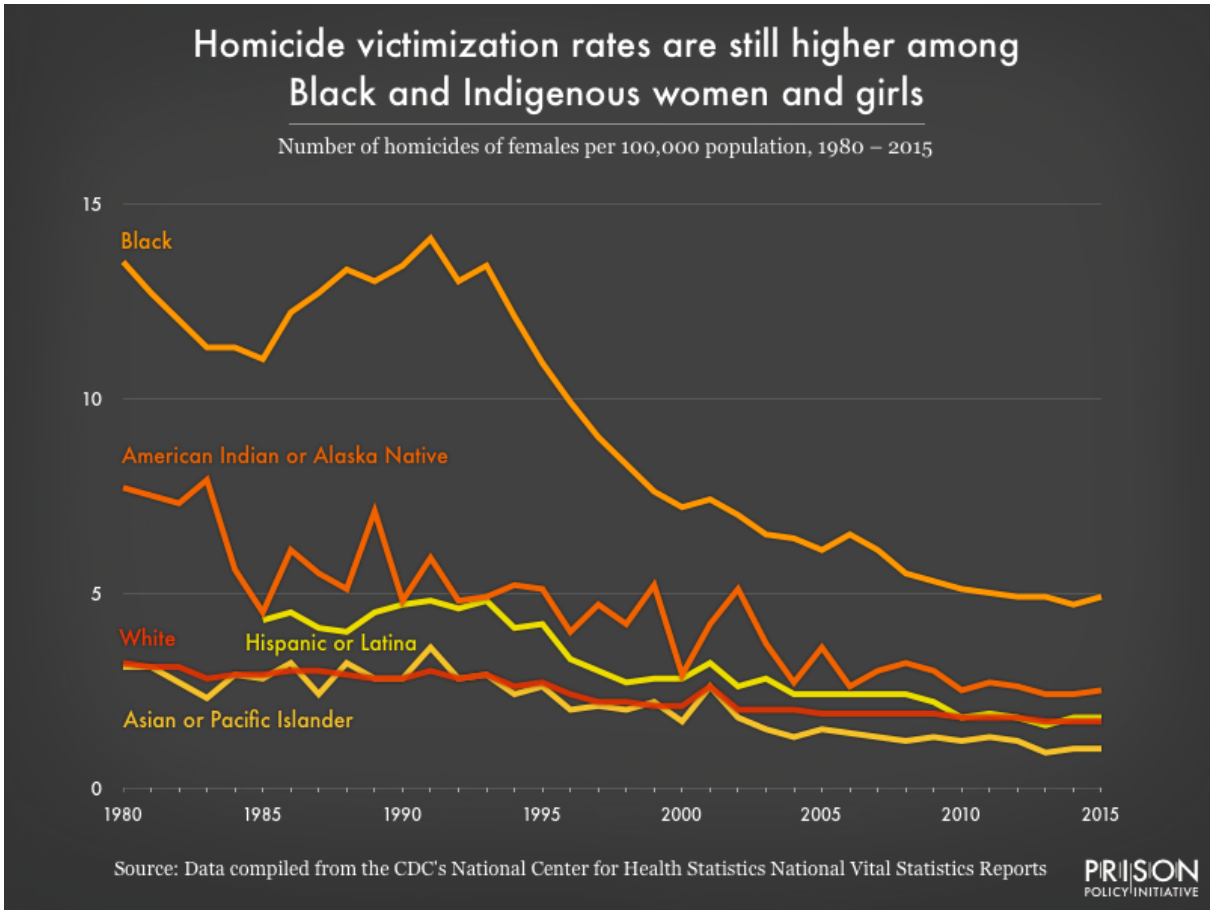

Racial inequities in homicide rates and homicide methods among Black and White women aged 25–44 years in the USA, 1999–2020: a cross-sectional time series study

Summary

Background In the USA, Black women aged 25–44 years are disproportionately murdered compared with their White counterparts. Despite ongoing efforts to reduce racial and structural inequities, the result of these efforts remains unclear, particularly in light of the COVID-19 pandemic.

Methods This study examined a cross-sectional time series of homicide death rates, by race, from the Centers for Disease Control and Prevention Wide-ranging Online Data for Epidemiologic Research system. We included data for women aged 25–44 years between 1999 and 2020 among 30 states in the USA. Homicide death was classified using underlying cause and multiple cause of death codes; mortality rates were calculated per 100 000 based on US Census Bureau population sizes. Homicide methods were classified as firearm, cutting or piercing, and other. Firearm homicides were compared with other homicides with logistic regression including covariates of race, time, and their interaction. We report odds ratios and 95% CIs.

Findings In 2020, the homicide rate among Black women was 11·6 per 100 000, compared with 3 per 100 000 among White women. This inequity has persisted over time and is virtually unchanged since 1999. Homicide inequities vary across US states; in 11 states, racial inequities have increased since 1999. The racial inequity was greatest in Wisconsin, where in 2019–20, Black women aged 25–44 years were 20 times more likely to die by homicide than White women. Homicide by firearm is increasing in frequency; women in the USA had 2·44 (95% CI 2·14–2·78) times the odds of homicide involving firearms in 2019–20 compared with 1999–2003. Firearm homicide deaths are disproportionately concentrated among Black women in every region in the USA.

Interpretation Our findings suggest that there is an urgent need to address homicide inequities among Black and White women in the USA. Enacting federal legislation that reduces gun access is a crucial step. Policy makers must address long-standing structural factors that underpin elevated gun violence by implementing sustainable wealth-building opportunities; developing desegregated, mixed income and affordable housing; and increasing green spaces in communities where Black women largely reside.

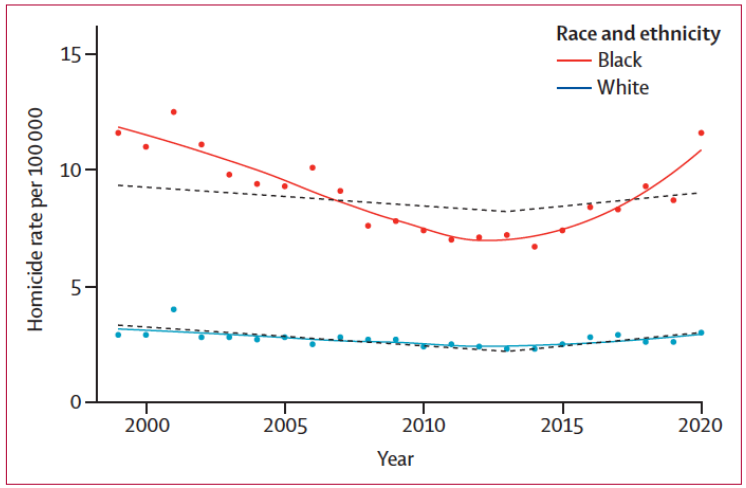

Figure 1: **Homicide rate per 100 000 among Black and White women aged 25–44 years in the USA from 1999 to 2020**

Includes locally estimated scatterplot smoothing regression estimated homicide rates and 95% CIs. Joinpoint regression analysis indicated that the best fitting model included two linear slopes (one joinpoint) for the Black trend line with a significant change in the magnitude of the slope in 2014 (1999–2013, slope −0·35, SE=0·04, p<0·010; 2014–20, slope 1·05, SE=0·15, p<0·010). The best fitting model included one linear slope (no joinpoints, slope −0·02, SE=0·01, p=0·080) for the White trend line. Additionally, we ran a parallel pairwise comparison to statistically test for parallelism between the two groups. This test rejected parallelism with a p value of <0·0010, indicating that the slopes were significantly different between Black and White women. Joinpoint estimates are visualised with black dashed lines.

	1999–2003	2004–08	2009–13	2014–18	2019–20	Difference in difference: 1999–2003 *vs* 2009–13	Difference in difference: 2009–13 *vs* 2019–20	Difference in difference: 1999–2003 *vs* 2019–20	Overall homicide rate per 100 000
South									
RR (95% CI)	2·88 (2·70 to 3·06)	2·56 (2·40 to 2·74)	2·45 (2·28 to 2·63)	2·46 (2·30 to 2·64)	2·78 (2·52 to 3·07)	0·86*	1·14*	0·96*	4·80
Rate difference (95% CI)	7·20 (6·60 to 7·70)	5·50 (5·10 to 6·10)	4·60 (4·20 to 5·10)	4·90 (4·40 to 5·30)	6·40 (5·60 to 7·10)	−2·60*	1·80*	−0·8*	..
Alabama									
RR (95% CI)	3·19 (2·47 to 4·10)	2·83 (2·14 to 3·75)	2·36 (1·74 to 3·20)	2·62 (1·98 to 3·47)	2·07 (1·35 to 3·16)	0·74*	0·88*	0·65*	6·60
Rate difference (95% CI)	10·35 (7·70 to 13·00)	7·65 (5·30 to 10·00)	5·30 (3·20 to 7·40)	6·98 (4·70 to 9·30)	5·48 (1·90 to 9·00)	−5·05*	0·19*	−4·87*	..
South Carolina									
RR (95% CI)	2·09 (1·58 to 2·78)	2·72 (1·99 to 3·71)	2·08 (1·51 to 2·88)	2·16 (1·58 to 2·95)	2·56 (1·67 to 3·93)	0·99*	1·24*	1·22*	5·70
Rate difference (95% CI)	5·31 (3·00 to 7·60)	6·19 (4·00 to 8·40)	4·07 (2·10 to 6·10)	4·32 (2·40 to 6·30)	6·89 (3·30 to 10·40)	−1·24*	2·82*	1·58*	..
Arkansas									
RR (95% CI)	4·42 (2·98 to 6·55)	3·91 (2·62 to 5·84)	3·45 (2·29 to 5·22)	2·98 (2·04 to 4·35)	6·06 (3·59 to 10·22)	0·79*	1·76*	1·37*	5·70
Rate difference (95% CI)	11·62 (7·30 to 16·00)	10·18 (6·00 to 14·30)	8·68 (4·80 to 12·60)	8·82 (4·80 to 12·80)	20·33 (12·00 to 28·70)	−2·94*	11·65*	8·71*	..
Tennessee									
RR (95% CI)	3·63 (2·83 to 4·66)	2·46 (1·86 to 3·25)	2·46 (1·84 to 3·29)	3·03 (2·30 to 4·01)	3·88 (2·64 to 5·69)	0·68*	1·58*	1·07*	5·20
Rate difference (95% CI)	10·44 (7·70 to 13·20)	5·86 (3·60 to 8·20)	5·31 (3·10 to 7·50)	6·92 (4·70 to 9·20)	10·68 (6·60 to 14·70)	−5·13*	5·37*	0·24*	..
Georgia									
RR (95% CI)	3·02 (2·47 to 3·71)	2·41 (1·94 to 3·01)	2·42 (1·89 to 3·11)	2·07 (1·65 to 2·59)	2·77 (1·96 to 3·90)	0·81*	1·15*	0·92*	4·80
Rate difference (95% CI)	7·25 (5·70 to 8·80)	4·68 (3·40 to 6·00)	3·62 (2·50 to 4·70)	3·47 (2·30 to 4·60)	5·37 (3·50 to 7·30)	−3·63*	1·75*	−1·88*	..
Oklahoma									
RR (95% CI)	2·73 (1·70 to 4·39)	2·55 (1·57 to 4·14)	3·01 (1·90 to 4·78)	2·08 (1·24 to 3·48)	5·13 (2·89 to 9·11)	1·11*	1·71*	1·88*	4·60
Rate difference (95% CI)	6·86 (2·23 to 11·50)	6·34 (1·80 to 10·90)	7·62 (3·00 to 12·30)	4·07 (3·41 to 7·80)	15·84 (6·90 to 24·80)	0·76*	8·22*	8·98*	..
Kentucky									
RR (95% CI)	2·57 (1·68 to 3·93)	1·90 (1·12 to 3·23)	3·35 (2·19 to 5·13)	1·76 (1·09 to 2·83)	3·93 (2·33 to 6·63)	1·31*	1·18*	1·53*	4·60
Rate difference (95% CI)	6·76 (2·40 to 11·10)	3·22 (−0·02 to 6·60)	8·12 (3·80 to 12·50)	3·40 (−0·05 to 6·90)	13·88 (5·60 to 22·20)	1·36*	5·76*	7·12*	..
Florida									
RR (95% CI)	2·22 (1·86 to 2·66)	2·48 (2·08 to 2·97)	2·53 (2·11 to 3·04)	2·21 (1·84 to 2·66)	2·08 (1·60 to 2·70)	1·14*	0·83*	0·94*	4·40
Rate difference (95% CI)	4·84 (3·50 to 6·20)	5·31 (4·00 to 6·60)	4·92 (3·70 to 6·10)	3·86 (2·80 to 4·90)	4·11 (2·40 to 5·90)	0·09*	−0·81*	−0·73*	..
North Carolina									
RR (95% CI)	2·74 (2·20 to 3·40)	2·17 (1·72 to 2·73)	1·78 (1·35 to 2·34)	2·45 (1·90 to 3·16)	3·22 (2·22 to 4·67)	0·65*	1·81*	1·18*	4·40
Rate difference (95% CI)	6·56 (4·80 to 8·30)	4·37 (2·80 to 5·90)	2·28 (1·00 to 3·50)	3·99 (2·70 to 5·30)	5·99 (3·70 to 8·30)	−4·28*	3·71*	−0·57*	..
Maryland									
RR (95% CI)	3·56 (2·67 to 4·74)	2·59 (1·89 to 3·53)	2·87 (2·02 to 4·08)	2·80 (1·98 to 3·95)	2·15 (1·34 to 3·48)	0·81*	0·75*	0·60*	4·30
Rate difference (95% CI)	6·94 (5·20 to 8·70)	4·36 (2·80 to 5·90)	3·97 (2·50 to 5·40)	4·03 (2·60 to 5·50)	3·71 (1·30 to 6·20)	−2·97*	−0·26*	−3·23*	..

(Table continues on next page)

	1999–2003	2004–08	2009–13	2014–18	2019–20	Difference in difference: 1999–2003 *vs* 2009–13	Difference in difference: 2009–13 *vs* 2019–20	Difference in difference: 1999–2003 *vs* 2019–20	Overall homicide rate per 100 000
(Continued from previous page)									
Texas									
RR (95% CI)	2·59 (2·18 to 3·06)	2·41 (2·04 to 2·86)	2·29 (1·92 to 2·74)	2·57 (2·19 to 3·01)	2·84 (2·24 to 3·59)	0·88*	1·25*	1·10*	4·00
Rate difference (95% CI)	5·54 (4·20 to 6·90)	4·92 (3·70 to 6·20)	3·93 (2·80 to 5·00)	5·01 (3·90 to 6·10)	5·72 (4·00 to 7·40)	−1·61*	1·79*	0·18*	..
Delaware									
RR (95% CI)	NA	2·67 (1·14 to 6·30)	NA	NA	NA	NA	NA	NA	3·60
Rate difference (95% CI)	NA	4·39 (−0·01 to 9·00)	NA	NA	NA	NA	NA	NA	..
Virginia									
RR (95% CI)	3·38 (2·62 to 4·36)	2·96 (2·21 to 3·97)	3·27 (2·36 to 4·51)	3·32 (2·45 to 4·49)	1·77 (1·08 to 2·89)	0·97*	0·55*	0·52*	3·50
Rate difference (95% CI)	7·02 (5·10 to 8·90)	4·76 (3·10 to 6·40)	4·33 (2·80 to 5·80)	4·93 (3·40 to 6·50)	2·13 (0·04 to 4·20)	−2·69*	−2·20*	−4·89	..
Midwest									
RR (95% CI)	6·16 (5·61 to 6·76)	5·36 (4·83 to 5·95)	4·32 (3·85 to 4·86)	4·85 (4·37 to 5·38)	7·22 (6·24 to 8·35)	0·70*	1·67*	1·17*	3·60
Rate difference (95% CI)	12·70 (11·60 to 13·70)	9·70 (8·70 to 10·60)	6·90 (6·10 to 7·70)	9·30 (8·30 to 10·20)	15·00 (13·20 to 16·70)	−5·80*	8·1*	2·30*	..
Missouri									
RR (95% CI)	4·56 (3·43 to 6·05)	4·92 (3·56 to 6·80)	5·38 (3·92 to 7·38)	6·06 (4·67 to 7·86)	5·59 (3·88 to 8·05)	1·18*	1·04*	1·22*	5·10
Rate difference (95% CI)	12·25 (8·80 to 15·70)	10·12 (7·00 to 13·30)	11·46 (8·20 to 14·80)	17·79 (13·80 to 21·80)	20·97 (14·20 to 27·70)	−0·79*	9·51*	8·72*	..
Indiana									
RR (95% CI)	6·56 (4·98 to 8·66)	5·34 (3·93 to 7·26)	2·08 (1·39 to 3·10)	5·09 (3·79 to 6·84)	6·22 (4·09 to 9·44)	0·32*	2·99*	0·95*	4·40
Rate difference (95% CI)	17·49 (13·10 to 21·90)	12·52 (8·80 to 16·30)	3·47 (1·00 to 5·90)	12·47 (8·90 to 16·00)	16·74 (10·60 to 22·80)	−14·02*	13·27*	−0·75*	..
Michigan									
RR (95% CI)	6·45 (5·24 to 7·95)	5·19 (4·08 to 6·60)	5·17 (3·90 to 6·87)	4·88 (3·78 to 6·30)	6·97 (4·72 to 10·28)	0·81*	1·35*	1·08*	4·30
Rate difference (95% CI)	14·77 (12·30 to 17·20)	10·24 (8·10 to 12·40)	8·03 (6·00 to 10·00)	9·54 (7·40 to 11·70)	13·18 (9·40 to 17·00)	−6·74*	5·15*	−1·59*	..
Michigan									
RR (95% CI)	4·47 (3·52 to 5·67)	5·05 (3·99 to 6·39)	3·73 (2·86 to 4·85)	3·46 (2·72 to 4·39)	5·26 (3·83 to 7·21)	0·84*	1·42*	1·18*	3·80
Rate difference (95% CI)	8·42 (6·40 to 10·50)	9·84 (7·70 to 12·00)	6·54 (4·70 to 8·40)	7·27 (5·30 to 9·20)	13·68 (9·90 to 17·50)	−1·88*	7·14*	5·26*	..
Kansas									
RR (95% CI)	6·15 (3·64 to 10·40)	4·83 (2·68 to 8·71)	4·30 (2·48 to 7·45)	3·68 (2·11 to 6·44)	6·57 (3·03 to 14·24)	0·70*	1·53*	1·07*	3·80
Rate difference (95% CI)	14·14 (6·70 to 21·60)	10·24 (3·70 to 16·80)	10·75 (4·00 to 17·50)	9·14 (2·90 to 15·40)	15·98 (4·20 to 27·70)	−3·39*	5·23*	1·84*	..
Illinois									
RR (95% CI)	6·81 (5·61 to 8·25)	5·34 (4·23 to 6·73)	4·84 (3·69 to 6·36)	6·02 (4·70 to 7·71)	11·21 (7·65 to 16·42)	0·72*	2·32*	1·65*	3·60
Rate difference (95% CI)	13·95 (11·90 to 16·00)	8·52 (6·80 to 10·20)	5·92 (4·50 to 7·40)	8·73 (7·00 to 10·50)	15·06 (11·70 to 18·50)	−8·03*	9·14*	1·11*	..
Wisconsin									
RR (95% CI)	6·42 (4·07 to 10·12)	5·42 (3·45 to 8·52)	5·55 (3·47 to 8·87)	5·19 (3·35 to 8·06)	20·16 (10·65 to 38·16)	0·86*	3·63*	3·14*	2·50
Rate difference (95% CI)	9·13 (5·00 to 13·20)	8·42 (4·50 to 12·30)	7·76 (4·10 to 11·40)	8·24 (4·60 to 11·90)	22·09 (13·60 to 30·60)	−1·37*	14·33*	12·96*	..

(Table continues on next page)

	1999–2003	2004–08	2009–13	2014–18	2019–20	Difference in difference: 1999–2003 *vs* 2009–13	Difference in difference: 2009–13 *vs* 2019–20	Difference in difference: 1999–2003 *vs* 2019–20	Overall homicide rate per 100 000
(Continued from previous page)									
Minnesota									
RR (95% CI)	3·87 (1·97 to 7·59)	7·36 (4·20 to 12·89)	5·55 (2·96 to 10·40)	NA	6·20 (2·88 to 13·37)	1·43*	1·12*	1·60*	1·60
Rate difference (95% CI)	4·65 (0·07 to 8·60)	7·84 (3·60 to 12·00)	4·91 (1·70 to 8·10)	NA	6·99 (2·00 to 12·00)	0·26*	2·08*	2·34*	..
West									
RR (95% CI)	3·36 (2·94 to 3·84)	3·67 (3·20 to 4·21)	2·36 (1·98 to 2·79)	2·73 (2·35 to 3·18)	2·78 (2·24 to 3·45)	0·71*	1·18*	0·83*	2·90
Rate difference (95% CI)	6·90 (5·70 to 8·10)	6·80 (5·60 to 7·90)	3·20 (2·30 to 4·00)	4·20 (3·30 to 5·10)	4·70 (3·30 to 6·20)	−3·70*	1·5*	−2·20*	..
Nevada									
RR (95% CI)	4·08 (2·49 to 6·67)	2·01 (1·15 to 3·51)	1·49 (0·76 to 2·94)	3·70 (2·32 to 5·90)	2·90 (1·35 to 6·24)	0·36*	1·95*	0·71*	4·60
Rate difference (95% CI)	13·65 (6·00 to 21·30)	4·73 (−0·02 to 9·6)	1·78 (−0·02 to 5·30)	8·73 (4·20 to 13·20)	5·83 (1·50 to 11·50)	−11·87	4·05	−7·82	..
Arizona									
RR (95% CI)	2·66 (1·63 to 4·34)	3·07 (1·91 to 4·92)	2·08 (1·21 to 3·56)	1·57 (0·88 to 2·78)	NA	0·79	NA	NA	3·90
Rate difference (95% CI)	7·97 (2·00 to 13·90)	7·43 (2·60 to 12·30)	3·54 (0·40 to 7·00)	1·76 (−0·09 to 4·50)	NA	−4·43	NA	NA	..
Colorado									
RR (95% CI)	4·26 (2·53 to 7·17)	3·37 (1·87 to 6·08)	2·51 (1·30 to 4·85)	1·91 (0·99 to 3·66)	NA	0·59*	NA	NA	2·90
Rate difference (95% CI)	8·96 (3·40 to 14·60)	6·04 (1·30 to 10·70)	3·62 (−0·02 to 7·40)	2·44 (−0·08 to 5·70)	NA	−5·34	NA	NA	
Washington									
RR (95% CI)	3·69 (2·05 to 6·64)	NA	NA	2·19 (1·22 to 3·91)	NA	NA	NA	NA	2·40
Rate difference (95% CI)	5·58 (1·40 to 9·80)	NA	NA	2·75 (−0·04 to 5·50)	NA	NA	NA	NA	..
Northeast									
RR (95% CI)	3·15 (2·82 to 3·51)	3·27 (2·86 to 3·73)	2·95 (2·55 to 3·42)	2·96 (2·55 to 3·43)	3·30 (2·64 to 4·12)	0·94*	1·12*	1·05*	2·70
Rate difference (95% CI)	6·00 (5·20 to 6·80)	4·40 (3·70 to 5·00)	3·40 (2·80 to 4·00)	3·20 (2·60 to 3·80)	4·10 (3·00 to 5·00)	−2·60*	0·70*	−1·9*	..
Pennsylvania									
RR (95% CI)	4·86 (3·88 to 6·10)	3·76 (2·91 to 4·87)	4·17 (3·21 to 5·41)	3·65 (2·85 to 4·69)	5·45 (3·80 to 7·81)	0·86*	1·31*	1·12*	3·50
Rate difference (95% CI)	9·87 (7·70 to 12·10)	6·55 (4·70 to 8·40)	6·96 (5·10 to 8·80)	6·65 (4·80 to 8·50)	10·39 (7·10 to 13·70)	−2·91*	3·43*	0·52*	..
New Jersey									
RR (95% CI)	3·19 (2·45 to 4·14)	4·52 (3·31 to 6·18)	4·13 (2·82 to 6·05)	3·47 (2·43 to 4·96)	2·71 (1·52 to 4·80)	1·29*	0·66*	0·85*	2·90
Rate difference (95% CI)	6·10 (4·30 to 8·00)	6·05 (4·30 to 7·80)	4·03 (2·60 to 5·50)	4·03 (2·50 to 5·60)	3·09 (0·08 to 5·30)	−2·07*	−0·94*	−3·05	..
New York									
RR (95% CI)	2·30 (1·96 to 2·69)	2·77 (2·23 to 3·46)	2·25 (1·76 to 2·86)	2·58 (1·95 to 3·42)	2·65 (1·76 to 4·00)	0·98*	1·18*	1·15	2·90
Rate difference (95% CI)	4·91 (3·80 to 6·10)	2·32 (2·40 to 4·20)	2·25 (1·40 to 3·10)	1·95 (1·20 to 2·70)	2·38 (1·10 to 3·60)	−2·66*	0·13*	−2·53	..
Connecticut									
RR (95% CI)	2·10 (1·13 to 3·88)	2·85 (1·61 to 5·06)	3·98 (2·10 to 7·54)	2·42 (1·28 to 4·58)	NA	1·89*	NA	NA	2·20
Rate difference (95% CI)	2·31 (−0·02 to 4·80)	3·60 (0·09 to 6·30)	3·83 (1·30 to 6·40)	2·47 (0·02 to 4·80)	NA	1·52*	NA	NA	..

(Table continues on next page)

	1999–2003	2004–08	2009–13	2014–18	2019–20	Difference in difference: 1999–2003 *vs* 2009–13	Difference in difference: 2009–13 vs 2019–20	Difference in difference: 1999–2003 *vs* 2019–20	Overall homicide rate per 100 000
(Continued from previous page)									
Massachusetts									
RR (95% CI)	2·50 (1·46 to 4·29)	3·36 (1·94 to 5·82)	1·77 (0·90 to 3·50)	2·56 (1·48 to 4·44)	NA	0·71	NA	NA	1·60
Rate difference (95% CI)	2·60 (0·04 to 4·80)	3·06 (0·09 to 5·20)	1·05 (–0·05 to 2·60)	2·19 (0·04 to 3·90)	NA	–1·55	NA	NA	..

Comparisons were made between women categorised as Black (with or without Hispanic ethnicity) and White (with or without Hispanic ethnicity). States in the table are organised from highest to lowest overall homicide rates. NA indicates a state that was excluded due to suppressed data by race on CDC WONDER (numerator or denominator <10). Included states are those with at least some time periods in which homicide death counts were not suppressed. 21 states were excluded due to suppressed data at all timepoints. Columns of difference in difference compare the magnitude of the rate ratio and rate difference between time periods. NA=not available. RR=rate ratio. *Indicates that the p value for the interaction test between race and ethnicity and time period was <0·050.

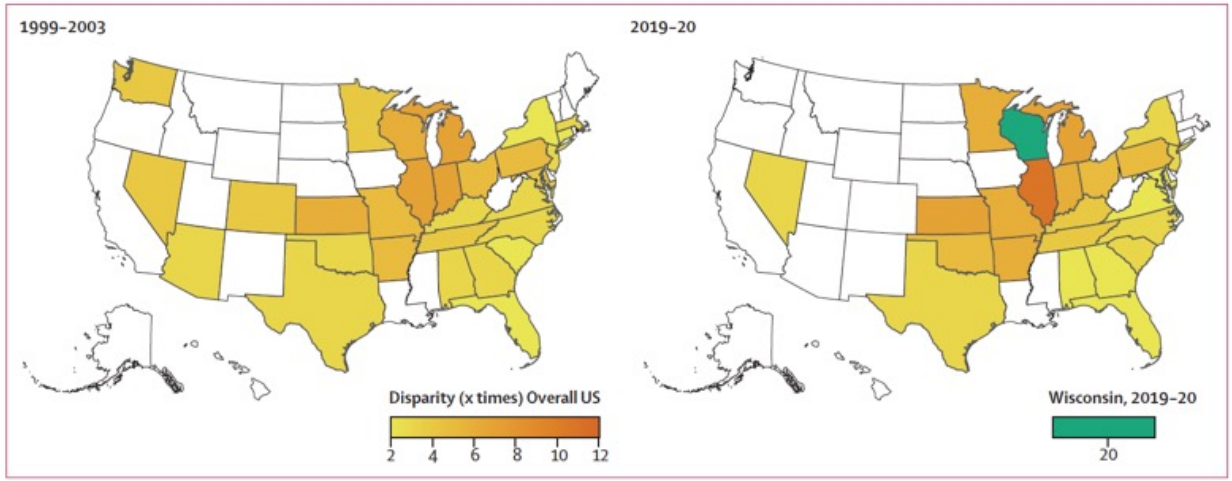

Figure 2: **Relative racial disparity in homicide (ratio of the Black homicide rate and White homicide rate) for 1999–2003 and 2019–20**
US states coloured in white did not have sufficient number of events for reporting. There were 29 states in the first study period and 24 states in the second study period with sufficient numbers of deaths (data source: CDC WONDER). The key indicates the relative homicide disparity between Black and White women. The magnitude of the disparity is indicated by the colour (ranging from yellow to orange for the USA and light orange to green for Wisconsin). The change in the disparity from 1999–2003 to 2019–20 can be visualised through the change in colour—ie, a change from a lighter yellow colour in 1999–2003 to a darker orange colour in 2019–20 indicates an increase in the disparity; a change from a darker colour to a lighter colour indicates a decrease in the disparity; no change in colour indicates no change in the disparity. In Wisconsin, the racial disparity in female homicide was substantially higher in 2019–20 (20 times) than the disparity between Black and White women for any other state in any time period, so we opted to show Wisconsin with a separate colour (green) in 2019–20.

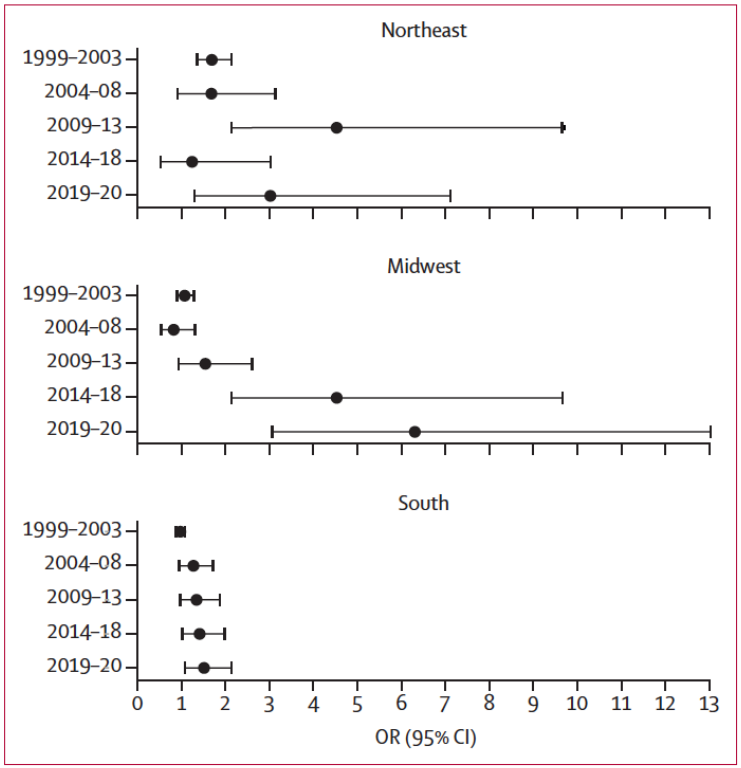

Figure 3: **Relationship between race and firearm deaths stratified by year and census region for the Northeast, Midwest, and South USA**
We did not have sufficient data to estimate the relationship between race and firearm death by year in the West. p values for joint test for interaction between year category and race: Northeast (p=0·090), Midwest (p<0·0001), and South (p=0·030). OR=odds ratio.

Research in context

Evidence before this study

Black women are more likely than women of any other racial group in the USA to be murdered; this is one of the most robust, long-standing, and widely reported findings about women in homicide epidemiology, yet data are scarce. Emerging evidence suggests a strong association between elevated homicide rates and the effects of long-standing structural inequities (eg, educational attainment, unemployment, economic status and wealth distribution, extreme poverty, and home ownership) across the USA. This finding implies that elevated rates of homicide among women might be preventable through social, structural, legislative, and policy changes; understanding the extent to which disparities change across time provides crucial surveillance on the nature and scope of the ongoing problem, and state-level analyses allow for concentrated focus on areas in the most need of intervention. Indeed, there is also some evidence to suggest that racial inequities in homicide among Black and White women are larger, on average, in states that perform worse on indices of structural equity, thus state-level assessment is crucial. Reasons for this trend are unclear, and there are important limitations to the existing evidence that preclude robust inferences about the contexts and conditions that give rise to, and those that mitigate and prevent, inequities in homicide rates among Black and White women, including potential disparities in the lethal means through which homicide is perpetuated. The evidence is largely cross-sectional, inclusive of 36% of US states (only accounting for 18 of 50 states) and, crucially, fails to account for homicide trends during the height of the COVID-19 pandemic.

Added value of this study

We used time-series data from the largest and most comprehensive dataset, Centers for Disease Control and Prevention Wide-ranging Online Data for Epidemiologic Research data from 1999 to 2020, reporting deaths in the USA among women aged 25–44 years. We examined the extent to which homicide rates varied between Black and White women across states, and how inequities in homicides between Black and White women shifted across 22 years, including during the height of the COVID-19 pandemic. We found strong evidence that indicates inequities in homicide rates between Black women and White women. Notably, Black women are murdered 6 times more often, on average, than their White peers. Further, Black women residing in the Midwest and Northeast were more likely to be killed with a firearm than Black women residing in any other area of the country. Importantly, we found the greatest inequities are in areas of the country where concentrated disadvantage is pronounced. This finding is a crucial initial step towards developing targeted solutions to reduce inequitable homicide rates among Black women.

Implications of all the available evidence

There is strong evidence that the size of racial inequalities in homicide rates is driven by social and structural contexts. Disparities in deaths by firearms underscore the ongoing role of gun violence in the USA. Against a backdrop of high and rising rates of homicide among Black women, there is an urgent need to understand the contexts and conditions that reduce the likelihood of their premature death.

Abdominal painful mass after prolonged standing: nephroptosis in a 30-year-old woman

A 30-year-old woman was referred to our urology clinic reporting a 2-year history of pain in the right flank. The patient said the pain was worse after physical exercise or after standing up for a long time; after these activities, she said a painful abdominal mass would be present, which subsequently disappeared when she rested for a few minutes in a supine decubitus position. Additionally, she reported that her symptoms, which had started without any identified reason, had been getting worse and had begun to affect her ability to carry out her daily routine. The patient had no medical history and said she was otherwise healthy.

On examination, she was generally well; blood pressure was 95/65 mm Hg, pulse was 70 beats per min, and oxygen saturation was 100%. We found no masses or organomegaly. However, she showed us photographs of the abdominal mass in her right iliac fossa, which appeared after standing up for 30 min or after doing physical exercise.

Laboratory investigations were within typical range—notably renal function was normal. Urinalysis showed proteinuria of >300 mg/dL (typical range <150) and microhaematuria.

A CT and MRI showed bilateral simple renal cysts and a calyceal diverticulum, but these findings were not a satisfactory explanation of the patient's symptoms; there was no dilation of any part of the urinary system.

Intravenous urography (IVU), while the patient was standing over a period of 30 min, initially showed the right kidney in a typical position in the abdomen with no dilation of any part of the urinary tract (figure). However, during the investigation, the right kidney gradually descended towards the pelvis causing increasing ureteral ectasia. And by the end of the 30 min, the right ureter had completed folded over itself producing an acute obstructive uropathy with the patient reporting intense pain (figure).

After discussion with the patient—who reiterated that the severity of the pain impacted upon her daily life—we proceeded to do a laparoscopic right nephropexy to the abdominal wall. The patient recovered and was allowed home 2 days after the operation.

6 months later, a diuretic renogram showed preserved parenchymal function and non-obstructive excretion curves. A multiphase renal CT scan showed no complications or stenosis of the upper urinary tract; the patient was able to return to work and to do physical exercise.

Nephroptosis, also known as floating kidney, is a differential diagnosis of unexplained abdominal pain which would include renal or intestinal infarction, nutcracker syndrome, ovarian vein syndrome or pelvic inflammatory disease in young women, and complications of a pelvic cyst—renal or ovarian.

Vertical nephroptosis, defined as a renal drop in the vertical position of ≥5 cm or the height of two vertebral bodies, is usually an accidental finding on IVU. Only 10% of patients—typically young, thin women—develop symptoms. Surgical correction is needed when it causes chronic complaints and worsens the quality of life—as in our patient. The symptoms, when present, are usually diagnostic. Complications include impaired renal function; ureteral obstruction and subsequent calculi and pyelonephritis; and hypertension and renal ischaemia resulting from elongation, twisting, or angulation of renal vessels.

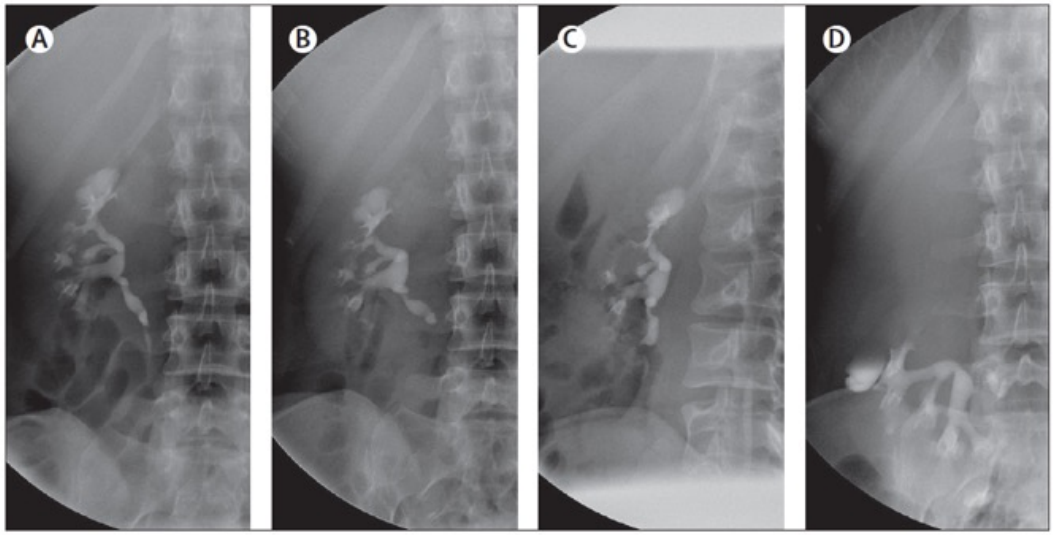

Figure: **Abdominal painful mass after prolonged standing: nephroptosis in a 30-year-old woman**
Intravenous urography, while the patient was standing over a period of 30 min, initially shows the right kidney in a typical position in the abdomen (A) with no dilation of any part of the urinary tract; during the investigation, the right kidney is shown as it gradually descends towards the pelvis (B; C), and after 30 min, the right ureter had completed folded over itself producing an acute obstructive uropathy with the patient reporting intense pain (D).

Menopause 1

An empowerment model for managing menopause

(Ermächtigung)

Menopause eventually happens to all people with typically functioning ovaries, and almost one billion women worldwide are postmenopausal. Although the biology of typical menopause is ubiquitous, the experience varies substantially. Factors contributing to the experience include not only individual factors, such as the nature and severity of symptoms, but also psychological, social, and contextual considerations, many of which are modifiable. In this first paper in the *Lancet* Series on menopause, we argue for a new approach that goes beyond the treatment of specific symptoms, to encompass a broad model to support women transitioning this life stage, using the model of empowerment. WHO defines empowerment as an active process of gaining knowledge, confidence, and self-determination to self-manage health and make informed decisions about care. Rather than focusing on menopause as an endocrine deficiency, we propose an empowerment model that recognises factors modifying the experience, in which the patient is an expert in their own condition and the health-care worker supports the patient to become an equal and active partner in managing their own care.

Menopause 2

Optimising health after early menopause

The typical age at menopause is 50–51 years in high-income countries. However, early menopause is common, with around 8% of women in high-income countries and 12% of women globally experiencing menopause between the ages of 40 years and 44 years. Menopause before age 40 years (premature ovarian insufficiency) affects an additional 2–4% of women. Both early menopause and premature ovarian insufficiency can herald an increased risk of chronic disease, including osteoporosis and cardiovascular disease. People who enter menopause at younger ages might also experience distress and feel less supported than those who reach menopause at the average age. Clinical practice guidelines are available for the diagnosis and management of premature ovarian insufficiency, but there is a gap in clinical guidance for early menopause. We argue that instead of distinct age thresholds being applied, early menopause should be seen on a spectrum between premature ovarian insufficiency and menopause at the average age. This Series paper presents evidence for the short-term and long-term consequences of early menopause. We offer a practical framework for clinicians to guide diagnosis and management of early menopause, which considers the nature and severity of symptoms, age and medical history, and the individual's wishes and priorities to optimise their quality of life and short-term and long-term health. We conclude with recommendations for future research to address key gaps in the current evidence.

Menopause 3

Promoting good mental health over the menopause transition

The potential risk for mental health conditions over the menopause transition shapes women's expectations and informs putative physiological mechanisms regulating women's mental health. We review evidence from prospective studies reporting on associations between mental health conditions and the menopause transition. Major depressive disorder and the more prevalent subthreshold depressive symptoms are the most common conditions studied. We reviewed 12 prospective studies reporting depressive symptoms, major depressive disorder, or both over the menopause transition and found no compelling evidence for a universal increased risk for either condition. However, specific subgroups of participants, primarily defined by menopause-related risk factors (ie, vasomotor symptoms that are severe or disturb sleep, a long duration of the transition, or reproductive hormone dynamics) and psychosocial risk factors (eg, stressful life events), were vulnerable to depressive symptoms. The increased risk of major depressive disorder over the menopause transition appears predominantly in individuals with previous major depressive disorder. Greater focus on recognising risk factors in primary care is warranted. On the basis of scarce data, we found no compelling evidence that risk of anxiety, bipolar disorder, or psychosis is universally elevated over the menopause transition. Potential misattribution of psychological distress and psychiatric disorders to menopause could harm women by delaying accurate diagnosis and the initiation of effective psychotropic treatments, and by creating negative expectations for people approaching menopause. A paradigm shift is needed. We conclude with recommendations for the detection and treatment of depressive symptoms or major depressive disorder and strategies to promote good mental health over the menopause transition, while responsibly preparing and supporting those at risk.

Menopause 4

Managing menopause after cancer

Globally, 9 million women are diagnosed with cancer each year. Breast cancer is the most commonly diagnosed cancer worldwide, followed by colorectal cancer in high-income countries and cervical cancer in low-income countries. Survival from cancer is improving and more women are experiencing long-term effects of cancer treatment, such as premature ovarian insufficiency or early menopause. Managing menopausal symptoms after cancer can be challenging, and more severe than at natural menopause. Menopausal symptoms can extend beyond hot flushes and night sweats (vasomotor symptoms). Treatment-induced symptoms might include sexual dysfunction and impairment of sleep, mood, and quality of life. In the long term, premature ovarian insufficiency might increase the risk of chronic conditions such as osteoporosis and cardiovascular disease. Diagnosing menopause after cancer can be challenging as menopausal symptoms can overlap with other common symptoms in patients with cancer, such as fatigue and sexual dysfunction. Menopausal hormone therapy is an effective treatment for vasomotor symptoms and seems to be safe for many patients with cancer. When hormone therapy is contraindicated or avoided, emerging evidence supports the efficacy of non-pharmacological and non-hormonal treatments, although most evidence is based on women older than 50 years with breast cancer. Vaginal oestrogen seems safe for most patients with genitourinary symptoms, but there are few non-hormonal options. Many patients have inadequate centralised care for managing menopausal symptoms after cancer treatment, and more information is needed about cost-effective and patient-focused models of care for this growing population.

Key messages

- More than 9 million women are diagnosed with cancer each year and treatments commonly induce early menopause and menopausal symptoms
- Many patients do not have access to effective treatments, even in high-income countries, with an even greater impairment of quality of life and psychological distress in low-income settings
- Diagnosing menopause after cancer can be challenging and many women resume menstruation within 2 years of chemotherapy completion; undetectable anti-Müllerian hormone at 30 months predicts menopause after chemotherapy for breast cancer and menopause is almost universal after ovarian radiation
- Women younger than 45 years without contraindications should be offered an individualised treatment plan including menopausal hormone therapy after cancer treatment
- If menopausal hormone therapy is contraindicated, non-pharmacological and non-hormonal treatments are available for vasomotor symptoms; vaginal oestrogen seems to be safe for most patients with cancer and growing evidence supports safety after breast cancer
- Multidisciplinary management of menopause after cancer is essential and should include primary care and, if appropriate, allied health practitioners
- Reaching the population who need treatment is a global problem and online platforms are being developed to better support and empower patients with cancer to make shared, evidenced-based decisions with their local health-care provider

Panel 1: Fictional clinical case study

- A 37-year-old woman with a male partner and two children aged 5 years and 3 years visited her primary care provider because of sleeping difficulties. The primary care provider knows her well. The patient previously had imaging to investigate right-sided pain, which revealed a complex ovarian mass. This mass was subsequently found to be stage 1C1 high-grade serous ovarian cancer. She had a total abdominal hysterectomy and removal of both ovaries, staging laparotomy, and adjuvant systemic chemotherapy. Genetic testing showed that she carried the *BRCA1* pathogenic variant, so both ovaries were removed. She also decided to undergo risk-reducing bilateral mastectomy with informed consent.
- When the primary care provider asked more about her sleeping problems, the patient started to cry. She was frustrated by this show of emotion and said that she was not herself anymore. She found that minor problems were harder to deal with and she easily became emotional, which had caused arguments with her partner and her parents. Her family members were concerned about her health during her cancer treatment, but now that she was cured, they did not understand why she was always angry or sad. When she tried to make up with her partner, he often wanted to initiate sex. However, sexual intercourse was painful. Also, she was self-conscious about her appearance after mastectomy.
- She was concerned about these changes and the effect they had on her life, especially at night. When she eventually fell asleep, she sometimes suddenly woke up feeling very hot, sweaty, and anxious. Sometimes these sensations also occurred during the day. After telling her story, she felt relieved to have told someone about her problems and was hopeful that the primary care provider could help to solve them.
- The primary care provider discussed with the patient that her symptoms (mood changes, vaginal dryness, hot flushes, and sleep disturbance) are all common after surgical menopause. This information gave great relief to the patient, who did not realise that removing her ovaries might have this effect. Previously she was blaming herself for feeling angry or sad, felt guilty about being unwilling to have penetrative intercourse, and was concerned about her relationship. She was also fearful that night sweats were a sign of brain metastases from her ovarian cancer. The primary care provider gave her information about symptoms after surgical menopause and possible treatments and made another appointment.
- When she returned a week later, the patient felt somewhat better. However, she continued to experience troublesome hot flushes, sleep disturbance, and vaginal dryness. The primary care provider had contacted the gynaecological oncologist to discuss treatment options. They advised that there were no contraindications to menopausal hormone therapy (MHT) in women with a history of high-grade serous ovarian cancer; however, the relevant studies had small sample sizes and short follow-up. Although the patient had a *BRCA1* pathogenic variant, there were no substantial concerns about breast cancer because she had undergone bilateral mastectomy and would be receiving oestrogen-only MHT.
- Together, the patient and the primary care provider discussed the treatment options. Initially, the patient was reluctant to consider pharmacological therapies because she had taken so much medication in the previous year. During an individualised discussion of the risks and benefits, the primary care provider explained that MHT was the most effective treatment for hot flushes and night sweats and would also prevent bone loss. The patient and the primary care provider made a joint decision that she should try MHT.
- A month later, the patient reported that her vasomotor symptoms were greatly improved and her sleep was much better. Her relationship with her family had improved and she had returned to work. She had recommenced sexual activity but continued to experience vaginal dryness, so the primary care provider offered vaginal topical oestrogen. However, the patient continued to experience anxiety, particularly a fear of cancer recurrence. Together, they agreed that help from a psychologist was needed, and the patient was referred for cognitive behavioural therapy.

Panel 2: Circumstances in which ovarian function can be preserved in gynaecological cancer

Consider ovarian preservation in premenopausal women with:

- Cervical cancer—stage 1 or 2A human papillomavirus-associated adenocarcinoma and squamous carcinoma of the cervix undergoing radical hysterectomy
- Endometrial cancer—stage 1 low grade (not associated with Lynch syndrome or *TP53* mutated); future molecular subtyping of endometrial cancer might improve stratification of care
- Ovarian cancer—stage 1 (A) low grade, contralateral ovary could be preserved after explaining the 6–13% risk of recurrence in the preserved ovary; germ cell tumours with early unilateral disease

Consider elective transposition in women younger than 40 years with:

- Cervical cancer—locally advanced, if primary chemoradiation is planned
- Rectal cancer—requiring neo-adjuvant chemoradiation
- Cancer requiring pelvic radiation (eg, anal, vulval, sarcoma)

Consider intra-operative transposition in women with:

- Cervical cancer—if radical hysterectomy is abandoned due to positive node or if adjuvant radiation is likely
- Rectal cancer—if adjuvant radiation is likely to be needed due to close margins or intra-operative complications

	Effect of MHT on cancer outcomes	Level of evidence	MHT use
Breast cancer: overall	Systematic review and meta-analysis (n=40 50) found increased risk of recurrence with tibolone or MHT (HR 1·46)[46]	Moderate	Avoid MHT
Breast cancer: oestrogen-receptor-negative	Subgroup analysis found no increased risk of recurrence with tibolone or MHT (HR 1·19)[46]	Moderate	Consider MHT in specific patients*
Breast cancer: oestrogen-receptor-positive	Subgroup analysis found increased risk of recurrence (HR 1·80) with tibolone or MHT[46]	Moderate	Avoid MHT
Uterine sarcomas	European guidelines suggest avoiding MHT, might be oestrogen sensitive[48]	Very low	Avoid MHT
Ovarian cancer: low-grade serous and granulosa cell	European guidelines suggest avoiding MHT, might be oestrogen sensitive[48]	Very low	Avoid MHT
Low-grade, early-stage endometrial cancer	Systematic review found no effect on cancer outcomes[49]	Moderate	Consider MHT
Cervical cancer	One small retrospective study (n=120) found no effect on cancer outcomes;[50] European guidelines suggest offering MHT[51]	Very low	Consider MHT
Haematological cancer	One small study (n=130) showed no effect on cancer outcomes[52]	Very low	Consider MHT
Early cutaneous malignant melanoma	One small study (n=206) showed no effect on cancer outcomes[53]	Very low	Consider MHT
Colorectal cancer	One large prospective study (n=834)[54] and one national cohort study[55] reported improved cancer outcomes	Low	Consider MHT
Hepatocellular cancer	One case-control study (n=244) reported improved cancer outcomes[56]	Very low	Consider MHT
Ovarian germ cell tumours	European guidelines suggest offering on an individualised basis[48]	Very low	Consider MHT
Epithelial ovarian cancer	Systematic review found uncertain evidence for efficacy or safety of MHT[57]	Moderate	Consider MHT
Vaginal, vulval, and anal squamous cell carcinoma	Do not express oestrogen receptors, MHT thought to be safe[58]	Very low	Consider MHT
Kidney cancer	Meta-analysis suggests better cancer outcomes with MHT[59]	Low	Consider MHT
Lung cancer	Mixed evidence: prospective cohort study (n=727)[60] and SEER data (n=485)[61] showed improved cancer outcomes; retrospective study (n=498)[62] and RCT[63] showed increased mortality	Moderate	Consider MHT

Figure 1: **Use of systemic MHT (or tibolone) by cancer type**
Red indicates that MHT should be avoided; yellow indicates that MHT should be considered. Grading uses the Grading of Recommendations, Assessment, Development, and Evaluation approach.[64] MHT=menopausal hormone therapy. HR=hazard ratio. RCT=randomised controlled trial. * After oestrogen-receptor-negative breast cancer, consider MHT if menopausal symptoms do not respond to non-hormonal treatments, particularly following bilateral mastectomy. Discuss with the patient that evidence to inform the safety of MHT in these circumstances is limited.[65–69]

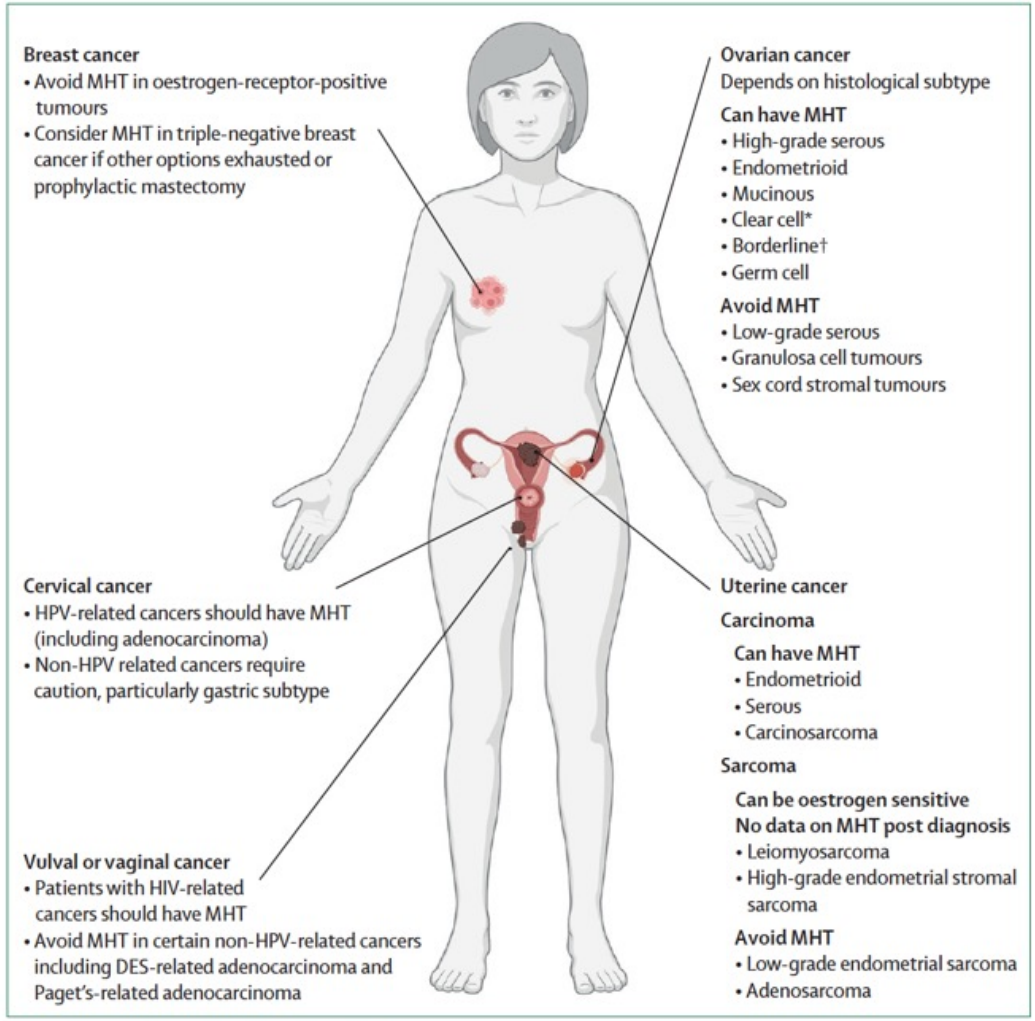

Figure 2: **Use of MHT after female-specific cancers**

MHT=menopausal hormone therapy. HPV=human papillomavirus. *Consider transdermal due to increased venous thromboembolism risk. †Fully resected, no invasive implants.

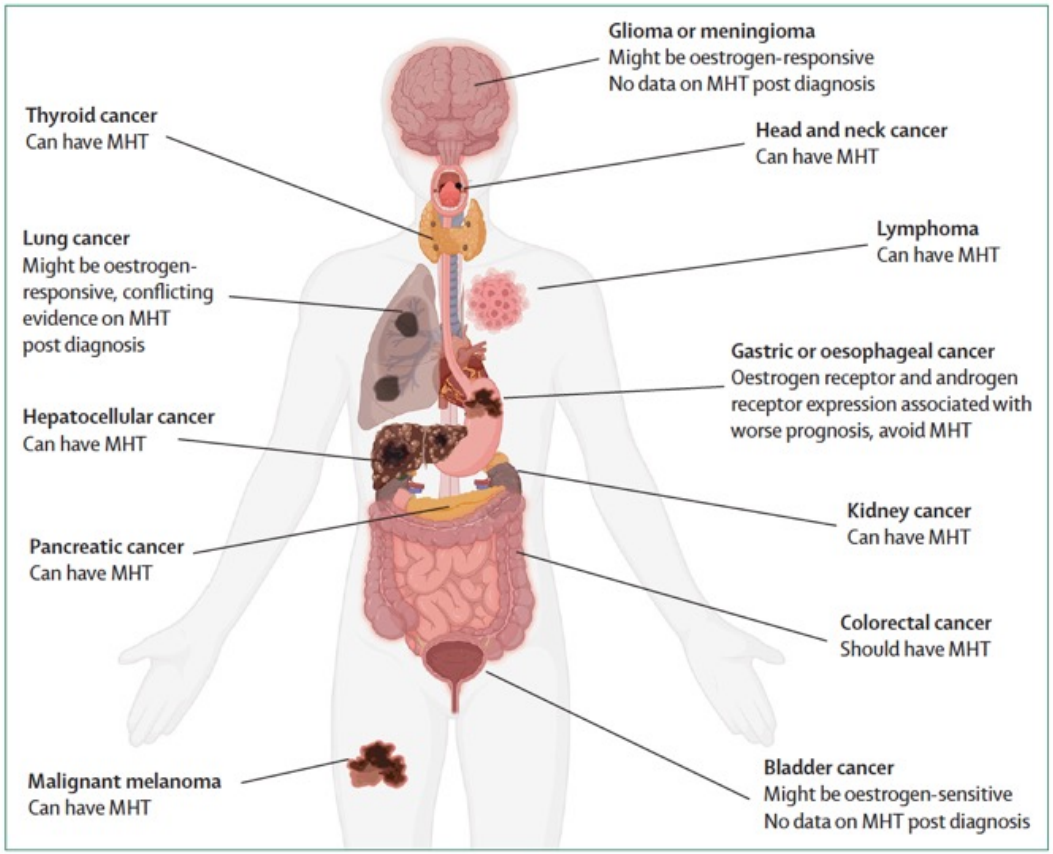

Figure 3: **Use of MHT after non-female specific cancers**
MHT=menopausal hormone therapy.

	Vasomotor symptoms	Sexual dysfunction	Vaginal dryness
Selected SSRIs and SNRIs	Likely	Unlikely*	Unlikely
Specific anticonvulsants	Likely	Unlikely	Unlikely
Oxybutynin	Likely	Unlikely	Unlikely
Clonidine	Likely	Unlikely	Unlikely
Vaginal lubricants or moisturisers	Unlikely	Possible	Possible
Vaginal carbon dioxide laser	Unlikely	Unlikely	Unlikely
Stellate ganglion block	Possible	Unlikely	Unlikely
Cognitive behavioural therapy	Likely	Likely	Unlikely
Physical exercise	Unlikely	Unlikely	Unlikely
Acupuncture	Possible	Unlikely	Unlikely
Hypnosis	Likely	Unlikely	Unlikely
Yoga and mindfulness-based stress reduction	Possible	Unlikely	Unlikely

Effectiveness is defined as likely (evidence from randomised controlled trials), possible (evidence from single-arm studies), or unlikely (no evidence of effectiveness). SNRIs=serotonin norepinephrine reuptake inhibitors. SSRIs=selective serotonin reuptake inhibitors. All trials are in patients with breast cancer. Adapted from Franzoi and colleagues with permission.[44] *Does not worsen sexual function when used for vasomotor symptoms.

Table: **Effectiveness of non-hormonal treatments for vasomotor symptoms, sexual difficulties, and vaginal dryness**

Evidence gaps

Almost all published studies of menopause and cancer are in early breast cancer, and less is known about advanced breast cancer or other cancers in women. There are no reliable ways of predicting who will experience severe or prolonged menopausal symptoms following cancer treatment. In breast cancer, vaginal dryness is more common with aromatase inhibitors than tamoxifen, and some evidence suggests that switching between tamoxifen and aromatase inhibitors can improve vasomotor symptoms in postmenopausal women.[13,118] Among premenopausal women, switching to tamoxifen plus ovarian function suppression or tamoxifen alone might improve vaginal dryness, and this treatment can be considered by the treating oncologist when weighing the advantages and disadvantages of disease risks and tolerance of therapy.[119] Decisions regarding the necessity and type of hormonal therapy used for breast cancer treatment depend on menopausal status, evolving literature, disease risk, and patients' comorbidities, tolerance over time, and preferences.

Although aromatase inhibitors have become the standard of care for many patients with oestrogen-positive breast cancer (with ovarian suppression in premenopausal women), there are commonly issues with access and cost for women in LMICs. Tamoxifen is widely used for premenopausal and postmenopausal women in these settings, and it is included in WHO's list of essential cancer medicines. More information is needed about the effect of long-term tamoxifen use on menopausal symptoms and quality of life for patients from LMICs, especially when they transition from premenopausal to postmenopausal. Most clinical trials of treatments for menopausal symptoms were done in older women but younger patients with cancer can experience severe symptoms and worse quality of life.[120] Little is known about the effects of cancer treatment in lesbian, gay, bisexual, transgender, queer or questioning, and intersex (LGBTQI+) individuals, but some people report hostility and prejudice from health-care providers and anxiety about disclosing their sexual orientation and gender identity.[121] In Australia, these data have informed a new information resource for LGBTQI+ people with cancer.

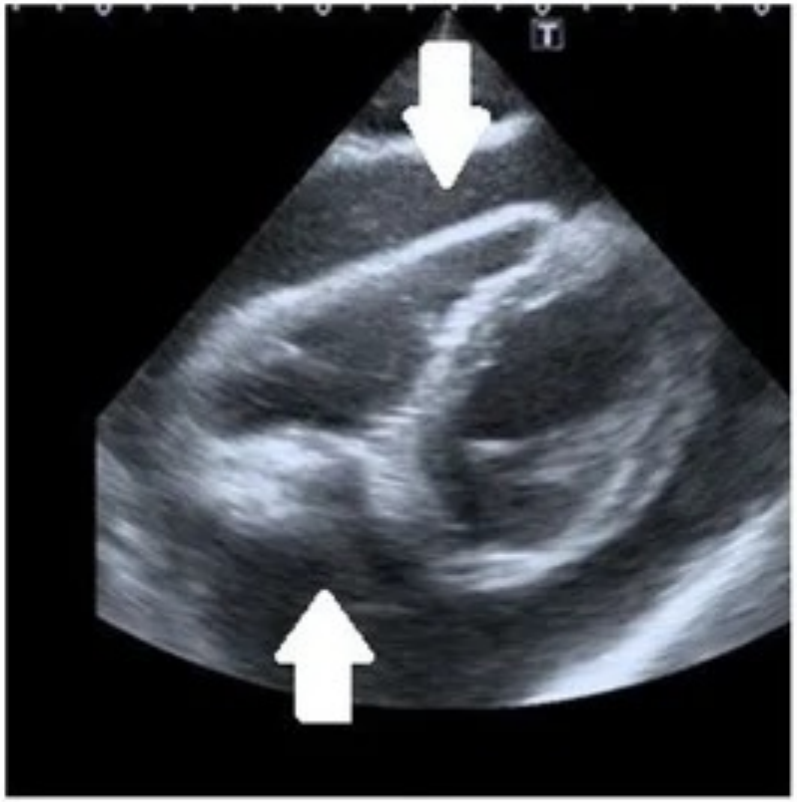

(a)

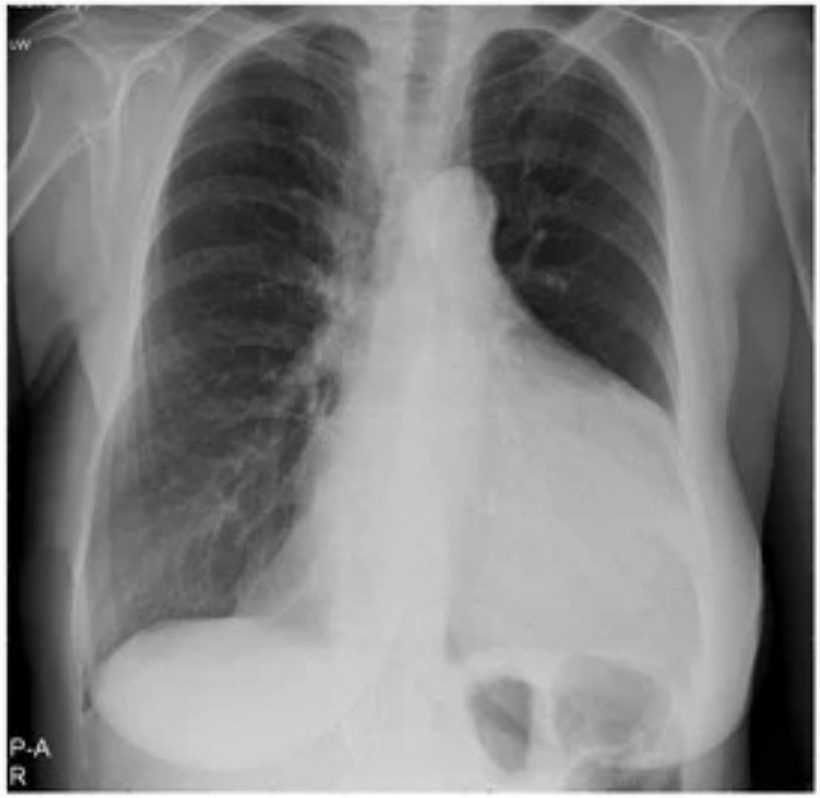

(b)

NEJM Knowledge+

Question of the Week

Which one of the following first-line therapies should be provided after pericardiocentesis in a 20-year-old man presenting with a first episode of a new large pericardial effusion, symptoms of acute pericarditis, an elevated erythrocyte sedimentation rate, and no risk factors for tuberculosis?

- Methotrexate
- Azathioprine
- Aspirin and colchicine
- Prednisone
- Intrapericardial triamcinolone

SUBMIT

Sorry, your answer is incorrect.

Methotrexate
Azathioprine
✓ Aspirin and colchicine
Prednisone
⊗ Intrapericardial triamcinolone

Key Learning Point

View Case Presentation ›

In a patient with a first episode of acute pericarditis, the best treatment for speeding recovery and reducing the risk for recurrence is aspirin and colchicine.

Detailed Feedback

This patient presents with a first episode of acute pericarditis. Tuberculous pericarditis is a possible alternative diagnosis, but in the absence of risk factors for tuberculosis, the patient can be treated for acute pericarditis. Initial treatment is with a combination of aspirin and colchicine, which markedly speeds symptomatic recovery and helps to prevent recurrence.

Several studies have shown that the use of glucocorticoids, such as prednisone, in acute pericarditis can increase the risk for recurrence. Consequently, glucocorticoid use should generally be restricted to patients with severely symptomatic recurrent pericarditis who are unresponsive to initial therapy with aspirin and colchicine.

Methotrexate or azathioprine may be used as a glucocorticoid-sparing therapy in cases of severe recurrent pericarditis, but the published literature on these agents is scant.

Data on intrapericardial delivery of triamcinolone in patients with acute pericarditis are limited. Although this approach has been successful in a small number of patients, it is not an established management option.

Transforming postsurgical care

Bioresorbable, shape-adaptive, ultrasound-readable materials structure (BioSUM) is an implantable device composed of small metal discs within a pH-responsive hydrogel. The device could allow recovery at home after surgery and rapid detection of postoperative complications. For example, when carrying out gastrointestinal (GI) anastomosis surgeries, BioSUM can be implanted. During recovery at home, the distance between the metal discs is measured by ultrasound. If a leak occurs, the hydrogel swells, so the metal discs are further apart. This early detection would prompt a return to the hospital before substantial organ damage arises.

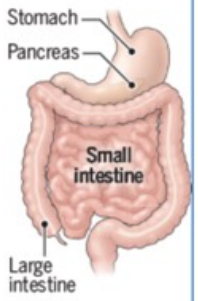

1 Device is implanted after GI repair surgery

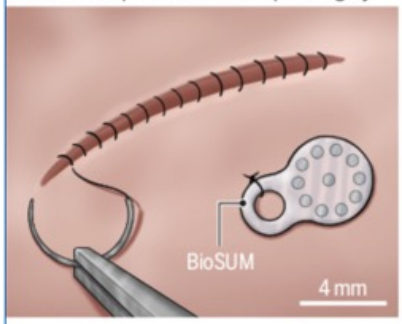

2 Device monitors for leaks postsurgery

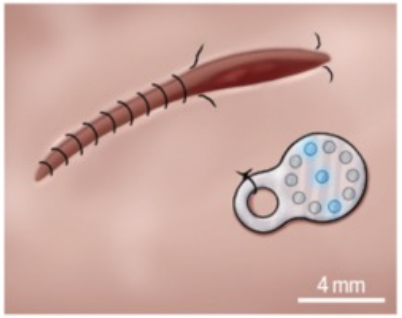

3 pH change from leak is sensed by hydrogel matrix, causing the device to swell

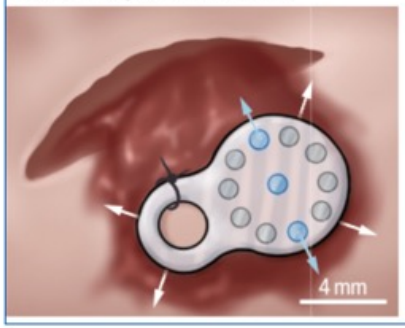

4 At-home monitoring is performed by the patient using an ultrasound device

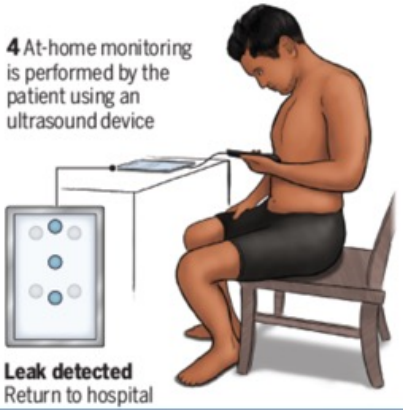

Leak detected
Return to hospital

BIOMEDICINE

Bioresorbable shape-adaptive structures for ultrasonic monitoring of deep-tissue homeostasis

Monitoring homeostasis is an essential aspect of obtaining pathophysiological insights for treating patients. Accurate, timely assessments of homeostatic dysregulation in deep tissues typically require expensive imaging techniques or invasive biopsies. We introduce a bioresorbable shape-adaptive materials structure that enables real-time monitoring of deep-tissue homeostasis using conventional ultrasound instruments. Collections of small bioresorbable metal disks distributed within thin, pH-responsive hydrogels, deployed by surgical implantation or syringe injection, allow ultrasound-based measurements of spatiotemporal changes in pH for early assessments of anastomotic leaks after gastrointestinal surgeries, and their bioresorption after a recovery period eliminates the need for surgical extraction. Demonstrations in small and large animal models illustrate capabilities in monitoring leakage from the small intestine, the stomach, and the pancreas.

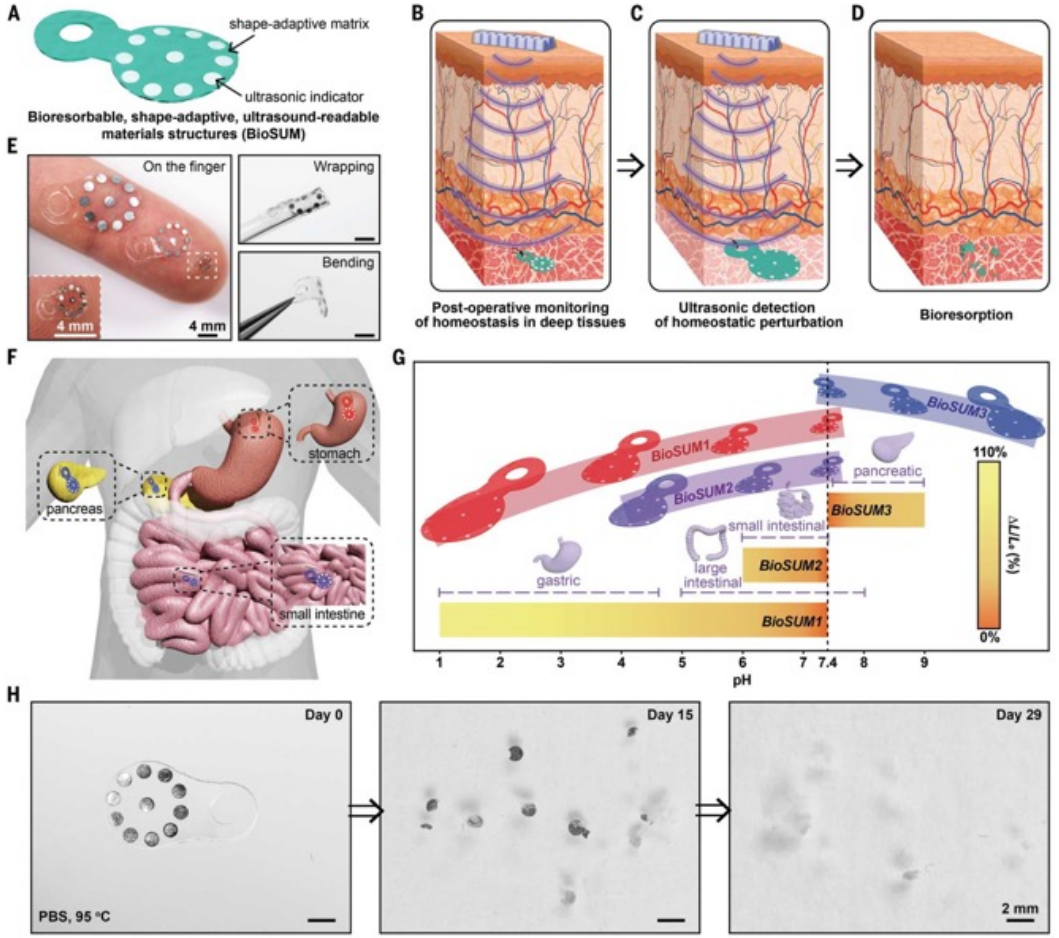

Fig. 1. Bioresorbable shape-adaptive ultrasound-readable materials structures (BioSUMs) for real-time monitoring of homeostasis in deep tissues. (**A**) Schematic illustration of our device, which includes a sparse collection of metal disks embedded in a thin hydrogel. (**B**) The BioSUM enables ultrasonic monitoring of homeostasis in deep tissues. (**C**) Ultrasonic signals from a BioSUM indicate homeostatic perturbations. (**D**) Subsequent bioresorption of the BioSUM eliminates the need for surgical extraction. (**E**) Miniaturized designs allow for implantation by laparoscopic surgery. Images of three BioSUMs of different dimensions (12, 7, and 3 mm in diameter) on the finger (left), wrapped around a plastic tube with an outer diameter of 3.175 mm (top right), and in a bent state (bottom right). (**F**) Schematic illustration of a BioSUM for detecting postsurgical leakage from the stomach, small intestine, and pancreas. (**G**) pH-responsive ranges for BioSUM1, BioSUM2, and BioSUM3, and the corresponding pH values of representative digestive juices. (**H**) Images of the accelerated dissolution of a BioSUM2 in PBS (pH 7.4) solution at 95°C.

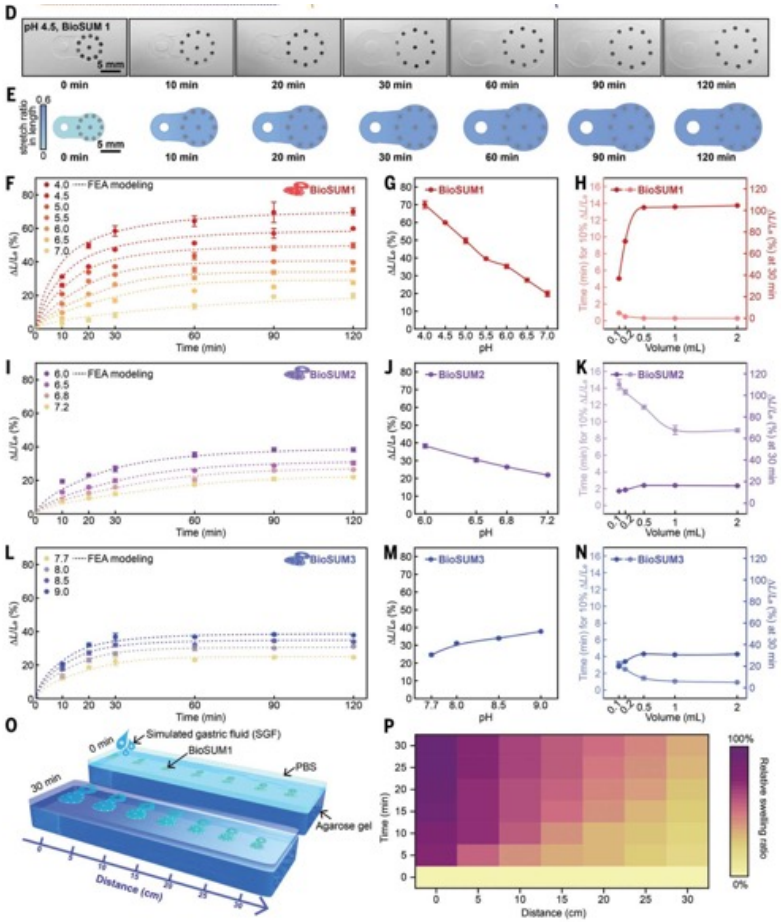

Fig. 2. pH-responsive behaviors of shape-adaptive materials structures. (**A**) Chemical structures of the monomers, oligomers, and cross-linker in the pH-responsive hydrogels used in the BioSUM system. (**B**) Schematic illustration of the mechanism for pH-responsive hydrogels in BioSUM1 and BioSUM2. (**C**) Schematic illustration of the mechanism for the pH-responsive hydrogel in BioSUM3. (**D**) Time-dependent response of a BioSUM1 when immersed in a solution with pH 4.5. (**E**) FEA modeling results of the case shown in (D). (**F**, **I**, and **L**) Ultrasonic measurement of time-dependent responses of BioSUM1, BioSUM2, and BioSUM3, respectively, to immersion in solutions with different pH values. $\Delta L/L_0$ (%) denotes the swelling ratio. (**G**, **J**, and **M**) Response of BioSUM1, BioSUM2, and BioSUM3, respectively, to immersion in solutions with different pH values at the equilibrium state. (**H**, **K**, and **N**) Optical measurement of sensitivity of a BioSUM to the introduction of different amounts of simulated GI fluids, including the response time for reaching 10% $\Delta L/L_0$ and $\Delta L/L_0$% at 30 min. (H) Response of a BioSUM1 to simulated gastric fluid. (K) Response of a BioSUM2 to simulated small intestinal fluid. (N) Response of a BioSUM3 to simulated pancreatic juice. (**O**) Schematic illustration of the setup for spatiotemporal mapping of pH with BioSUM1s. (**P**) Spatiotemporal characteristics, determined through optical methods, of BioSUM1s in response to the introduction of simulated gastric fluid at one end of the system. BioSUMs are fully swollen in PBS (pH 7.4) for 24 hours before the measurements presented here. Error bars in (F) to (N) represent ±SD.

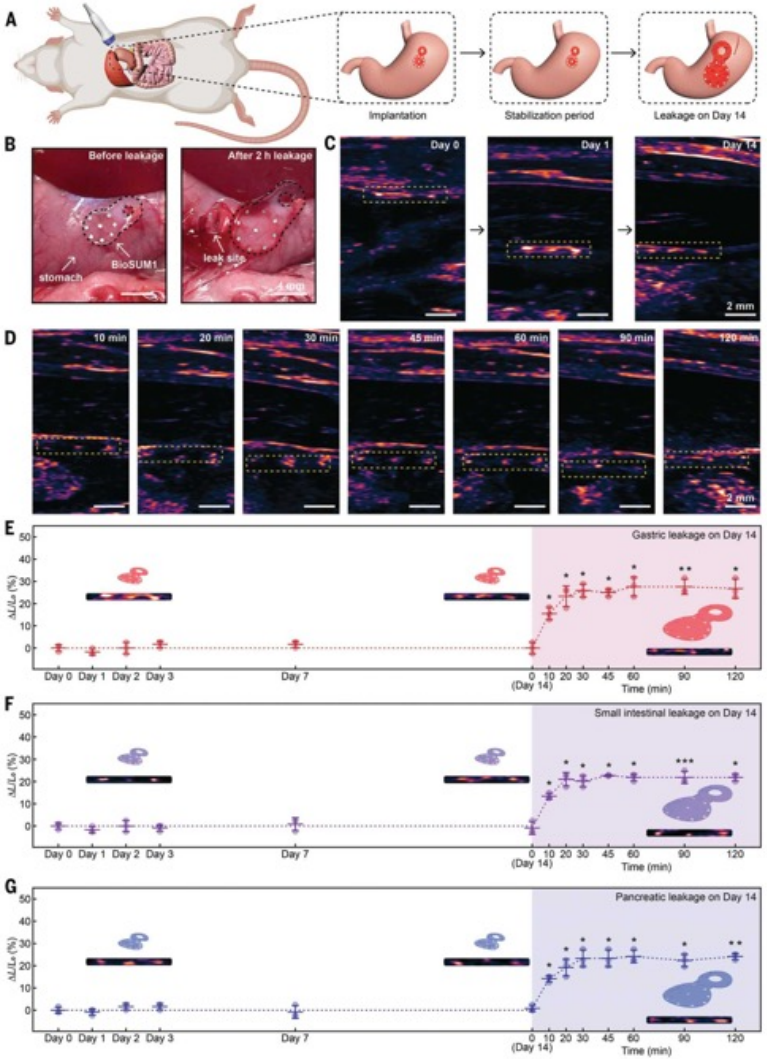

Fig. 4. Longitudinal monitoring of pH homeostasis of the rat gastrointestinal system. (**A**) Schematic illustration of the implantation and sensing procedure for a BioSUM1 on the stomach of a rat. [Created with Biorender.com] (**B**) Images showing the expansion of a BioSUM1 2 hours after creating a single gastrotomy. (**C**) Ultrasound images of a BioSUM1 on the stomach over a 14-day stabilization period without induced gastric leakage. The depth of the array of Zn disks changes between day 0 and day 1 because of postoperative relocation of organs. (**D**) Longitudinal ultrasound images of BioSUM1 on the stomach after acute gastrotomy. (**E**) Summary data showing the swelling ratios of a BioSUM1 during the stabilization period and after acute gastrotomy. $n = 3$ biologically independent animals. Repeated measures (RM) one-way analysis of variance (ANOVA), $P = 0.0008$. Holm-Sidak's multiple comparison test versus day 14 (0 min): 10 min, $P = 0.0208$; 20 min, $P = 0.0208$; 30 min, $P = 0.0198$; 45 min, $P = 0.0207$; 60 min, $P = 0.0208$; 90 min, $P = 0.0092$; and 120 min, $P = 0.0207$. Inset ultrasound images representing day 1, day 14, and 120 min were extracted from (C) and (D). (**F**) Same as (E), but for a BioSUM2 and enterotomy. RM one-way ANOVA, $P = 0.0009$. Holm-Sidak's multiple comparison test versus day 14 (0 min): 10 min, $P = 0.0254$; 20 min, $P = 0.0254$; 30 min, $P = 0.0141$; 45 min, $P = 0.0254$; 60 min, $P = 0.0254$; 90 min, $P = 0.0005$; and 120 min, $P = 0.0254$. Inset ultrasound images representing day 1, day 14, and 120 min were extracted from fig. S43. (**G**) Same as (E), but for a BioSUM3 and pancreatic leakage. RM one-way ANOVA, $P = 0.0021$. Holm-Sidak's multiple comparison test versus day 14 (0 min): 10 min, $P = 0.0231$; 20 min, $P = 0.0359$; 30 min, $P = 0.0359$; 45 min, $P = 0.0359$; 60 min, $P = 0.0348$; 90 min, $P = 0.0325$; and 120 min, $P = 0.0089$. Dots represent individual animals. Line represents B-spline. Error bars represent ±SD. $^{*}P < 0.05$, $^{**}P < 0.01$, $^{***}P < 0.001$. Inset ultrasound images representing day 1, day 14, and 120 min were extracted from fig. S44. BioSUMs were fully swollen in PBS (pH 7.4) for 24 hours before implantation, in all cases.

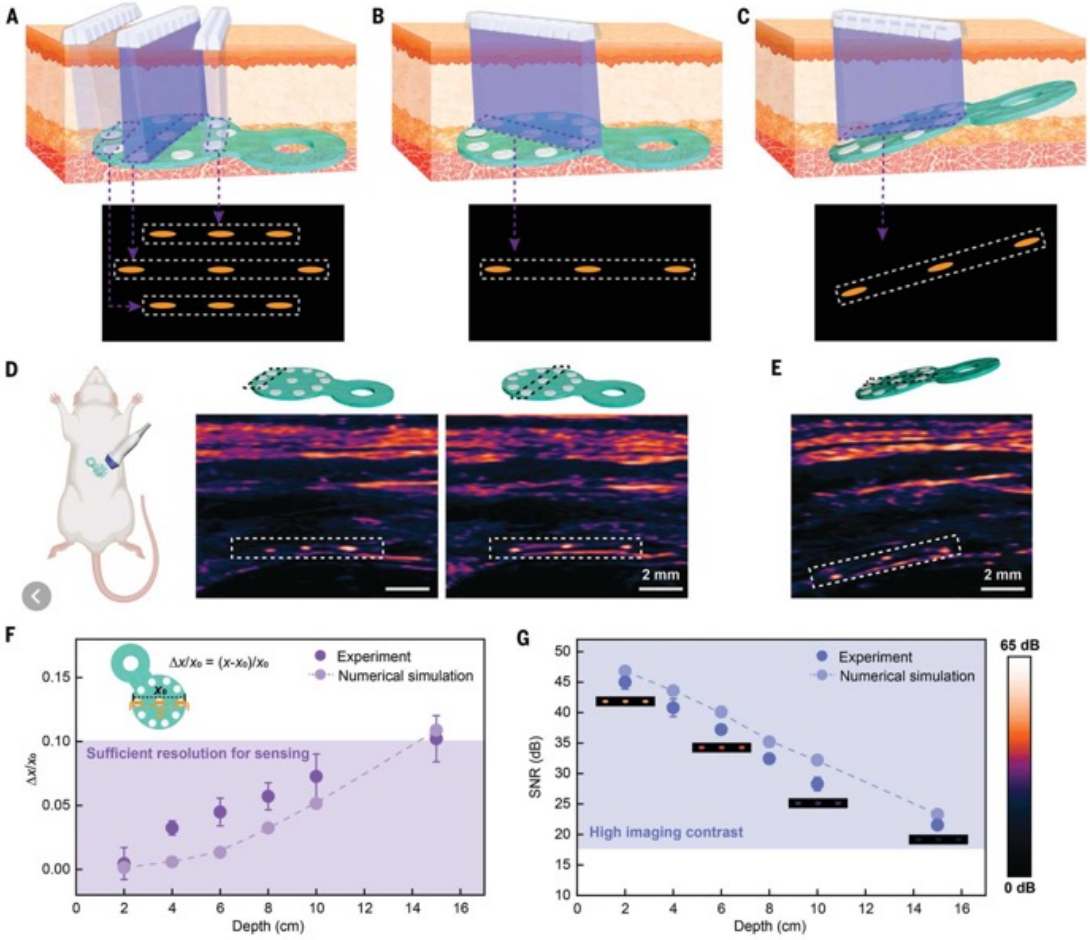

Fig. 3. Sensing by ultrasound imaging in deep tissues. (**A**) Schematic illustration of the cross-sectional position of acoustic waves relative to a BioSUM in different cases, and the corresponding signals in the ultrasound B-mode image. (**B**) The symmetric design enables ultrasonic visualization independent of the orientation of the transducer. (**C**) Schematic illustration of a BioSUM in a tilted case, and the corresponding signals in the ultrasound B-mode image. (**D**) Ultrasound B-mode images of a BioSUM on the stomach in a rat model demonstrating the cross-sectional position of acoustic waves in different cases, correlated to the schematic illustration in (A). (**E**) Ultrasound B-mode image of a BioSUM in a tilted case on the stomach in a rat model, corresponding to the schematic illustration in (C). (**F**) Experimental and numerical simulation results for the measurement accuracy of a BioSUM at different depths. $\Delta x/x_0$ is the deviation of measured length divided by the actual length. (**G**) Experimental and numerical simulation results for the signal-to-noise ratio at different depths. Inset images are schematic illustrations of the image contrast in decibels. Error bars in (F) and (G) represent ±SD.

Conclusions

We introduce bioresorbable shape-adaptive structures that enable rapid, noninvasive measurements of homeostasis in deep tissues by conventional ultrasound imaging techniques. The swelling of thin films of a responsive hydrogel matrix induced by homeostatic perturbations leads to changes in separations between sparse collections of bioresorbable metal elements functioning as indicators whose positions can be determined accurately by ultrasound. The large mismatch between the acoustic impedance of these elements and the surrounding materials produces high contrast in ultrasound images, thereby allowing for accurate measurements of their separations, and thus local physical or chemical characteristics of the surrounding tissues in shallow or deep locations. An envisioned clinical scenario is in real-time detection of anastomotic leakage through changes in pH during a period of recovery after a GI surgery, to allow for early intervention. The devices survive for a relevant timeframe and then naturally bioresorb, eliminating the need for secondary surgical extraction procedures. In vivo demonstrations of this concept in small and large animals validate materials designs tailored for use in gastric, small intestinal, and pancreatic leakage.

Woman fosters obese dog; throngs of fans watch canine lose weight

Golden retriever Frannie was severely overweight, and had lived outside for her entire life. Her owners were planning to euthanize her.

Frannie was 125 pounds when she was fostered in mid-December. She has since lost 31 pounds. (Frannie's Fight)

Frannie was living in a backyard when she was rescued by Rover's Retreat. (Frannie's Fight)

Bram put Frannie on a container to help her learn to stand on her legs. (Frannie's Fight)

Bram and Frannie in February. (Frannie's Fight)

CENTRAL ILLUSTRATION: Sex Differences in Physical Activity-Associated Mortality Risk Reduction

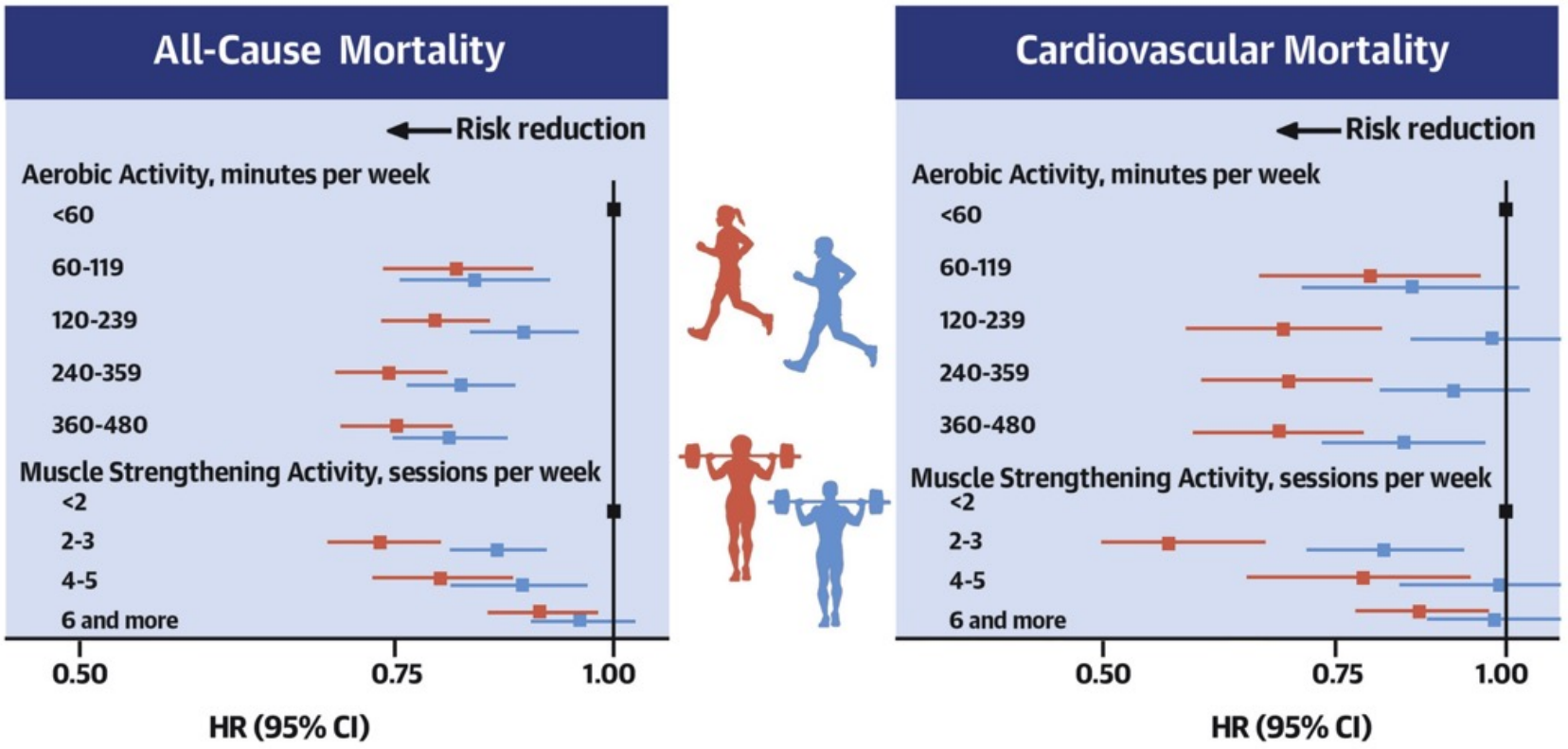

Ji H, et al. J Am Coll Cardiol. 2024;83(8):783-793.